Genetics and Epigenetics of Alveolar Capillary Dysplasia

From bedside to bench

Evelien Slot

Cover and layout: Publiss | www.publiss.nl

Layout: Publiss | www.publiss.nl

Printing: Ridderprint | www.ridderprint.nl

Genetics and Epigenetics of Alveolar Capillary Dysplasia

From bedside to bench

Genetica en epigenetica van alveolaire capillaire dysplasie

Van kliniek tot laboratorium

Proefschrift

ter verkrijging van de graad van doctor aan de

Erasmus Universiteit Rotterdam

op gezag van de rector magnificus

Prof.dr. A.L. Bredenoord

en volgens besluit van het College voor Promoties.

De openbare verdediging zal plaatsvinden op

woensdag 1 december 2021 om 13.00 uur

door

Evelien Slot

geboren te Lelystad, Nederland.

Erasmus University Rotterdam

Promotiecommissie:

Promotor: prof. dr. em. D. Tibboel

Overige leden: prof. dr. ir. N.J. Galjart

prof. dr. R.P.M. Steegers - Theunissen

prof. dr. P.S. Hiemstra

Copromotoren: dr. J.E.M.M. de Klein

dr. R.J. Rottier

TABLE OF CONTENTS

CHAPTER 1

GENERAL INTRODUCTION

ACD/MPV CASE ILLUSTRATION

SCOPE OF THIS THESIS

GENERAL INTRODUCTION

Human lung development

The human lung develops from four weeks of gestation throughout early childhood and is characterized by five stages: the embryonic stage, pseudoglandular stage, canalicular stage, saccular stage and alveolar stage (extensively reviewed elsewhere (1, 2)). In the embryonic stage (weeks 4-6), lung buds appear from the primitive gut and expand into lobar and segmental branches on either side of the future oesophagus. Already at this early stage of lung development, a vascular plexus connected to the embryonic circulation surrounds the early lung structures (3). In the pseudoglandular stage (weeks 6-17), airway branching morphogenesis continues and results in the formation of a complex tree-like structure of pre-acinar airways. At this stage, the airway tubules are lined by columnar epithelial cells while the distal parts are lined by cuboidal epithelial cells which represent the distal progenitor cells. The surrounding vascular network extends simultaneously through angiogenesis. During the canalicular stage (weeks 16-25), branching morphogenesis is completed. Each respiratory bronchioli terminates in an acinus where distal cuboidal epithelial cells differentiate into type 1 and type 2 alveolar cells. The vascular network expands into the surrounding mesenchyme and forms a capillary network close to the flattening epithelium. In this way, the first blood-airway barrier arises. In the saccular phase (weeks 24-38), the airspaces expand, interstitial tissue decreases and neighbouring capillary networks form a bi-layer in the intersaccular septae. In the last phase of lung development, the alveolar phase (week 38- first years of life), the intersaccular septae divide into thin alveolar septae and extra capillaries are formed through angiogenesis. The final alveolar spaces are lined by type 1 (90%) and type 2 (10%) alveolar cells that share their basement membrane with the vascular endothelial cells to provide optimal gas exchange.

Alveolar capillary dysplasia with or without misalignment of the pulmonary veins

Alveolar capillary dysplasia with or without misalignment of the pulmonary veins (ACD/MPV) is a rare and lethal congenital lung disorder of which the pathogenesis is poorly understood. Typically, ACD/MPV patients are born at term after an uncomplicated

pregnancy but suffer from severe respiratory distress, caused by progressive pulmonary hypertension and oxygen insufficiency. There is no long term treatment for ACD/MPV and with a few exceptions most patients eventually die. Life supportive care is often put to a halt as soon as the diagnosis is clear. However, the only way to diagnose ACD/MPV is by means of histological examination of the lung and thus, most patients are diagnosed post-mortem through autopsy or by exclusion of other diagnosis in the absence of histological material. The main histological characteristics of ACD/MPV lungs are the lack of alveolar capillaries and thickened alveolar septae leading to insufficient gas exchange (Figure 1). Further, hypertrophy of the peripheral arterial walls is observed, corresponding to the clinically observed pulmonary hypertension. Whether these abnormal arterial walls are either the cause or the result of the pulmonary hypertension is still topic of discussion. Lastly, in the majority of ACD/MPV patients, veins are found in the bronchovascular bundle adjacent to the pulmonary arteries and are the so-called "misaligned pulmonary veins" (MPV). The origin of these misaligned veins is not clear.

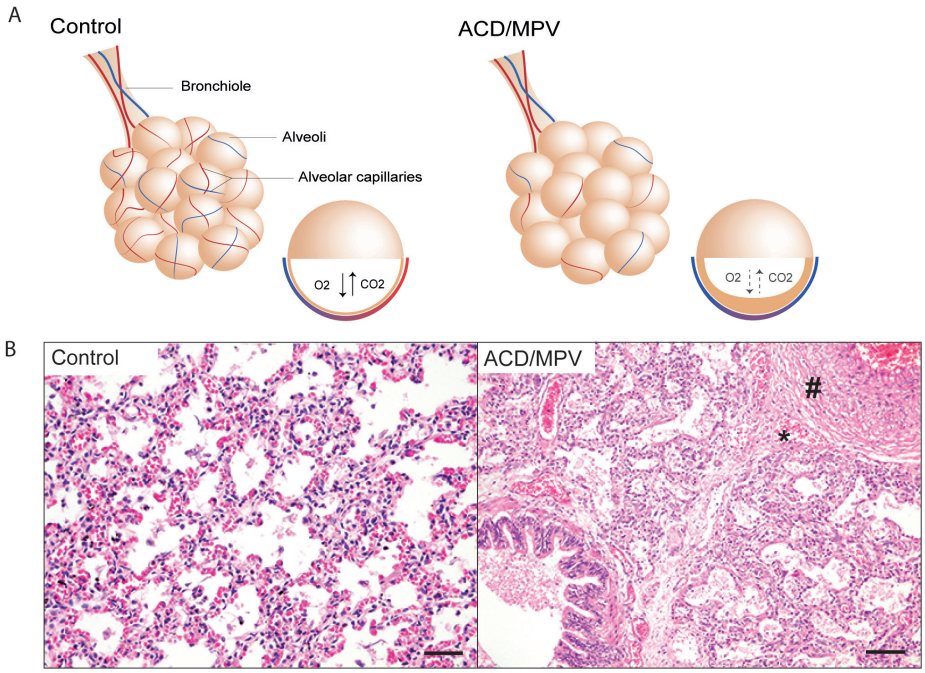

Figure 1. ACD/MPV lung characteristics *A: Schematic illustration of reduced alveolar capillaries and thickening of alveolar septa in ACD/MPV lungs blocking sufficient gas exchange. Control left, ACD/MPV right. B: H&E staining of ACD/MPV lung tissue (right) and lung tissue of an age-matched control (left) (adapted from Kool et al. 2014(4)) showing arterial wall hypertrophy (#), misaligned pulmonary veins (*) and central positioning of capillaries in alveolar septa. Scale bar: 100μM*

Genetics of ACD/MPV

Over the last ten years, multiple studies have focused on the pathogenesis of ACD/MPV. The most important discovery was by the group of Stankiewicz who found that heterozygous mutations and deletions involving the *FOXF1* locus are associated with ACD/MPV (5-7). According to our current knowledge, the *FOXF1* locus consists of a two-exon gene and a 60 kilo base (kb) enhancer region located 250 kb upstream of the gene (Figure 2) (8). *FOXF1* encodes for Forkhead Box F1 (FOXF1), a transcription factor that is expressed in the mesenchymal and vascular cells during embryonic pulmonary development (9, 10). Since the association between ACD/MPV and *FOXF1* was discovered, over 100 different mutations and deletions have been identified (11-17). Many of the genetic diagnoses were the result of retrospective genetic testing on research basis but the number of ACD/MPV patients being genetically tested in the clinic in the early stages of disease increases (5, 7, 11-14, 18, 19). Genetic testing is less invasive than obtaining a lung biopsy and could therefore be an accessible method for diagnosing ACD/MPV in the early stages of disease. In case of familial occurrence, a genetic diagnosis could provide information about the recurrence risk in future pregnancies. For mutation detection, Sanger sequencing or whole exome sequencing (WES) are currently the most commonly used genetic techniques. However, to detect large deletions in the *FOXF1* gene or its 60kb enhancer region, array comparative genomic hybridization or SNP array is often used. Although all of these techniques work well, they need to be combined for ACD/MPV which makes their use time consuming and expensive. Whole genome sequencing (WGS), a more advanced genetic testing technique, enables detection of mutations and large deletions in both coding and non-coding regions in the same run. However, WGS has only recently become available for routine diagnostic testing and thus, a genetic diagnosis is only rarely given before lung biopsy or autopsy is performed. Furthermore, to fully replace histological lung examination as gold standard for diagnosing ACD/MPV with genetic testing, the exact effects of different *FOXF1* alterations on lung development and the phenotype need to be clarified.

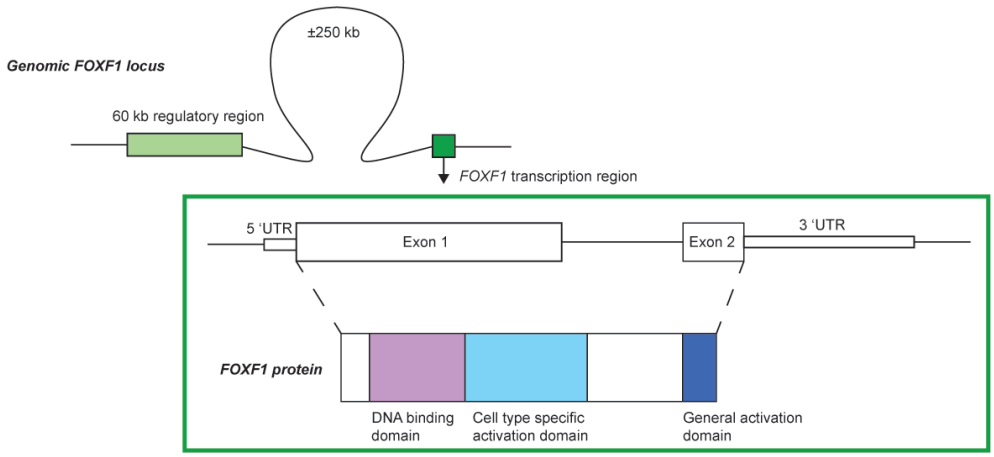

Figure 2. Schematic overview of the FOXF1 locus and the FOXF1 protein *The FOXF1 gene, consisting of two exons, is located on chromosome 16 and is (partly) regulated by a 60kb regulatory region located ±250 kb upstream on chromosome 16 (6, 8, 16). The FOXF1 protein contains a general Forkhead box (FOX) DNA binding domain, a lung cell type specific activation domain and a general activation domain (20).*

Epigenetics of ACD/MPV

In a few of the genetically tested ACD/MPV patients, no genomic *FOXF1* alteration was observed nor could any other potentially causative genomic alteration be identified (16). Apart from genomic changes, epigenetic changes have a large influence on gene expression as well and could play a role in the pathogenesis of ACD/MPV. The most studied epigenetic mechanism is DNA methylation in which a methyl-group is added to the cytosine molecule that is directly followed by a guanine (CpG site), converting the cytosine into a 5-methylcytosine. In the human genome, about 70-80% of CpG sites are methylated and these specific methylation patterns influence gene expression and gene regulation (21). An example of gene regulation through methylation is parental imprinting in which either the paternally derived or maternally derived allele is inactive due to an allele specific methylation pattern. Since ACD/MPV is caused by heterozygous mutations and deletions, it has been hypothesized that the *FOXF1* gene is also subject to parental imprinting (6, 16, 22). Studies revealed that point mutations involving the *FOXF1* transcription region are found on both alleles, which would be in conflict with imprinting of the gene itself. However, all but one large deletions detected in ACD/MPV patients that involve the 60kb *FOXF1* enhancer region were found on the maternal allele, which could imply imprinting of the 60kb *FOXF1* enhancer (6, 16, 22, 23). To get a better understanding

of epigenetic *FOXF1* regulation in lung tissue and its role in ACD/MPV, which is especially important for the cases without a genomic *FOXF1* alteration, more studies should be conducted on (ab)normal methylation patterns in human lung tissue.

The role of FOXF1 in lung development

Mice studies revealed that the levels of Foxf1 expression in mesenchymal and endothelial cells play a critical role for normal lung development. Homozygous loss of Foxf1 is embryonically lethal before the embryonic stage of lung development, whereas mice with heterozygous loss of *Foxf1* show variable pulmonary defects correlated to the level of *Foxf1* expression (9, 10, 24). Interestingly, also overexpression of *Foxf1* in all tissues is embryonically lethal and overexpression of *Foxf1* in endothelial and hematopoietic lineages results in pulmonary, vascular, lymphatic and platelet defects (25). *Foxf1* is a downstream target of the Sonic hedgehog signalling pathway and is upregulated through binding of GLI2 (8, 9, 26). FOXF1 induces endothelial cell proliferation and angiogenesis during lung development and lung regeneration through regulation of endothelial genes including Flt1, Flk1, Pdgfb, Pecam1, Tie2 and Cdh5 (27-32). Mesenchymal deletion of *Foxf1* demonstrated impaired lung branching, and disrupted epithelial development in the trachea and oesophagus indicating an important role for FOXF1 in the mesenchymal-epithelial signalling during embryonic development (26, 33). Although studies in mice form the basis for our understanding of the function of FOXF1 in pulmonary (vascular) development, studies on FOXF1 in human are scarce. Similar to mice, endothelial deletion of FOXF1 in human derived endothelial colony forming cells reduced vascular sprouting (31). Furthermore, expression analyses of ACD/MPV lung tissues demonstrated a deregulation of genes involved in lung development, angiogenesis and pulmonary hypertension (30). However, direct FOXF1 target genes have not been identified in human yet and little is known about the effects of the different genomic *FOXF1* variants detected in ACD/MPV patients which could, among others, involve downregulation of FOXF1, impaired DNA binding or changes in protein complex forming. To get a better understanding of the pathogenesis involved in ACD/MPV, the (ab)normal function of FOXF1 is ideally studied in primary pulmonary vascular cells of ACD/MPV patients and age-matched controls during lung development. However, ACD/MPV is hardly ever diagnosed during pregnancy and even of postnatally diagnosed ACD/MPV patients, there

is very little fresh lung tissue available for isolation of vascular cells. Therefore, the use of *in vitro* models that mimic lung development provide an alternative but effective method to study the role of FOXF1 during embryonic development in human.

Pulmonary vascular development in a dish

The introduction of induced human pluripotent stem cells (iPSCs)(34) created a new opportunity to mimic human pulmonary and vascular development in a dish (35-37). Similar to embryonic stem cells (ESCs), iPSCs have extensive self-renewal capability and can be differentiated into a variety of differentiated cell types, including vascular endothelial cells. Whereas ESCs need to be isolated from the undifferentiated inner mass of an embryo, iPSCs can be generated from easy accessible cells like skin fibroblasts or blood cells (38-41). This allows research on vascular endothelial cells, in the context of the patient's genome.

ACD/MPV CASE ILLUSTRATION

Text translated by Jennifer de Wolf-Collins from: 'Myla, een verhaal over hoop, geloof en liefde' written by Mathijs Lourens

November 23rd-25th

Upon arriving in Rotterdam on Wednesday we first took Alec to the Speeldek, which is a daycare sponsored by the Ronald McDonald House Charities where siblings of sick children are lovingly taken care of by various volunteers. Yet again I am walking through the hallways of the hospital together with Jessica to visit Myla. She is doing fairly well and is stable, but she is not really progressing. Last Monday it looked like she was improving, but that hope unfortunately turned out to be unfounded. Now, unexpectedly, we are taken aside by one of the physicians, who suddenly paints a grim scenario for us. Because Myla is not improving, they are starting to suspect that she could be suffering of ACD. Alveolar Capillary Dysplasia. A lung disorder that simply is not compatible with life and which is untreatable. Bam! After a couple of 'quiet' days we feel like we are back in an emotional rollercoaster. The harsh reality has struck and yet again confirms our daughter Myla's worrying situation. The horrible part is that we cannot even get a confirmation of her diagnosis without invasive surgery to obtain a piece of lung to investigate. A biopsy. Because this is such a huge risk in her case as she is on ECMO (heart-lung machine), this is simply not possible.

December 16th

My daughter has Alveolar Capillary Dysplasia, which is not compatible with life, as they say with such nice words. Jessica falls apart completely. I can hardly take it in. I cry, but feel ready for battle. But fighting is no longer necessary, it is pointless. Even though that is what I am so very good at. I submit to dr. C. "That's it, enough is enough" I tell her. She nods affirmatively. Our little brave Myla has fought like a lion. She kept getting back up, never backing down, but she never stood a chance. Dr. V. takes care of Jessica together with E., while I talk some more with Dr. C. Mostly we talk about what happens next. Tomorrow morning they first need to convene with the entire teams of physicians to discuss the results from Seattle. They will stabilize Myla throughout the night and we will be allowed to say our goodbyes however we want to. And then what it comes down to is that they will turn off the machine tomorrow morning. She will die shortly after. The conversation passes in a blur. I just do not know what to do with myself, what a final blow. Knockout.

SCOPE OF THIS THESIS

ACD/MPV is a rare congenital disorder with symptoms that are not specific for ACD/MPV such as respiratory distress, and a mortality rate of almost 100%. Before ACD/MPV is diagnosed by histological examination of the lung, patients spend significant time in the hospital receiving invasive and sometimes expensive treatments like extra corporeal membrane oxygenation (ECMO). Moreover, it is believed that ACD/MPV cases have been misdiagnosed for idiopathic pulmonary hypertension for many years, due to the lack of lung tissue examination. To improve clinical care for ACD/MPV patients, the studies described in this thesis aimed at increasing awareness among clinicians, improving diagnostics and increasing our understanding of the pathogenesis of ACD/MPV. In **CHAPTER 1**, I give a short introduction into lung development and ACD/MPV, and I discuss the gaps in our current knowledge of the pathogenesis of ACD/MPV.

Although awareness of ACD/MPV is increasing, ACD/MPV is still not often in the top differential diagnosis when a patient presents with severe respiratory symptoms. To emphasize on ACD/MPV as possible diagnosis in a new-born presenting with respiratory distress, this thesis includes an extensive overview of the clinical and genetic aspects of ACD/MPV (**CHAPTER 2**) (42).

In **CHAPTER 3,** I aimed to contribute to a faster diagnosis of ACD/MPV by improving current diagnostic methods. As mentioned before, the gold standard to diagnose ACD/MPV is histological lung examination. However, performing an open lung biopsy is invasive, especially during ECMO treatment, and is therefore not performed before other possible causes are excluded. In practice, this can take several weeks with the result that many patients die prior to biopsy and get diagnosed post-mortem through autopsy. For more incentive to proceed with lung biopsy in an earlier stage of symptom presentation, it would help to have information about the presence or absence of genomic *FOXF1* variants. Because genetic testing techniques that were available at the start of this thesis (2017) did not meet the criteria for fast and cost-effective detection of *FOXF1* mutations and deletions, **CHAPTER 3** presents the development and validation of a *FOXF1* targeted NGS panel for detection of mutations and deletions associated with ACD/MPV (43).

Retrospective testing of ACD/MPV patients with the newly developed NGS panel confirmed the absence of genomic *FOXF1* alterations in a subset of patients. Whether epigenetic

changes are involved in the pathogenesis of ACD/MPV is unclear. Therefore, **CHAPTER 4** demonstrates the investigation of DNA methylation patterns in lung tissues of ACD/MPV patients and age-matched controls to identify abnormally methylated regions that might contribute to ACD/MPV.

Over the past ten years, retrospective genetic testing of ACD/MPV patients demonstrated a wide variety in genomic *FOXF1* variants associated with ACD/MPV. Yet, very little is known about the effects of these *FOXF1* mutations on the expression and function of FOXF1, and how this leads to abnormal pulmonary vascular development. As fresh tissue from ACD/MPV patients is scarce which impedes the investigation of *FOXF1* mutations in patient derived cells, **CHAPTER 5** describes the generation of three iPSC lines from skin fibroblasts of two ACD/MPV patients with different missense mutations located in the *FOXF1* DNA binding domain (44). Since iPSCs can be differentiated into many cell types of interest, this reduces the need for fresh ACD/MPV tissue to study specific *FOXF1* variants.

One of the most important cell types involved in pulmonary vascular development are endothelial cells. Therefore, **CHAPTER 6** describes the differentiation of patient derived iPSCs into vascular endothelial cells. Using RNA sequencing, gene expression trends during differentiation are analysed, and functional assays are used to investigate the angiogenic potential of the *FOXF1* mutated endothelial cells.

The general discussion (**CHAPTER 7**) reviews the results that are obtained in the studies described in this thesis. Furthermore, this chapter elaborates on the hypotheses and perspectives for future research.

The final chapter of this thesis, **CHAPTER 8** contains the summary in English in Dutch.

REFERENCES

1. Morrisey EE, Hogan BL. Preparing for the first breath: genetic and cellular mechanisms in lung development. Dev Cell. 2010;18(1):8-23.
2. Mullassery D, Smith NP. Lung deve-lopment. Semin Pediatr Surg. 2015;24(4):152-5.
3. Parera MC, van Dooren M, van Kempen M, de Krijger R, Grosveld F, Tibboel D, et al. Distal angiogenesis: a new concept for lung vascular morphogenesis. Am J Physiol Lung Cell Mol Physiol. 2005;288(1):L141-9.
4. Kool H, Mous D, Tibboel D, de Klein A, Rottier RJ. Pulmonary vascular development goes awry in congenital lung abnormalities. Birth Defects Res C Embryo Today. 2014;102(4):343-58.
5. Stankiewicz P, Sen P, Bhatt SS, Storer M, Xia Z, Bejjani BA, et al. Genomic and genic deletions of the FOX gene cluster on 16q24.1 and inactivating mutations of FOXF1 cause alveolar capillary dysplasia and other malformations. Am J Hum Genet. 2009;84(6):780-91.
6. Szafranski P, Dharmadhikari AV, Brosens E, Gurha P, Kolodziejska KE, Zhishuo O, et al. Small noncoding differentially methylated copy-number variants, including lncRNA genes, cause a lethal lung developmental disorder. Genome Res. 2013;23(1):23-33.
7. Szafranski P, Herrera C, Proe LA, Coffman B, Kearney DL, Popek E, et al. Narrowing the FOXF1 distant enhancer region on 16q24.1 critical for ACDMPV. Clin Epigenetics. 2016;8:112.
8. Szafranski P, Dharmadhikari AV, Wambach JA, Towe CT, White FV, Grady RM, et al. Two deletions overlapping a distant FOXF1 enhancer unravel the role of lncRNA LINC01081 in etiology of alveolar capillary dysplasia with misalignment of pulmonary veins. Am J Med Genet A. 2014;164A(8):2013-9.
9. Mahlapuu M, Enerback S, Carlsson P. Haploinsufficiency of the forkhead gene Foxf1, a target for sonic hedgehog signaling, causes lung and foregut malformations. Development. 2001;128(12):2397-406.
10. Mahlapuu M, Ormestad M, Enerback S, Carlsson P. The forkhead transcription factor Foxf1 is required for differentiation of extra-embryonic and lateral plate mesoderm. Development. 2001;128(2):155-66.
11. Abu-El-Haija A, Fineman J, Connolly AJ, Murali P, Judge LM, Slavotinek AM. Two patients with FOXF1 mutations with alveolar capillary dysplasia with misalignment of pulmonary veins and other malformations: Two different presentations and outcomes. Am J Med Genet A. 2018;176(12):2877-81.
12. Goel D, Oei JL, Lui K, Ward M, Shand AW, Mowat D, et al. Antenatal gastrointestinal anomalies in neonates subsequently found to have alveolar capillary dysplasia. Clin Case Rep. 2017;5(5):559-66.
13. Ito Y, Akimoto T, Cho K, Yamada M, Tanino M, Dobata T, et al. A late presenter and long-term survivor of alveolar capillary dysplasia with misalignment of the pulmonary veins. Eur J Pediatr. 2015;174(8):1123-6.
14. Jourdan-Voyen L, Touraine R, Masutti JP, Busa T, Vincent-Delorme C, Dreyfus L, et al. Phenotypic and genetic spectrum of alveolar capillary dysplasia: a retrospective cohort study. Arch Dis Child Fetal Neonatal Ed. 2019.
15. Ma Y, Jang MA, Yoo HS, Ahn SY, Sung SI, Chang YS, et al. A Novel De Novo Pathogenic Variant in FOXF1 in a Newborn with Alveolar Capillary Dysplasia with Misalignment of Pulmonary Veins. Yonsei Med J. 2017;58(3):672-5.
16. Szafranski P, Gambin T, Dharmadhikari AV, Akdemir KC, Jhangiani SN, Schuette J, et al. Pathogenetics of alveolar capillary dysplasia with misalignment of pulmonary veins. Hum Genet. 2016;135(5):569-86.
17. Hayasaka I, Cho K, Akimoto T, Ikeda M, Uzuki Y, Yamada M, et al. Genetic basis for childhood interstitial lung disease among Japanese infants and children. Pediatr Res. 2018;83(2):477-83.
18. Al-Hathlol K, Phillips S, Seshia MK, Casiro O, Alvaro RE, Rigatto H. Alveolar capillary dysplasia. Report of a case of prolonged life without extracorporeal membrane oxygenation (ECMO) and review of the literature. Early Hum Dev. 2000;57(2):85-94.
19. Sen P, Gerychova R, Janku P, Jezova M, Valaskova I, Navarro C, et al. A familial case of alveolar capillary dysplasia with misalignment of pulmonary veins supports paternal imprinting of FOXF1 in human. Eur J Hum Genet. 2013;21(4):474-7.

20. Hellqvist M, Mahlapuu M, Samuelsson L, Enerback S, Carlsson P. Differential activation of lung-specific genes by two forkhead proteins, FREAC-1 and FREAC-2. J Biol Chem. 1996;271(8):4482-90.
21. Bird A. DNA methylation patterns and epigenetic memory. Genes Dev. 2002;16(1):6-21.
22. Alsina Casanova M, Monteagudo-Sanchez A, Rodiguez Guerineau L, Court F, Gazquez Serrano I, Martorell L, et al. Maternal mutations of FOXF1 cause alveolar capillary dysplasia despite not being imprinted. Hum Mutat. 2017;38(6):615-20.
23. Dharmadhikari AV, Szafranski P, Kalinichenko VV, Stankiewicz P. Genomic and Epigenetic Complexity of the FOXF1 Locus in 16q24.1: Implications for Development and Disease. Curr Genomics. 2015;16(2):107-16.
24. Kalinichenko VV, Lim L, Stolz DB, Shin B, Rausa FM, Clark J, et al. Defects in pulmonary vasculature and perinatal lung hemorrhage in mice heterozygous null for the Forkhead Box f1 transcription factor. Dev Biol. 2001;235(2):489-506.
25. Dharmadhikari AV, Sun JJ, Gogolewski K, Carofino BL, Ustiyan V, Hill M, et al. Lethal lung hypoplasia and vascular defects in mice with conditional Foxf1 overexpression. Biol Open. 2016;5(11):1595-606.
26. Nasr T, Holderbaum AM, Chaturvedi P, Agarwal K, Kinney JL, Daniels K, et al. Disruption of a hedgehog-foxf1-rspo2 signaling axis leads to tracheomalacia and a loss of sox9+ tracheal chondrocytes. Dis Model Mech. 2020.
27. Bolte C, Flood HM, Ren X, Jagannathan S, Barski A, Kalin TV, et al. FOXF1 transcription factor promotes lung regeneration after partial pneumonectomy. Sci Rep. 2017;7(1):10690.
28. Cai Y, Bolte C, Le T, Goda C, Xu Y, Kalin TV, et al. FOXF1 maintains endothelial barrier function and prevents edema after lung injury. Sci Signal. 2016;9(424):ra40.
29. Pradhan A, Dunn A, Ustiyan V, Bolte C, Wang G, Whitsett JA, et al. The S52F FOXF1 Mutation Inhibits STAT3 Signaling and Causes Alveolar Capillary Dysplasia. Am J Respir Crit Care Med. 2019.
30. Sen P, Dharmadhikari AV, Majewski T, Mohammad MA, Kalin TV, Zabielska J, et al. Comparative analyses of lung transcriptomes in patients with alveolar capillary dysplasia with misalignment of pulmonary veins and in foxf1 heterozygous knockout mice. PLoS One. 2014;9(4):e94390.
31. Sturtzel C, Lipnik K, Hofer-Warbinek R, Testori J, Ebner B, Seigner J, et al. FOXF1 Mediates Endothelial Progenitor Functions and Regulates Vascular Sprouting. Front Bioeng Biotechnol. 2018;6:76.
32. Ren X, Ustiyan V, Pradhan A, Cai Y, Havrilak JA, Bolte CS, et al. FOXF1 transcription factor is required for formation of embryonic vasculature by regulating VEGF signaling in endothelial cells. Circ Res. 2014;115(8):709-20.
33. Ustiyan V, Bolte C, Zhang Y, Han L, Xu Y, Yutzey KE, et al. FOXF1 Transcription Factor Promotes Lung Morphogenesis by Inducing Cellular Proliferation in Fetal Lung Mesenchyme. Dev Biol. 2018.
34. Takahashi K, Tanabe K, Ohnuki M, Narita M, Ichisaka T, Tomoda K, et al. Induction of pluripotent stem cells from adult human fibroblasts by defined factors. Cell. 2007;131(5):861-72.
35. Clevers H. Modeling Development and Disease with Organoids. Cell. 2016;165(7):1586-97.
36. Dye BR, Hill DR, Ferguson MA, Tsai YH, Nagy MS, Dyal R, et al. In vitro generation of human pluripotent stem cell derived lung organoids. Elife. 2015;4.
37. Orlova VV, van den Hil FE, Petrus-Reurer S, Drabsch Y, Ten Dijke P, Mummery CL. Generation, expansion and functional analysis of endothelial cells and pericytes derived from human pluripotent stem cells. Nat Protoc. 2014;9(6):1514-31.
38. Kang M, Thebaud B. Stem cell biology and regenerative medicine for neonatal lung diseases. Pediatr Res. 2018;83(1-2):291-7.
39. Martin U. Therapeutic Application of Pluripotent Stem Cells: Challenges and Risks. Front Med (Lausanne). 2017;4:229.
40. Nawroth JC, Barrile R, Conegliano D, van Riet S, Hiemstra PS, Villenave R. Stem cell-based Lung-on-Chips: The best of both worlds? Adv Drug Deliv Rev. 2019;140:12-32.

41. Pollard BS, Pollard HB. Induced pluripotent stem cells for treating cystic fibrosis: State of the science. Pediatr Pulmonol. 2018;53(S3):S12-S29.
42. Slot E, Edel G, Cutz E, van Heijst A, Post M, Schnater M, et al. Alveolar capillary dysplasia with misalignment of the pulmonary veins: clinical, histological, and genetic aspects. Pulm Circ. 2018;8(3):2045894018795143.
43. Slot E, von der Thusen JH, van Heijst A, van Marion R, Magielsen F, Dubbink HJ, et al. Fast detection of FOXF1 variants in patients with alveolar capillary dysplasia with misalignment of pulmonary veins using targeted sequencing. Pediatr Res. 2020.
44. Slot E, de Klein A, Rottier RJ. Generation of three iPSC lines from two patients with heterozygous FOXF1 mutations associated to Alveolar Capillary Dysplasia with Misalignment of the Pulmonary Veins. Stem Cell Res. 2020;44:101745.

CHAPTER 2

ALVEOLAR CAPILLARY DYSPLASIA WITH MISALIGNMENT OF THE PULMONARY VEINS: CLINICAL, HISTOLOGICAL, AND GENETIC ASPECTS

Evelien Slot[1,2], Gabriela Edel[1], Ernest Cutz[3], Arno van Heijst[4], Martin Post[5], Marco Schnater[1], Rene Wijnen[1], Dick Tibboel[1], Robbert Rottier[1] and Annelies de Klein[2]

1. Department of Pediatric Surgery, Sophia Children's Hospital, Erasmus University Medical Center, Rotterdam, The Netherlands
2. Department of Clinical Genetics, Erasmus University Medical Center, Rotterdam, The Netherlands
3. Division of Pathology, Department of Paediatric Laboratory Medicine, Hospital for Sick Children, Toronto, ON, Canada
4. Department of Neonatology, Radboud University Medical Center – Amalia Children's Hospital, Nijmegen, The Netherlands
5. Department of Translational Medicine, Hospital for Sick Children, Toronto, ON, Canada

Published in Pulmonary Circulation, 2018

ABSTRACT

Alveolar capillary dysplasia with misalignment of the pulmonary veins (ACD/MPV) is a rare and lethal disorder mainly involving the vascular development of the lungs. Since its first description, significant achievements in research have led to a better understanding of the underlying molecular mechanism of ACD/MPV and genetic studies have identified associations with genomic alterations in the locus of the transcription factor FOXF1. This in turn has increased the awareness among clinicians resulting in over 200 cases reported so far, including genotyping of patients in most recent reports. Collectively, this promoted a better stratification of the patient group, leading to new perspectives in research on the pathogenesis. Here, we provide an overview of the clinical aspects of ACD/MPV, including guidance for clinicians, and review the ongoing research into the complex molecular mechanism causing this severe lung disorder.

CLINICAL PRESENTATION

The clinical presentation of alveolar capillary dysplasia with misalignment of the pulmonary veins (ACD/MPV) is characterized by respiratory distress and cyanosis caused by severe pulmonary hypertension (PH) and insufficient oxygen uptake.[1–3] Ninety-five percent of ACD/MPV patients are born at full term with normal birth weights and Apgar scores[4,5] and most patients develop symptoms within the first 24 h of life.[1,6,7] In up to 80% of the cases, associated malformations are found for which surgery is occasionally needed.[3,8–14] These malformations predominantly affect the gastrointestinal tract, but also affect the cardiovascular and urogenital system.[2–5,9,15,16] Irrespective of the co-morbidities, the mortality of ACD/MPV is almost 100%. The vast majority succumb to hypoxemic respiratory failure within days to weeks after presentation despite receiving supportive care including extracorporeal membrane oxygenation (ECMO).4,12,17–24 Atypical, milder cases of ACD/MPV patients that present after 24 h of life or survive beyond the neonatal period have sporadically been described and will be discussed in the histology section.

INCIDENCE

Since ACD/MPV was first described in 1981, over 200 cases have been reported.[3,25] In 2000, Al-Hathlol et al. reported two ACD/MPV patients among 226 infants autopsied over a 10-year period in the province of Manitoba, Canada.[4] During these 10 years, the total number of deliveries was 170,000, with 340 infants dying within the neonatal period. It is unclear whether other ACD/MPV cases were among the remaining deceased neonates because an autopsy or biopsy is needed for confirmation. Based on this study, the incidence can be estimated at approximately 1/100,000. In The Netherlands, the incidence can be estimated at 1/200,000 if calculated from the total number of ACD/MPV patients (20) diagnosed in either the Radboudumc Amalia Children's Hospital Nijmegen or the Sophia Children's Hospital Rotterdam since 1993 and the total number of living births during this period (4.3 million[26]). However, also in The Netherlands, it is likely that ACD/MPV is underdiagnosed and sometimes misdiagnosed as idiopathic PH due to the lack of autopsies.

DIAGNOSIS

The current gold standard to unambiguously diagnose ACD/ MPV is histological examination of the lungs. In the majority of studies, most cases were diagnosed postmortem by autopsy.[4,5,27] In one study, 85% of cases were diagnosed premortem by open lung biopsy.[1] In this study, the median time from admission to lung biopsy was 6.5 days. Of neonatal patients who underwent an open lung biopsy during ECMO therapy in the Sophia Children's Hospital Rotterdam or the Radboudumc Amalia Children's Hospital Nijmegen, 32% were diagnosed with ACD/MPV. In all these patients, treatment was withdrawn due to futility. In order to avoid unnecessary and expensive ECMO treatment, it is recommended to perform a lung biopsy before starting ECMO therapy or, if it has been initiated already, within the first week of ECMO.[28] Considering the non-uniformly distribution of lung involve-ment observed in some patients, it is recommended to obtain more than one lung sample to avoid false-negatives. Echocardiography is used to confirm PH and to exclude structural cardiovascular abnormalities.[1,4,7,10,18,19,21,29] An X-ray of the lungs does not show features specific for ACD/MPV, but can show unspecific diffuse haziness or pneumothoraces, most likely caused by mechanical ventila-tion.[4,7,10,18,19,29] A computed tomography (CT) scan may show bilateral widespread ground-glass infiltrates with septal line thickening,[12,21] while a CT angiography does not result in the diagnosis either due to the limitations of imaging most peripheral capillaries of the lung. Photoacoustic imaging, however, is able to perform molecular imaging at a high resolution inside different tissues and therefore overcomes the limitations of a CT angiography. So far, photoacoustic imaging has only been used in bio-medical research settings, but since studies in humans are very promising, it could provide an excellent tool to diagnose ACD/ MPV in the future.[30] During pregnancy, there are no clinical signs associated with ACD/ MPV. However, if there is a high suspicion for ACD/MPV, for instance after an earlier familial case, fetal genetic testing for deletions and mutations in the FOXF1 locus could contribute to an early diagnosis.[16,31] In addition, a decreased total fetal lung volume (FLV) measured by prenatal magnetic resonance imaging (MRI) and ultrasound together with a lowered MRI signal intensity can be used to detect fetal pulmonary hypoplasia associated with multiple diffuse lung developmental disorders among others, including ACD/MPV.[32] An early detection of ACD/MPV allows adequate prenatal counseling regarding the dismal prognosis although the postnatal clinical course must be observed as it differs between patients. Histological examination will be necessary to confirm the diagnosis.

HISTOLOGY

On gross examination, the lungs in cases of ACD/MPV appear bulky with up to a threefold increase in expected weight due to increased interstitial tissue.[33–35] The most significant differences between ACD/MPV and healthy lungs are noted on a microscopic level. In normal lungs, the alveolar capillaries are in close contact with the alveolar epithelium lined by flattened type 1 pneumocytes to provide sufficient gas exchange. In cases of ACD/MPV, the lung tissue is characterized by diffuse thickening of interalveolar septa and marked reduction of pulmonary alveolar capillaries. In addition, these scanty alveolar capillaries are located away from the alveolar epithelium which is predominantly composed of hyperplastic cuboidal type 2 pneumocytes (Fig. 1a).[3–5,33–35]

Typically, in cases of ACD/MPV, the walls of small peripheral pulmonary arteries are thickened due to hypertrophic smooth muscle cells in the media (Fig. 1b). Further, the majority of ACD/MPV patients present with peripheral veins in the bronchovascular bundle adjacent to the pulmonary arteries outside the interlobular septa while normally they are located within the septa. This phenomenon is called "misalignment of the pulmonary veins" (Fig. 1c).

It is postulated that the milder phenotype of atypical ACD/MPV patients, including late presenters and longterm survivors, is correlated with the extent of affected lung tissue.[12,19–21,24,36] Although a few atypical patients with diffuse histological findings similar to the typical patients have been described,[18,22] a very recent study showed a heterogeneous non-uniform distribution of histological findings in all atypical ACD/MPV patients.[36] Nevertheless, correlating the histological features with phenotypical differences between patients remains difficult due to factors such as incomplete autopsy records, varying co-existing malformations, and variations in treatment, especially concerning treatment withdrawal.[5] Either way, when a biopsy is obtained to confirm the diagnosis of ACD/MPV, consideration should be given to the possibility of uneven distribution of lesions. This is especially important if no other life-threatening co-malformations are found and the prognosis is based solely on the severity of lung lesions.

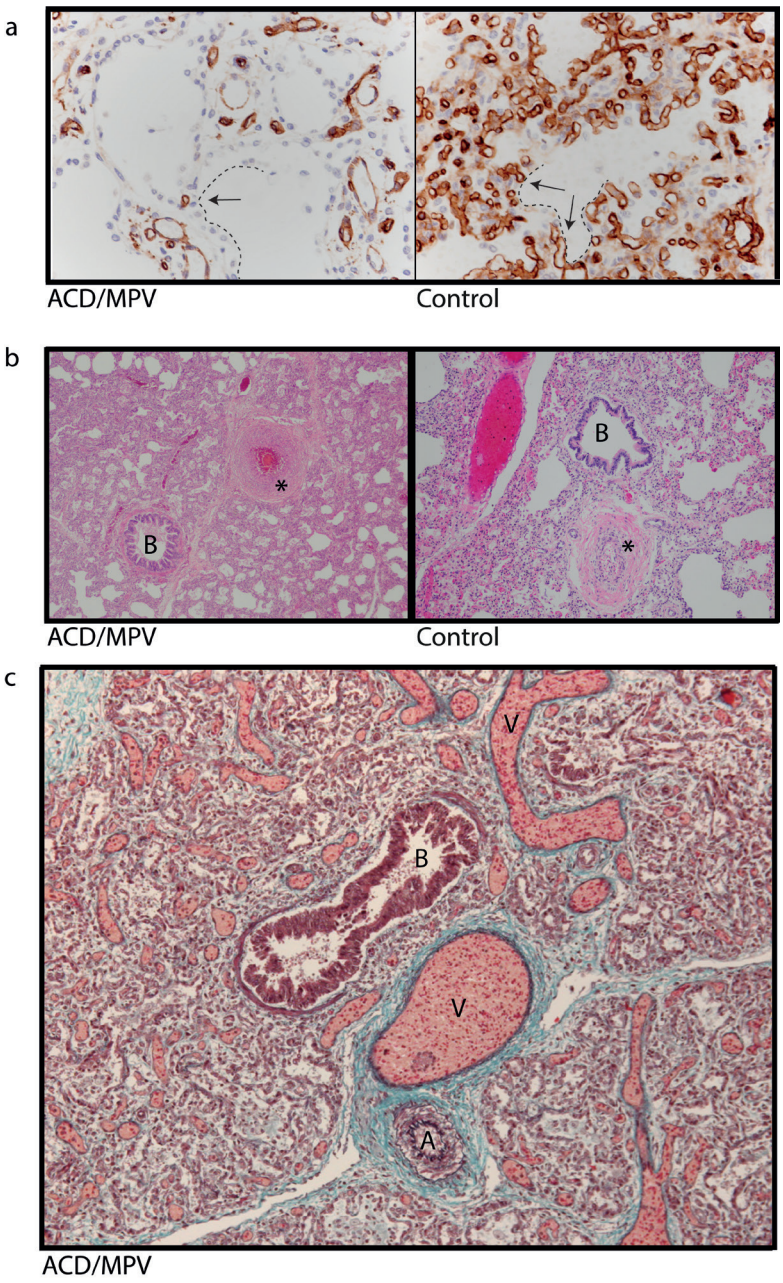

Fig 1. Lung histology of a 2-week-old infant with ACD/MPV. *(a) Immunostaining for CD31 (brown color) highlighting a reduced number of alveolar capillary endothelial cells located away (arrows) from the inner side of the alveoli (dashed lines) in ACD/MPV compared to control lung. (b) Illustration of a hypertrophic arterial wall (*) in hematoxylin and eosin stained lung tissue from an ACD/MPV case compared to control. (c) Illustration of the misaligned pulmonary veins (V) adjacent to the bronchiole (B) and thickened pulmonary arteriole (A) in trichrome stained ACD/MPV lung tissue. Magnifications: (a) 200; (b) 50; (c) 100.*

TREATMENT

Similar to persistent PH of the newborn (PPHN), the clinical approach to ACD/MPV consists of general supportive cardiorespiratory care and vasodilatory agents to reduce PH. In most cases, intubation and mechanical ventilation are immediately required at time of presentation due to the very low oxygen saturation levels. Rarely, only supplemental oxygen is temporarily enough to stabilize the patient before mechanical ventilation is needed.[4,7,10,15,17,20,37] To reduce the pulmonary vascular resistance, inhaled nitric oxide and oral or intravenous vasodilatory agents such as milrinone, sildenafil, or epoprostenol are used. In the short term, this can improve the saturation levels, but literature shows that the dosage needs to be increased repeatedly and that eventually the severe hypoxemia will be fatal.[4,5,7,10,18,20,22,23,37,38] Interestingly, one atypical ACD/MPV patient was still alive on oral vasodilators and supple-mental oxygen at the age of 38 months when the case report was written.[21]

ECMO therapy can be used to stabilize infants in life-threatening conditions if the diagnosis is not clear. Yet, the vast majority of ACD/MPV patients cannot be weaned from ECMO, while ECMO itself is invasive, comes with risks of complications, and is expensive.[1,4,7,8,19,23,28,29,37] Ideally, an open lung biopsy is performed before ECMO therapy has started or at least before a "second-run" ECMO therapy is considered.[7,14,27,28] On the other hand, ECMO therapy can provide an excellent bridge to lung transplantation in ACD/MPV patients with a mild pheno-type.[12,36] To date, seven ACD/MPV patients receiving bilateral lung transplantation have been reported in the United States with a comparable five-year survival (56%) to infants transplanted for other indications at the St. Louis Children's Hospital, Missouri.[36,39] All of the transplanted ACD/MPV patients had an atypical milder phenotype than the classical ACD/MPV patients.[12,36,40] Although the overall survival in this young age group is still disappointing, ECMO therapy followed by lung transplantation is the potential treatment of choice for selected ACD/MPV patients.[36,41–43]

PATHOGENESIS

Although the pathogenesis of ACD/MPV has not yet been fully defined, several hypotheses implicating various factors and events have been proposed. It is thought that ACD/ MPV is caused by an early disturbance in embryonic lung development. Already at the end of the embryonic phase of lung development (five weeks of gestation), the

two lung buds are surrounded by a vascular network that is connected to the systemic circulation. During the pseudoglandular phase (5–16 weeks of gestation), this network expands by angiogenesis when the two buds branch into the loose mesenchymal tissue. In the canalicular and saccular stage (16–26 and 26–38 weeks of gestation, respectively), expansion of the network continues, increasing the capillary dens-ity in the developing lung.[44,45] The deficiency of capillaries in ACD/MPV lung tissue implies a disturbance already in the early embryonic and pseudoglandular phase. The presence of thickened septa and simplified acini with a reduced number of type 1 pneumocytes in ACD/MPV lungs indicate that also the saccular stage is affected, in which normally the alveolar saccules are formed with thin septa covered by type 1 pneumocytes.[35,46,47]

The cause of PH in ACD/MPV is still a topic of discussion. It was suggested that chronic hypoxemia in the new-born induces hypertrophic arterial changes which cause PH.[35,38] However, this seems unlikely because the extent of arterial changes in ACD/MPV newborns would imply the presence of hypoxemia already during early fetal life when the oxygen is still provided by the placenta. Moreover, this theory is inconsistent with the poor outcome of ACD/MPV patients despite mechanical ventilation or ECMO therapy which diminishes the hypoxemia. Another, more acceptable, theory is that the PH results from a marked reduction in the alveolar capillary bed.[18,33] However, abrupt deterioration in late presenters without any signs of PH during the time before deterioration questions this theory as well.[4,18,23,33,34] Collectively, the progressive PH combined with structural histological changes in all ACD/MPV patients suggests a disturbance in normal pulmonary vascular development and is currently the subject of several studies in different laboratories.

The origin of the “misaligned pulmonary veins” found in peripheral ACD/MPV lung tissue, and whether they are indeed malpositioned, is not clear. Considering the presence of valves, it is more likely that the anomalous veins originate from bronchial veins that normally do not extend beyond the larger bronchopulmonary branches.[33–35] This theory is supported by a study showing “misaligned pulmonary veins” originating from bronchial veins and act as shunt vessels between the bronchial and pulmonary veins.[48]

ROLE OF FOXF1 IN ACD/MPV

In 2009, Stanckiewizc and Shaw-Smith suggested an association between ACD/MPV and haploinsufficiency of the Forkhead Box F1 (*FOXF1*) gene.[2] Since then, they have accumulated the largest ACD/MPV sample collection of 141 patients in which they identified 86 pathogenic variants containing copy number variations (CNVs), point mutations, and one complex rearrangement, all involving the *FOXF1* gene or its regulatory region.[49] This regulatory region was identified by defining the shortest region of overlapping genomic deletions in ACD/MPV patients.[50,51] The remaining 55 cases were not genetically tested due to insufficient DNA quality.[49] Additionally, a variety of heterozygous genomic variants in the *FOXF1* locus of ACD/MPV patients have been reported by other research groups.[8,16,20] Most of the variants are collected in the Leiden Open Variation Database (LOVD).[52]

FOXF1, first described by Pierrou et al. in 1994, is a member of the Forkhead box transcription factors (TFs) and plays a role during embryonic development, specifically in lung development.[53] Studies in rodent embryos show that FOXF1 is already expressed at the primitive streak stage in the mesodermal lateral plate and continues to be expressed during development in mesenchymal lung tissue.[54–58] Very little is known about FOXF1 expression during human lung development, but in newborns FOXF1 is expressed in mesenchymal stromal cells from tracheal aspirates.[59] FOXF1 is regulated by Sonic hedgehog (SHH) signaling, one of the key regulators of embryonic development.[60] Further research on the signaling pathways involving FOXF1 is ongoing. A recent study showed that the serotonin transporter (SERT) protein, important during pulmonary vascular remodeling and adaptation at birth, might be one of the downstream targets of FOXF1 as the expression of SERT protein was completely absent in ACD/MPV patients while expression levels in other disorders causing PH in the newborn were normal.[61] Although rodent models enable us to study the function of FOXF1 during lung development, the phenotype of heterozygous *Foxf1* mice does not completely correlate with ACD/MPV. Similar to ACD/MPV, heterozygous deletion of FoxF1 gives rise to multiple foregut and lung defects including lobular and alveolar underdevelopment, compact lung mesenchyme, and hemorrhagic lesions. However, the pulmonary branching defects dominate in these models while the main problem in ACD/MPV is the underdeveloped pulmonary vascularization.[62] These differences illustrate the difficulties of studying the pathogenesis of ACD/MPV.

IMPRINTING OF FOXF1

The question why a heterozygous genomic alteration in the *FOXF1* gene or its regulatory region causes haploinsufficiency and results in ACD/MPV is still unanswered. The most suggested and studied explanation is parental imprinting where epigenetic marks determine if a particular gene is only expressed on the paternal or maternal allele.[2,50,54,63]

Assuming this hypothesis is true, all genomic alterations associated with ACD/MPV would be located on the same parental chromosome. Indeed, all but one of the deletions located in the regulatory region did arise on the maternal chromosome. However, mutations located in the FOXF1 transcription region are found on both paternal and maternal alleles. Still, this might implicate parental imprinting of the regulatory region instead of the transcription region itself.[49] Unfortunately, detailed studies on imprinting of the FOXF1 locus in fetal, neonatal, and adult lung tissue have not been able to confirm this idea.[50,64]

PHENOTYPICAL DIFFERENCES OF ACD/MPV

Although earlier studies suggested a high correlation between ACD/MPV and genomic alterations in the *FOXF1* locus, familial cases show large phenotypical differences and, again, illustrate the complexity of the molecular mechanisms causing ACD/MPV. In total, eight ACD/MPV families with associated genomic variants in the *FOXF1* transcription region have been reported so far (Fig. 2; Table 1).[49,63,65,66] In six of these families, the pathogenic variant was also found in one of the parents including two fathers who were mosaic. None of those parents exhibited signs of ACD/MPV. The phenotypical variance is also illustrated by family 6 (Fig. 2) that was previously described by Reiter et al.[66] In this family, two children were affected by ACD/MPV but only one of them showed classical features of ACD/MPV. The other child presented with an atypical form and survived. Interestingly, another sister carried the same mutation but was unaffected.[49,66] The genotype– phenotype variation might be associated with altered FOXF1 expression levels, similar to *Foxf1* heterozygote knock-out mice that show variation in the phenotype severity correlated to *Foxf1* expression levels.[58] Different expression levels can be the result of so-called "modifier genes" that modify the expression of the *FOXF1* gene. In combination with mutations or deletions in the *FOXF1* locus, alterations in these modifier genes might lead to ACD/MPV. This idea is supported by the finding that the survival of heterozygous *Foxf1* knock-out mice depends on their genetic background.[62]

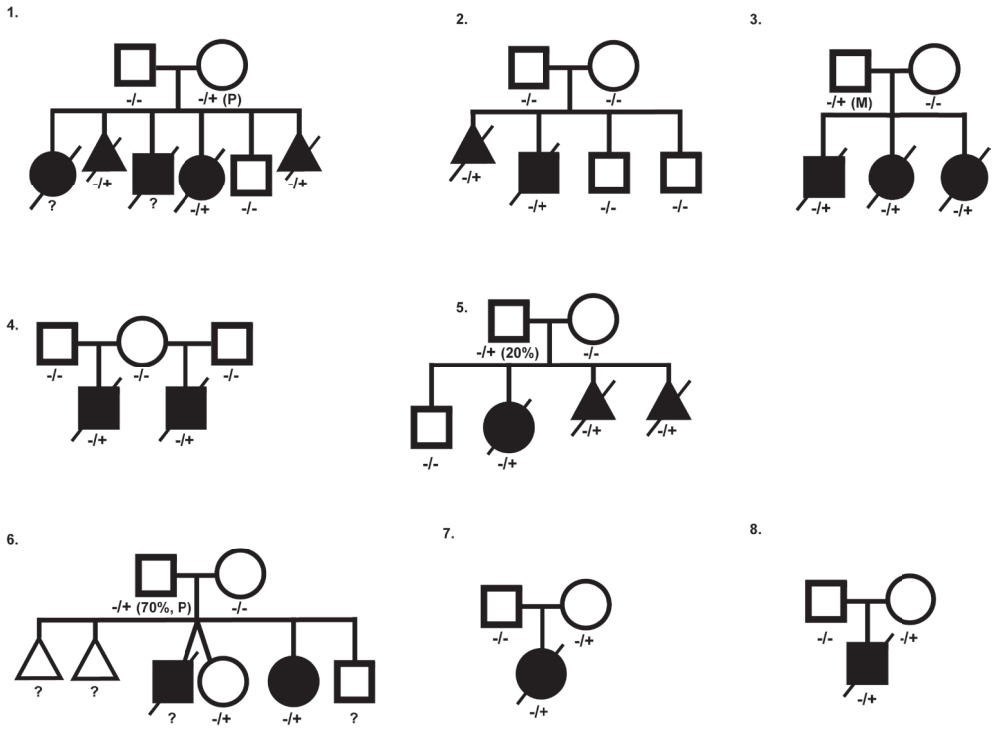

Fig. 2. Pedigrees of published ACD/MPV families corresponding to Table 1, illustrating the complex inheritance pattern. *Filled square or circle=affected male or female; open square or circle=unaffected male or female; crossed out=deceased; open triangle=spontaneous abortion; crossed-out filled triangle=terminated pregnancy. -/+, presence of heterozygous variant in the FOXF1 gene; -/-, no variant in FOXF1 gene present; P, variant located on paternal allele; M, variant located on maternal allele.*

Table 1. Overview of published ACD/MPV families with genomic alterations in the *FOXF1* gene.

Family number (Fig. 2)	Genomic alteration (all located in first *FOXF1* exon)	Protein change	Inheritance	Parental inheritance	Reference
1	c.416G > T	Arg139Leu	Maternal	De novo paternal allele	Sen et al., 2013
2	c.253T >A	Phe85Ile	Not found in parental DNA: germline mosaicism?	—	Sen et al., 2013
3	Insertion 5 UTR side	Unknown	Paternal	De novo maternal allele	Szafranski et al., 2016
4	c.849_850del	p.Ile285fs	Not found in parental DNA: maternal germline mosaicism?	—	Szafranski et al., 2016

Family number (Fig. 2)	Genomic alteration (all located in first *FOXF1* exon)	Protein change	Inheritance	Parental inheritance	Reference
5	c90_96del	p.Ser31fs	Paternal; 20% mosaicism in blood nucleated cells	De novo, allele unknown	Szafranski et al., 2016
6	c.231C > A	p.Phe77Leu	Paternal; 70% mosaicism in blood nucleated cells	De novo paternal allele	Reiter et al., 2016
7	c.253T > C	p.Phe85Leu	Maternal	Unknown	Sen et al., 2013
8	c.294C > A	p.His98Gln	Maternalw	Unknown	Sen et al., 2013

SUMMARY

ACD/MPV is a rare, almost uniformly lethal, developmental disorder of the lungs. Patients suffer from severe hypoxemia and PH that progresses over time. Although the awareness of ACD/MPV is growing among clinicians, it can be confused with idiopathic PH as the clinical picture is similar. This prolongs the time to confirm the diagnosis and contributes to unnecessary suffering of patients and a high cost of therapy. As soon as the response to medical treatment deviates from the expected, a histological examination should be performed. Moreover, an open lung biopsy is ideally performed before ECMO therapy or surgical interventions for co-occurring anomalies are initiated. For a very small selection of atypical ACD/MPV patients, a lung transplantation can be considered although survival rates are still disappointing. ACD/MPV is associated with haploinsufficiency of FOXF1, a TF regulated by SHH that plays a significant role during early lung development. Although phenotypical differences are present, prenatal or postnatal genetic testing could contribute to earlier detection and allows adequate consultation about the prognosis and the process of decision-making.

REFERENCES

1. Eulmesekian P, Cutz E, Parvez B, et al. Alveolar capillary dys-plasia: a six-year single center experience. J Perinat Med 2005; 33: 347–352.
2. Stankiewicz P, Sen P, Bhatt SS, et al. Genomic and genic dele-tions of the FOX gene cluster on 16q24.1 and inactivating muta-tions of FOXF1 cause alveolar capillary dysplasia and other malformations. Am J Hum Genet 2009; 84: 780–791.
3. Bishop NB, Stankiewicz P and Steinhorn RH. Alveolar capil-lary dysplasia. Am J Respir Crit Care Med 2011; 184: 172–179.
4. Al-Hathlol K, Phillips S, Seshia MK, et al. Alveolar capillary dysplasia. Report of a case of prolonged life without extracorporeal membrane oxygenation (ECMO) and review of the literature. Early Hum Dev 2000; 57: 85–94.
5. Sen P, Thakur N, Stockton DW, et al. Expanding the pheno-type of alveolar capillary dysplasia (ACD). J Pediatr 2004; 145: 646-65.
6. Al-Hathlol K, Idiong N, Hussain A, et al. A study of breathing pattern and ventilation in newborn infants and adult subjects. Acta Paediatr 2000; 89: 1420–1425.
7. Michalsky MP, Arca MJ, Groenman F, et al. Alveolar capil-lary dysplasia: a logical approach to a fatal disease. J Pediatr Surg 2005; 40: 1100–1105.
8. Ma Y, Jang MA, Yoo HS, et al. A novel de novo pathogenic variant in FOXF1 in a newborn with alveolar capillary dys-plasia with misalignment of pulmonary veins. Yonsei Med J 2017; 58: 672–675.
9. Arreo Del Val V, Avila-Alvarez A, Schteffer LR, et al. Alveolar capillary dysplasia with misalignment of the pulmon-ary veins associated with aortic coarctation and intestinal mal-rotation. J Perinatol 2014; 34: 795–797.
10. Miranda J, Rocha G, Soares H, et al. Alveolar capillary dys-plasia with misalignment of pulmonary veins (ACD/MPV): a case series. Case Rep Crit Care 2013; 2013: 327250.
11. Rabah R and Poulik JM. Congenital alveolar capillary dyspla-sia with misalignment of pulmonary veins associated with hypoplastic left heart syndrome. Pediatr Dev Pathol 2001; 4: 167–174.
12. Szafranski P, Dharmadhikari AV, Wambach JA, et al. Two deletions overlapping a distant FOXF1 enhancer unravel the role of lncRNA LINC01081 in etiology of alveolar capillary dysplasia with misalignment of pulmonary veins. Am J Med Genet A 2014; 164A: 2013–2019.
13. Garola RE and Thibeault DW. Alveolar capillary dysplasia, with and without misalignment of pulmonary veins: an asso-ciation of congenital anomalies. Am J Perinatol 1998; 15: 103–107
14. Gerrits LC, De Mol AC, Bulten J, et al. Omphalocele and alveolar capillary dysplasia: a new association. Pediatr Crit Care Med 2010; 11: e36–37.
15. Antao B, Samuel M, Kiely E, et al. Congenital alveolar capil-lary dysplasia and associated gastrointestinal anomalies. Fetal Pediatr Pathol 2006; 25: 137–145.
16. Prothro SL, Plosa E, Markham M, et al. Prenatal diagnosis of alveolar capillary dysplasia with misalignment of pulmonary veins. J Pediatr 2016; 170: 317–318.
17. Abdallah HI, Karmazin N and Marks LA. Late presentation of misalignment of lung vessels with alveolar capillary dyspla-sia. Crit Care Med 1993; 21: 628–630.
18. Ahmed S, Ackerman V, Faught P, et al. Profound hypoxemia and pulmonary hypertension in a 7-month-old infant: late presentation of alveolar capillary dysplasia. Pediatr Crit Care Med 2008; 9: e43–46
19. Boggs S, Harris MC, Hoffman DJ, et al. Misalignment of pul-monary veins with alveolar capillary dysplasia: affected sib-lings and variable phenotypic expression. J Pediatr 1994; 125–128
20. Goel D, Oei JL, Lui K, et al. Antenatal gastrointestinal anomalies in neonates subsequently found to have alveolar capillary dysplasia. Clin Case Rep 2017; 5: 559–566.
21. Ito Y, Akimoto T, Cho K, et al. A late presenter and long-term survivor of alveolar capillary dysplasia with misalignment of the pulmonary veins. Eur J Pediatr 2015; 174: 1123–112.

22. Kodama Y, Tao K, Ishida F, et al. Long survival of congenital alveolar capillary dysplasia patient with NO inhalation and epoprostenol: effect of sildenafil, beraprost and bosentan. Pediatr Int 2012; 54: 923–926.
23. Shankar V, Haque A, Johnson J and Pietsch J. Late presenta-tion of alveolar capillary dysplasia in an infant. Pediatr Crit Care Med 2006; 7: 177–179.
24. Oldenburg J, Van Der Pal HJ, Schrevel LS, et al. Misalignment of lung vessels and alveolar capillary dysplasia. Histopathology 1995; 27: 192–194.
25. Janney CG, Askin FB and Kuhn C 3rd. Congenital alveolar capillary dysplasia–an unusual cause of respiratory distress in the newborn. Am J Clin Pathol 1981; 76: 722–727.
26. Central Bureau for Statistics. (2018, June 5). Statistics Netherlands: Birth; key figures. Retrieved from http://stat-line.cbs.nl/Statweb/publication/?DM¼SLEN&PA¼37422eng&D1¼0,3-27,32-39,48-51,53-54&D2¼0,5,10,15,20,25,30,35,43-66&LA¼EN&HDR¼T&STB¼G1&VW¼T
27. Inwald D, Brown K, Gensini F, et al. Open lung biopsy in neonatal and paediatric patients referred for extracorporeal membrane oxygenation (ECMO). Thorax 2004; 59: 328–333.
28. Houmes RJ, Ten Kate CA, Wildschut ED, et al. Risk and relevance of open lung biopsy in pediatric ECMO patients: the Dutch experience. J Pediatr Surg 2017; 52: 405–409.
29. Ng PC, Lewindon PJ, Siu YK, et al. Congenital misalignment of pulmonary vessels: an unusual syndrome associated with PPHN. Acta Paediatr 1995; 84: 349–353.
30. Zackrisson S, van de Ven S and Gambhir SS. Light in and sound out: emerging translational strategies for photoacoustic imaging. Cancer Res 2014; 74: 979–1004.
31. Parris T, Nik AM, Kotecha S, et al. Inversion upstream of FOXF1 in a case of lethal alveolar capillary dysplasia with misalignment of pulmonary veins. Am J Med Genet A 2013; 161A: 764–770.
32. Zirpoli S, Munari AM, Rustico M, et al. Fetal-MRI prenatal diagnosis of severe bilateral lung hypoplasia: alveolar capillary dysplasia case report. J Prenat Med 2016; 10: 15–19.
33. Cullinane C, Cox PN and Silver MM. Persistent pulmonary hypertension of the newborn due to alveolar capillary dysplasia. Pediatr Pathol 1992; 12: 499–514.
34. Sirkin W, O'Hare BP, Cox PN, et al. Alveolar capillary dys-plasia: lung biopsy diagnosis, nitric oxide responsiveness, and bronchial generation count. Pediatr Pathol Lab Med 1997; 17: 125–132.
35. Haraida S, Lochbuhler H, Heger A, et al. Congenital alveolar capillary dysplasia: rare cause of persistent pulmonary hypertension. Pediatr Pathol Lab Med 1997; 17: 959–975.
36. Towe CT, White FV, Grady RM, et al. Infants with atypical presentations of alveolar capillary dysplasia with misalignment of the pulmonary veins who underwent bilateral lung trans-plantation. J Pediatr 2018; 194: 158–164.
37. Castilla-Fernandez Y, Copons-Fernandez C, Jordan-Lucas R, et al. Alveolar capillary dysplasia with misalignment of pul-monary [corrected] veins: concordance between pathological and molecular diagnosis. J Perinatol 2013; 33: 401–403.
38. Steinhorn RH, Cox PN, Fineman JR, et al. Inhaled nitric oxide enhances oxygenation but not survival in infants with alveolar capillary dysplasia. J Pediatr 1997; 130: 417–422.
39. Eldridge WB, Zhang Q, Faro A, et al. Outcomes of lung trans-plantation for infants and children with genetic disorders of surfactant metabolism. J Pediatr 2017; 184: 157–164.
40. Boston US, Fehr J, Gazit AZ, et al. Paracorporeal lung assist device: an innovative surgical strategy for bridging to lung transplant in an infant with severe pulmonary hypertension caused by alveolar capillary dysplasia. J Thorac Cardiovasc Surg 2013; 146: e42–43.
41. Khan MS, Heinle JS, Samayoa AX, et al. Is lung transplant-ation survival better in infants? Analysis of over 80 infants. J Heart Lung Transplant 2013; 32: 44–49.
42. Benden C, Edwards LB, Kucheryavaya AY, et al. The Registry of the International Society for Heart and Lung Transplantation: Sixteenth Official Pediatric Lung and Heart-Lung Transplantation Report–2013; focus theme: age. J Heart Lung Transplant 2013; 32: 989–997.

43. Hayes D Jr., Naguib A, Kirkby S, et al. Comprehensive evalu-ation of lung allograft function in infants after lung and heart-lung transplantation. J Heart Lung Transplant 2014; 33: 507–513.
44. Parera MC, van Dooren M, van Kempen M, et al. Distal angiogenesis: a new concept for lung vascular morphogenesis. Am J Physiol Lung Cell Mol Physiol 2005; 288: L141–149.
45. Schachtner SK, Wang Y and Scott Baldwin H. Qualitative and quantitative analysis of embryonic pulmonary vessel forma-tion. Am J Respir Cell Mol Biol 2000; 22: 157–165.
46. Ameis D, Khoshgoo N and Keijzer R. Abnormal lung devel-opment in congenital diaphragmatic hernia. Semin Pediatr Surg 2017; 26: 123–128.
47. Schittny JC. Development of the lung. Cell Tissue Res 2017; 367: 427–444.
48. Galambos C, Sims-Lucas S, Ali N, et al. Intrapulmonary vas-cular shunt pathways in alveolar capillary dysplasia with mis-alignment of pulmonary veins. Thorax 2015; 70: 84–85.
49. Szafranski P, Gambin T, Dharmadhikari AV, et al. Pathogenetics of alveolar capillary dysplasia with misalign-ment of pulmonary veins. Hum Genet 2016; 135: 569–586.
50. Szafranski P, Dharmadhikari AV, Brosens E, et al. Small non-coding differentially methylated copy-number variants, includ-ing lncRNA genes, cause a lethal lung developmental disorder. Genome Res 2013; 23: 23–33.
51. Szafranski P, Herrera C, Proe LA, et al. Narrowing the FOXF1 distant enhancer region on 16q24.1 critical for ACDMPV. Clin Epigenetics 2016; 8: 112.
52. Fokkema IF, Taschner PE, Schaafsma GC, et al. LOVD v.2.0: the next generation in gene variant databases. Hum Mutat 2011; 32: 557–563.
53. Pierrou S, Hellqvist M, Samuelsson L, et al. Cloning and char-acterization of seven human forkhead proteins: binding site specificity and DNA bending. EMBO J 1994; 13: 5002–5012.
54. Dharmadhikari AV, Szafranski P, Kalinichenko VV, et al. Genomic and epigenetic complexity of the FOXF1 locus in 16q24.1: implications for development and disease. Curr Genomics 2015; 16: 107–116.
55. Mahlapuu M, Pelto-Huikko M, Aitola M, et al. FREAC-1 contains a cell-type-specific transcriptional activation domain and is expressed in epithelial-mesenchymal interfaces. Dev Biol 1998; 202: 183–195.
56. Peterson RS, Lim L, Ye H, et al. The winged helix transcrip-tional activator HFH-8 is expressed in the mesoderm of the primitive streak stage of mouse embryos and its cellular deriva-tives. Mech Dev 1997; 69: 53–69.
57. Mahlapuu M, Ormestad M, Enerback S, et al. The forkhead transcription factor Foxf1 is required for differentiation of extra-embryonic and lateral plate mesoderm. Development 2001; 128: 155–166.
58. Kalinichenko VV, Lim L, Stolz DB, et al. Defects in pulmon-ary vasculature and perinatal lung hemorrhage in mice hetero-zygous null for the Forkhead Box f1 transcription factor. Dev Biol 2001; 235: 489–506.
59. Bozyk PD, Popova AP, Bentley JK, et al. Mesenchymal stro-mal cells from neonatal tracheal aspirates demonstrate a pat-tern of lung-specific gene expression. Stem Cells Dev 2011; 20: 1995–2007.
60. Ormestad M, Astorga J, Landgren H, et al. Foxf1 and Foxf2 control murine gut development by limiting mesenchymal Wnt signaling and promoting extracellular matrix production. Development 2006; 133: 833–843.
61. Castro EC, Sen P, Parks WT, et al. The role of serotonin transporter in human lung development and in neonatal lung disorders. Can Respir J 2017; 2017: 9064046.
62. Mahlapuu M, Enerback S and Carlsson P. Haploinsufficiency of the forkhead gene Foxf1, a target for sonic hedgehog signaling, causes lung and foregut malformations. Development 2001; 128: 2397–2406.
63. Sen P, Gerychova R, Janku P, et al. A familial case of alveolar capillary dysplasia with misalignment of pulmonary veins sup-ports paternal imprinting of FOXF1 in human. Eur J Hum Genet 2013; 21: 474–477.
64. Alsina Casanova M, Monteagudo-Sanchez A, Rodiguez Guerineau L, et al. Maternal mutations of FOXF1 cause alveolar capillary dysplasia despite not being imprinted. Hum Mutat 2017; 38: 615–620.

65. Sen P, Yang Y, Navarro C, et al. Novel FOXF1 mutations in sporadic and familial cases of alveolar capillary dysplasia with misaligned pulmonary veins imply a role for its DNA binding domain. Hum Mutat 2013; 34: 801–811.
66. Reiter J, Szafranski P, Breuer O, et al. Variable phenotypic presentation of a novel FOXF1 missense mutation in a single family. Pediatr Pulmonol 2016; 51: 921–927.

CHAPTER 3

FAST DETECTION OF *FOXF1* VARIANTS IN PATIENTS WITH ALVEOLAR CAPILLARY DYSPLASIA WITH MISALIGNMENT OF PULMONARY VEINS USING TARGETED SEQUENCING

Evelien Slot[1,2], Jan H. von der Thüsen[3], Arno van Heijst[4], Ronald van Marion[3], Frank Magielsen[1], Hendrikus J. Dubbink[3], Martin Post[5], Anne Debeer[6], Dick Tibboel[2], Robbert J. Rottier[2], Annelies de Klein[1]*

1. Department of Clinical Genetics, Erasmus University Medical Center, Rotterdam, The Netherlands
2. Department of Pediatric Surgery, Sophia Children's Hospital, Erasmus University Medical Center, Rotterdam, The Netherlands
3. Department of Pathology, Erasmus University Medical Center, Rotterdam, The Netherlands
4. Department of Neonatology, Radboud University Medical Center-Amalia Children's Hospital, Nijmegen, The Netherlands
5. Department of Translational Medicine, Hospital for Sick Children, Toronto, ON, Canada
6. Department of Neonatology, University Hospitals Leuven, Leuven, Belgium

Published in Pediatric Research, 2020

ABSTRACT

Background

Alveolar capillary dysplasia with misalignment of pulmonary veins (ACD/MPV) is a lethal congenital lung disorder associated with heterozygous variants in the *FOXF1* gene or its regulatory region. Patients with ACD/MPV unnecessarily undergo invasive and expensive treatments while awaiting a diagnosis. The aim of this study was to reduce the time to diagnose ACD/MPV by developing a targeted next generation sequencing (NGS) panel that detects *FOXF1* variants.

Methods

A *FOXF1*-targeted NGS panel was developed for detection of mutations and large genomic alterations and used for retrospective testing of ACD/MPV patients and controls. Results were confirmed with Sanger sequencing and SNP array analysis.

Results

Each amplicon of the *FOXF1*-targeted NGS panel was efficiently sequenced using DNA isolated from blood or cell lines of 15 ACD/MPV patients and 8 controls. Moreover, testing of ACD/MPV patients revealed 6 novel and 6 previously described pathogenic or likely pathogenic *FOXF1* alterations.

Conclusion

We successfully designed a fast and reliable targeted genetic test to detect variants in the *FOXF1* gene and its regulatory region in one run. This relatively non-invasive test potentially prevents unnecessary suffering for patients and reduces the use of futile and expensive treatments like extra-corporeal membrane oxygenation.

INTRODUCTION

Patients with alveolar capillary dysplasia with misalignment of pulmonary veins (ACD/MPV) unnecessarily undergo invasive and expensive treatments while awaiting a diagnosis. Patients with this rare and lethal congenital lung disorder usually present shortly after birth with respiratory distress caused by therapy resistant pulmonary hypertension (PH) and insufficient oxygen uptake. In addition, 80% of the patients suffer from malformations in the gastrointestinal, urogenital or cardiovascular system (1). Currently, ACD/MPV can only be confirmed by histological examination of the lung, which is characterized by alveolar septal thickening, reduced numbers of alveolar capillaries, peripheral arterial wall hypertrophy and, in most patients, misaligned pulmonary veins (MPV) (1, 2). Although most neonatologists and pediatric pulmonologists are aware of this disorder, ACD/MPV is not always recognized timely and patients receive multiple futile therapies directed at the PH such as antihypertensive pharmacotherapy and extra-corporeal membrane oxygenation (ECMO). If necessary, additional surgeries are carried out for co-malformations. Due to the risks of an open lung biopsy, especially during anticoagulation while on ECMO, it takes several days to weeks before the decision is made to take a biopsy. Moreover, retrospective studies have shown that most patients are diagnosed post-mortem by autopsy (1, 3-5) and there is a high probability that many patients are not diagnosed at all. While histology is the gold standard for diagnosis of ACD/MPV, increased availability of non-invasive genetic testing makes it possible to obtain a genetic diagnosis in infants with respiratory failure and severe pulmonary hypertension, especially in the setting of congenital anomalies. To minimize the unnecessary suffering for both patients and parents, as well as reducing the use of ineffective, expensive and futile therapies, this study was aimed at developing a fast and specific genetic test to shorten the time between hospitalization and diagnosing ACD/MPV.

ACD/MPV is primarily caused by haploinsufficiency of Forkhead Box F1 (*FOXF1*) , which is a transcription factor that plays a role in early embryonic lung development (6, 7). Genomic alterations detected in ACD/MPV patients are either point mutations or indels in the *FOXF1* gene or large copy number variations (CNVs) involving the gene or its 60-kilobase pair (kb) regulatory region (7-10). Therefore, genetic testing of ACD/MPV patients requires a combination of Sanger sequencing with SNP array or array comparative genomic hybridization (aCGH). To detect the different ACD/MPV variants in one run, whole genome

sequencing (WGS) can be used. However, this technique is expensive and provides an excessive amount of information about the whole genome which takes a long time to be analyzed and might lead to incidental findings. Furthermore, whole exome sequencing (WES) is not sufficient to detect CNVs in the regulatory region and the same applies to the available NGS panels that include the *FOXF1* gene (11). In this study, we present a new targeted next generation sequencing (NGS) panel to identify variants associated to ACD/MPV in one run. This testing method is fast, cost-effective and prevents unwanted incidental findings in other regions of the genome. Further, by routine testing of DNA samples from ACD/MPV patients, new genomic alterations involving the *FOXF1* locus could be identified which contributes to the knowledge on the complex pathogenesis of ACD/MPV.

METHODS

Sample collection

Blood samples, cell lines and formalin-fixed and paraffin-embedded lung tissues of patients with histologically confirmed ACD/MPV were collected from the Sophia Children's Hospital - Erasmus University Medical Center Rotterdam, the Radboudumc Amalia Children's Hospital Nijmegen, the VU University Medical Center Amsterdam, the Hospital for Sick Children Toronto, the University Hospitals Leuven and the Charles University and General University Hospital in Prague. Blood samples of age-matched controls without ACD/MPV were collected from the Sophia Children's Hospital - Erasmus University Medical Center Rotterdam. In this study, we only used bodily material that was previously obtained for diagnostic purposes. All samples were anonymized before genetic testing was performed. Before the start of the study, the research proposal was reviewed and approved by the Daily Board of the Medical Ethics Committee (METC) Erasmus University Medical Center Rotterdam, The Netherlands.

NGS with the ACD/MPV panel

A specific ACD/MPV panel was designed with the Ion Ampliseq Designer 6.0 (ThermoFisher Scientific, Waltham, MA, USA) and included 157 amplicons targeted at the *FOXF1* gene and its regulatory region. To enable detection of copy number variations (CNVs), 119

amplicons were designed to cover selected single nucleotide polymorphisms (SNPs) with a minor allele frequency (MAF) above 0.4 (12). The majority of these 119 SNPs were selected in and around the *FOXF1* gene and its regulatory region, with a distance of 50 to 500 base pairs (bp) between the SNPs. The other SNPs were located across the remaining parts of chromosome 16 with a distance of approximately two to four Megabase pairs (Mb). For the detection of single nucleotide substitutions and small deletions or duplications in the *FOXF1* gene, 38 overlapping amplicons were designed that together cover the *FOXF1* gene. The final library was constructed with the AmpliSeq Library Kit 2.0 (ThermoFisher Scientific), according to the manufacturer's instructions. The sequences and coverages were analyzed with the Ion S5 XL Sequencing System and the Torrent Suite Software v5.6 (ThermoFisher Scientific) as described previously (13). Due to the high GC-content, the first 6 bp at the start of exon 1 could not be covered by amplicons, as well as a 187 bp strech in the 3' untranslated region (UTR). These regions were additionally sequenced with Sanger sequencing.

Staining

The pathologists affiliated to the providing hospitals confirmed ACD/MPV by histological examination of lung tissue at the time of diagnosis. To review the diagnosis of patients without *FOXF1* alterations, an additional immunohistochemical staining was performed with hematoxylin-eosin (HE) and CD31 (JC70 clone) (Cell Marque, Rocklin, CA, USA) at the Department of Pathology of the Erasmus Medical Center. The staining was performed with ready-to-use antibodies on a Benchmark Ultra system, using an Ultraview Dab kit for visualization (all from Ventana Medical Systems, Oro Vally, AZ, USA).

DNA isolation

To isolate DNA from skin fibroblasts or FFPE lung tissues, the QIAamp DNA Mini Kit (Qiagen, Hilden, Germany) was used according to the manufacturer's instructions. For DNA isolation from FFPE lung tissue, 8-10 sections of 10µm were pre-treated with xylene to remove the paraffin and with sodium thiocyanate to permeabilize the tissue. To isolate DNA from blood, the Chemagic DNA Blood Kit special (PerkinElmer chemagen Technology, Baesweiler, Germany), the Gentra Puregene Blood Kit (Qiagen) or the 'Salting out' method (14) was used. DNA concentrations were measured with the Quant-iT Picogreen assay kit (ThermoFisher Scientific) according the manufacturer's instructions.

Variant analysis

Single nucleotide substitutions, small deletions and small duplications were identified with the Variant Caller v5.6 plugins (ThermoFisher Scientific) and summarized in Variant Caller Files. Variants were notated as potential disease causing variants if they were present in more than 30% of the sequencing reads and located in one of the exons, the 3' UTR or the 5' UTR. Variants were excluded if they have been reported with an MAF above 1% in the *1000 Genomes-, UCSC common SNP 151-, ExAc-, GONL-, ESP-, gnomAD-* or *SwissProt Variants* databases. Additionally, the *FOXF1* gene was manually checked for variants with the Integrative Genomic Viewer (15). Variants were described as recommended by the Human Genome Variation Society (16) and classified according to the guidelines of the American College of Medical Genetics and Genomics (17). For classification, the following in silico prediction algorithms were used: PolyPhen-2, MutationTaster, SIFT Align Protein Sequences, PANTHER and GeneSplicer. If parental DNA was available, it was used for Sanger sequencing to determine whether the variants arose *de novo* or were inherited from one of the parents.

CNV analysis

CNVs were identified by analyzing the percentages of sequencing reads per amplicon and allele frequencies of the common SNPs, using the Torrent Suite Software v5.6 (ThermoFisher Scientific) and Microsoft Excel (2010). Allele frequencies of the SNPs were obtained from the Variant Caller Files. A deletion was identified if multiple consecutive amplicons contained a lower percentage of reads than other samples, combined with loss of heterozygosity. A gain was called if multiple consecutive amplicons contained higher read percentages combined with an allelic imbalance. The coordinates of the CNVs are based on the 3'-end and the 5'-end of the amplicons that are located upstream and downstream of the amplicons with altered read counts. The CNVs were classified according to the joint consensus recommendation of the American College of Medical Genetics and Genomics (ACMG) and the Clinical Genome Resource (ClinGen) for interpretation and reporting of CNVs (18). If parental DNA was available, it was used for SNP array to determine on which allele the CNV arose.

Confirmation of the NGS results

The presence of small variants located in the *FOXF1* gene were confirmed with Sanger sequencing using the 3730xl DNA Analyzer (Applied Biosystems, ThermoFisher Scientific) with custom designed primers (primer sequences available upon request). Sequences were aligned and compared with the reference sequences GRCh37/hg19 from the Ensemble genome database (ENSG00000103241), using SeqScape Software v3.0 (Applied Biosystems, ThermoFisher Scientific). CNVs were confirmed with SNP array using the Infinium Global Screening Array v1.0 (Illumina, San Diego, CA, USA). Array results were analyzed with Nexus Software 9.0 (BioDiscovery, El Segundo, CA, USA).

RESULTS

Sample collection

In total, we collected blood or skin fibroblasts of eight controls and 15 ACD/MPV patients (Table 1). The characteristic finding of misalignment of the pulmonary veins (MPV) was present in all these patients, except for patient 5. Control 1 was a sibling of ACD/MPV patient 3 and had several congenital malformations but no ACD/MPV. Control 2 and 3 were neonates that suffered from congenital alveolar dysplasia (CAD). The five other controls were anonymous controls with normal lung histology. Furthermore, we collected 18 FFPE lung tissue samples of deceased ACD/MPV patients of whom no blood or cell lines were stored.

Patient no.	Sample no.	Year of birth	Time between birth and de-compensation	Age at death in days	Total amount of days on ECMO	Co-malformati-on(s)	Mutation/CNV	Inheritance	Location	Coding effect	ACMG classification
1	P_003874[a]	2012	< 1 hr	17	26	None	g.86544428T>A	*De novo*	Exon 1	p.(Phe85Ile)	P
2	P_003884[a]	2011	n/a	15	13	PDA	g.86544447G>T g.86547445T>C	*De novo* Present in the father	Exon 1 3' UTR	p.(Gly91Val) unknown	LP LB
3	P_003877[b]	1999	< 24 hrs	21	14	None	Loss: g.86137510-86286682 (≈149kb)	*De novo* (M)	Regulatory region	--	P
4	P_003854[b]	2000	< 24 hrs	19	17	Omphalecele, hydronephrosis	Loss: g.86137510-86339166 (≈201kb)	*De novo* (M)	Regulatory region	--	P
5	P_004155[c]	2003	< 24 hrs	13	6	Bilateral hydrone-phrosis	g.86544531G>A	Parental DNA not available	Exon 1	p.(Gly119Asp)	LP
6	P_004157[c]	2004	< 24 hrs	12	10	Omphalocele	g.86544866_86544873del	Parental DNA not available	Exon 1	p.(A-la231Argfs*61)	LP
7	P_003871	2014	< 24 hrs	35	0	Hirshsprung (clinical diagnosis)	g.86544341C>G g.86547445T>C	Parental DNA not available	Exon 1 3' UTR	p.(Leu56Val) unknown	LP LB
8	P_004152	1998	< 1 hr	17	7	Intestinal malro-tation	g.86545125del	Parental DNA not available	Exon 1	p.(Asn-317Thrfs*62)	LP
9	P_003881	2015	<1 hr	28	25	Chylothorax	Loss: g.86243180-87703229 (≈1,5mb)	*De novo* (M)	Regulatory region and *FOXF1* gene	--	P
10	P_004156	2004	< 24 hrs	11	4	None	Loss g.:86144118-86289385 (≈145kb)	Parental DNA not available	Regulatory region	--	P
11	P_004444	2016	10 days	20	6	PFO	Loss: g.86137629-86287477 (≈150kb)	*De novo* (M)	Regulatory region	--	P
12	P_004439	2018	< 1hr	1	0	None	g.86547909_86547922dup	Present in the father	3' UTR	Unknown	LB
13	P_003890	2007	< 1 hr	10	5	None	None	--	--	--	--
14	P_003887	2008	< 1 hr	11	12	None	None	--	--	--	--
15	P_004237	2001	< 1hr	1	0	Facial dysmor-phism, toe defor-mities	None	--	--	--	--

Patient no.	Sample no.	Year of birth	Time between birth and de-compensation	Age at death in days	Total amount of days on ECMO	Co-malformati-on(s)	Mutation/CNV	Inheritance	Location	Coding effect	ACMG classification
C1	Control 1	2000	--	GA 15	--	Shortened distal spine, cloacal exstrophy, abdom-inal wall defect	None	--	--	--	
C2	Control 2	2006	< 1 hr	3	3	CAD	None	--	--	--	
C3	Control 3	2015	<1 hr	13	12	CAD	None	--	--	--	
C4	Control 4	--	--	--	--	--	None	--	--	--	
C5	Control 5	--	--	--	--	--	None	--	--	--	
C6	Control 6	--	--	--	--	--	None	--	--	--	
C7	Control 7	--	--	--	--	--	g.86544215G>C g.86547445T>C	Parental DNA not available	Exon 1 3' UTR	p.(Gly14Arg) unknown	B LB
C8	Control 8	--	--	--	--	--	None	--	--	--	

Table 1. Clinical details of ACD/MPV patients and controls with the results of FOXF1 targeted NGS. *PDA: patent ductus arteriosus. PFO: patent foramen ovale. GA: gestational age in weeks. CAD: congenital alveolar dysplasia. (M): maternal allele. ACMG classification B/LB/VUS/LP/P: benign/likely benign/variant of uncertain significance/likely pathogenic/pathogenic.* [a]*: Patients previously tested by Sen et al. (19)* [b]*: Patients previously tested by Szafranski et al. (20) (20) (20) (20)* [c]*: Patients carrying a mutation that has been described in other ACD/MPV patients (19). Grey shaded rows: pair of siblings. Genomic coordinates are based on Chr16(GRCh37); RefSeq NM_001451.2.*

Identification of FOXF1 variants using targeted NGS

If DNA samples isolated from blood or cell lines were used, each amplicon of the NGS panel (Figure 1) was sequenced more than 10 times and the mean coverage per amplicon was above 1716. All genomic alterations found with the NGS panel corresponded to the genomic alterations found with Sanger sequencing and SNP array, indicating a sensitivity and specificity of 100% compared to current available techniques. In 11 (73%) of the 15 DNA samples isolated from blood or cell lines, we detected heterozygous *FOXF1* alterations classified as pathogenic (P) or likely pathogenic (LP) (Table 1). Six of them were single nucleotide substitutions, small deletions or small duplications located in the first *FOXF1* exon. The remaining five variants were CNVs of which one encompassed both the *FOXF1* gene and its regulatory region, and four encompassed only the regulatory region. Two of the identified *FOXF1* variants (g.86544531G>A, p.(Gly119Asp) and g.86544866_86544873del, p.(Ala231Argfs*61)) have been previously described by Sen and colleagues in other ACD/MPV patients (19) (Table 1).

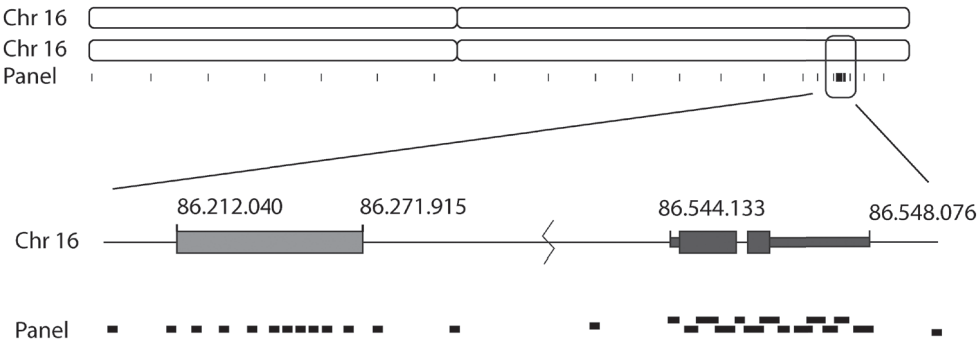

Figure 1. Schematic overview of the custom designed ACD/MPV panel consisting of amplicons distributed over chromosome 16. *Dark grey: FOXF1 gene with its two exons. Light grey: 60-kb regulatory region. The illustration is not in accordance with actual distances*

Since skin fibroblasts and blood samples of previously diagnosed ACD/MPV patients are limited, we also included four ACD/MPV patients of whom DNA was already tested with Sanger sequencing and array comparative genomic hybridization in collaboration with the group of Stankiewicz in 2013 (19, 20) (Table 1). With the ACD/MPV NGS panel we confirmed the findings of the studies in 2013. However, in 2013 we included additional Sanger sequencing to investigate the exact breakpoints of the CNVs, therefore the coordinates of the CNVs differ slightly from the results we show here (patient 3 and 4 of Table 1) (20). Further, we showed in 2013 that these CNVs were located on the maternal

allele (20). To investigate whether the other CNVs identified with the NGS panel were also located on the maternal allele, we performed SNP array on parental DNA. Indeed, the CNVs in patients 9 and 11 were also located on the maternal allele. Of patient 10, there was no parental DNA available for allele identification (Table 1).

In one patient we only detected a likely benign (LB) variant and, in three patients we could not detect any *FOXF1* variants, neither by SNP array or Sanger sequencing. To make sure that these patients were not misdiagnosed, lung samples were re-examined by a specialized pathologist of the Erasmus University Medical Center who again confirmed ACD/MPV (Figure 2).

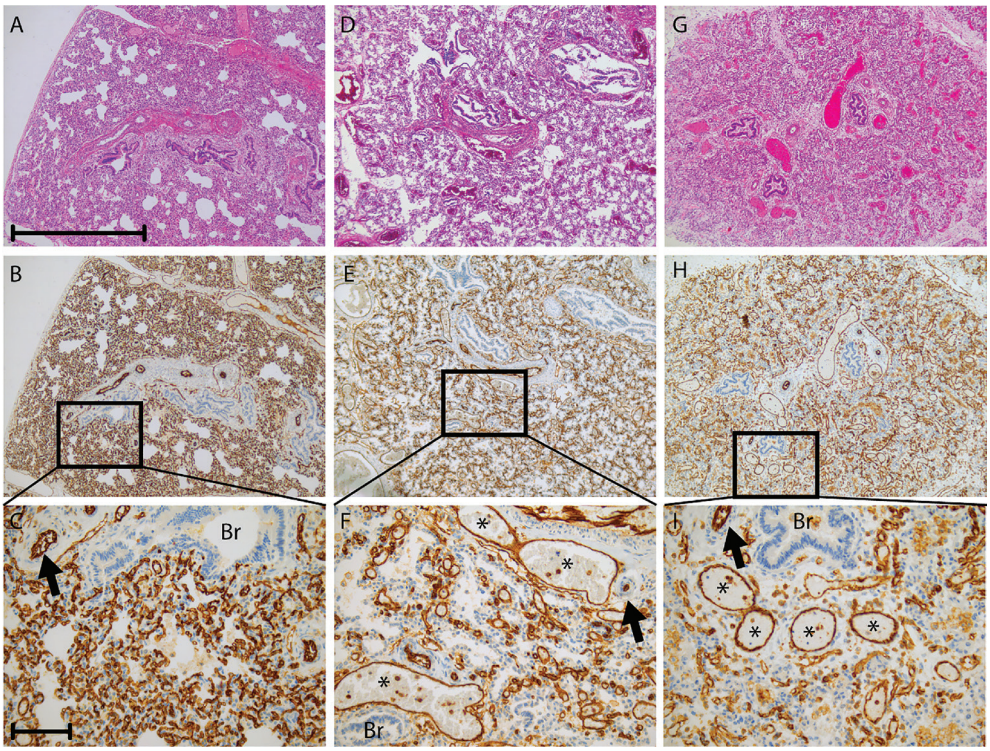

Figure 2. Hematoxylin-eosin (top row) and CD31 staining on lung tissue of an age-matched control (A-C) and two ACD/MPV patients (D-F; G-I). *ACD/MPV lung tissues demonstrate misalignment of pulmonary veins (MPV; asterisks) and disordered capillary networks in alveolar septa. In DNA of ACD/MPV patient P_003854 (D-F), a deletion involving the FOXF1 regulatory region was found. In DNA of ACD/MPV patient P_003890 (G-I), no FOXF1 alteration was found. Br: bronchiole; arrows: arterioles. Scale bars: 1 mm (A); 100 µm (C).*

In one of the eight control samples, we detected two variants that were classified as LB. There were no *FOXF1* alterations found in the other seven control samples.

To investigate whether this test can also be used when only formalin-fixed and paraffin-embedded (FFPE) tissue is available, we tested 18 DNA samples isolated from FFPE lung tissue. The use of these samples resulted in a large variability of sequencing depths between amplicons and between samples. Therefore, the read percentages could not be compared to each other and CNV analysis was not possible (Supplemental Figure S1 (online)). Furthermore, multiple amplicons showed a low read depth (<10 reads) with the result that the *FOXF1* gene was not fully sequenced in four samples. However, in one sample we could confirm a previously described mutation (19) and in another sample we detected one novel mutation (Supplemental Table S1 (online)). Both mutations were confirmed with Sanger sequencing.

DISCUSSION

In this study, our aim was to develop a new targeted NGS panel to detect genomic alterations associated with ACD/MPV which has the potential to reduce the time to diagnose ACD/MPV in clinical practice. Retrospective testing of ACD/MPV patients and controls showed that the panel works efficiently with DNA isolated from fresh tissue and resulted in identification of 6 novel and 6 previously described *FOXF1* alterations classified as pathogenic or likely pathogenic.

Two of the previous described *FOXF1* alterations were identified in other ACD/MPV patients. Interestingly, the clinical presentations differed between patients carrying the same mutation. For instance, patient 5 from the current study needed ECMO therapy directly at the start of symptoms, while the patient described by Sen et al. (patient 26) survived for 21 days without ECMO therapy (19). Furthermore, the patient from our study suffered from a bilateral hydronephrosis whereas the patient described by Sen et al. suffered from a megaduodenum, pyloric stenosis and an annular pancreas (19). In accordance with previous studies, these observations suggest that the severity of ACD/MPV and the extent of accompanying malformations cannot be correlated to specific *FOXF1* variants (1, 6). Recently, Szafranski et al. reported that the phenotypical differences might be caused by the presence or absence of rare single nucleotide variants located in the *FOXF1* enhancer, which could result in different expressions of *FOXF1* (21). Furthermore, it has been suggested that parental imprinting of *FOXF1* modulates FOXF1

expression (20, 22). In line with earlier studies, the CNVs identified in the current study were located on the maternal allele and support that at least the regulatory region of *FOXF1* is paternally imprinted.

Stated turn-around times for available FOXF1 genetic studies are generally longer than two to three weeks, in contrast to the 72 hours for our approach using the NGS panel (Figure 3A). Currently, ACD/MPV patients receive life supportive care and invasive treatments for several days to weeks while awaiting a diagnosis (1) (Figure 3B, left segment). By testing DNA isolated from a small blood sample with the NGS ACD/MPV panel, the time between hospitalization and diagnosis can be shortened (Figure 3B, middle segment). The ACD/MPV panel is especially effective when a likely pathogenic or pathogenic alteration is found. This gives clinicians the chance to confirm the diagnosis earlier with lung biopsy and allows clinicians to better inform and counsel the parents (22). In the majority of patients, an earlier diagnosis leads to earlier treatment withdrawal and thus, reduces the use of invasive and expensive treatments like ECMO therapy (23). For exceptional ACD/MPV cases with an atypical less severe phenotype, lung transplantation might be an option (24, 25). Based on the patient's condition, one could argue to omit the lung biopsy if a likely pathogenic or pathogenic *FOXF1* alteration is detected. Since the genotype-phenotype correlation is still not fully understood, we recommend to histologically confirm the diagnosis. Hopefully, future studies will clarify the mechanisms behind the genotype-phenotype relation with the result that eventually, genetic testing could obviate the need for a lung biopsy (Figure 3B, right segment).

Given that ACD/MPV is a rare cause of PH in newborns, we recommend to continue therapy if there are no variants identified that can be classified as likely pathogenic or pathogenic (Figure 3B, middle and right segment). However, our findings show that the absence of *FOXF1* alterations does not always exclude ACD/MPV. Four of the 15 (27%) histologically confirmed ACD/MPV patients were negative for pathogenic or likely pathogenic *FOXF1* alterations, even with additional testing by Sanger sequencing and SNP array. Since we are not the first group to describe ACD/MPV patients without pathogenic alterations in the *FOXF1* region (9), these results suggest that the pathogenesis of ACD/MPV might involve epigenetic changes or genetic changes in other genes or regulatory regions. Therefore, a lung biopsy should still be performed if symptoms progress over time, especially when a variant of uncertain significance is found. In the absence of a

FOXF1 alteration, further genome wide testing can contribute to the search for other genes or regulatory regions involved in the pathogenesis of ACD/MPV.

Additional to the care related beneficial aspects of the ACD/MPV panel, it is also a cost-effective technique. For testing of DNA with the ACD/MPV panel, the Erasmus Medical Center charges €900 whereas for the combination of Sanger sequencing and SNP array, €1700 is charged. Although WGS is not yet available as a standard diagnostic test, the charges for diagnostic WGS will certainly exceed the charges for WES (€1800). Furthermore, each extra day of hospitalization at a neonatal intensive care unit that can be prevented by an earlier diagnosis, can save up to thousands of euros. (22)

Clearly, there are some limitations to the present study. First of all, because of the low incidence of ACD/MPV, our approach was retrospective to infants already identified as having ACD/MPV through histopathologic analysis of lung tissue, rather than demonstrating prospectively that we provide a rapid diagnostic test. However, the results of this study can be the starting point for a prospective study that investigates the impact of the ACD/MPV panel on the patient's quality of life, the diagnostic yield, and the cost-effectiveness. Another limitation would be that the current study focused solely on detection of *FOXF1* variants whereas the phenotype of ACD/MPV overlaps with the phenotypes of other congenital lung disorders. Based on the successful results of the current study, we are expanding the panel by adding more genes and loci so that other congenital lung disorders can be diagnosed without the need for additional WGS. Furthermore, by using an updated version of the Ion Ampliseq Designer, the GC-rich regions that were uncovered in the current ACD/MPV panel can be included in the expanded panel.

In this study, DNA samples isolated from FFPE tissues worked not as efficient as DNA isolated from fresh tissue. It has been shown that DNA fragmentation and degradation are higher in FFPE tissues than fresh tissues and that they increase after longer storage (26, 27). In this study, only three of the 18 FFPE lung samples were processed after 2009, including one of the samples in which a mutation was identified. Presumably, as shown in previous studies, the use of more recently fixed FFPE tissues will result in more efficient sequencing (13). Furthermore, other tissues like spleen or liver may provide better results than lung tissue.

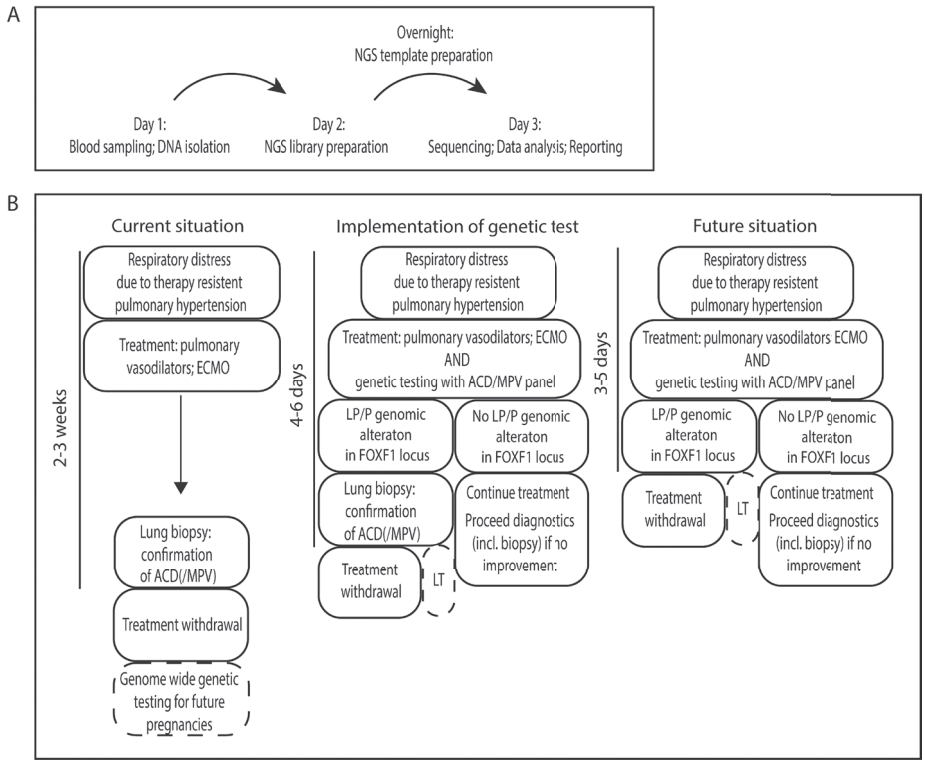

Figure 3. Schematic overview of the FOXF1-targeted NGS pipeline and implementation in clinical practice. *Illustration of the NGS steps within 72 h (a). Implementation of NGS with the ACD/MPV panel potentially reduces the time between hospitalization and diagnosis (b). LP likely pathogenic, P pathogenic, No LP/P all variants that are not classified as pathogenic or likely pathogenic, including variants of unknown significance, LT lung transplantation.*

To summarize, we developed a *FOXF1* targeted NGS panel to detect mutations and deletions associated with ACD/MPV and showed that the panel works efficiently with DNA isolated from fresh tissues like blood. To our knowledge, this is the first NGS panel that targets both the *FOXF1* gene and the enhancer region in the same run. Therefore this test is able to detect CNVs in the non-coding enhancer region without the need for expensive and time consuming whole genome approaches. Although the current study is based on retrospective testing of ACD/MPV patients, the results suggest that the panel can be used for relatively non-invasive and quick screening for *FOXF1* alterations in future ACD/MPV patients. Thereby, it has the potential to increase the diagnostic yield and reduce the use of futile and high cost techniques like ECMO therapy. Moreover, once the correlation between *FOXF1* alterations and ACD/MPV is well-defined, an invasive lung biopsy might no longer be needed to confirm ACD/MPV.

ACKNOWLEDGEMENT

We thank the VU University Medical Center Amsterdam and the Charles University and General University Hospital Prague for their contribution to our sample collection. Further, we thank the Friends from Sophia Foundation for their support and, we thank the Royal Netherlands Academy of Arts and Sciences for the Ter Meulen Grant.

AUTHOR CONTRIBUTIONS

AdK, RR and DT designed the study. AvH, MP and AD provided samples. Experiments were performed by ES, RvM, FM and JvdT. Data was analyzed and interpreted by ES, RvM, JvdT, AdK, HJD, and RR. ES wrote the manuscript and AvH, AdK, RR, HJD, and DT critically commented and edited the manuscript. All authors had final approval of the submitted and published versions.

Statement of Financial support: We received financial support from The Friends from Sophia Foundation and The Royal Netherlands Academy of Arts and Sciences.

REFERENCES

1. Slot E, et al. 2018 Alveolar capillary dysplasia with misalignment of the pulmonary veins: clinical, histological, and genetic aspects. Pulm Circ 8:2045894018795143.
2. Kool H, Mous D, Tibboel D, de Klein A, Rottier RJ 2014 Pulmonary vascular development goes awry in congenital lung abnormalities. Birth Defects Res C Embryo Today 102:343-358.
3. Al-Hathlol K, Phillips S, Seshia MK, Casiro O, Alvaro RE, Rigatto H 2000 Alveolar capillary dysplasia. Report of a case of prolonged life without extracorporeal membrane oxygenation (ECMO) and review of the literature. Early Hum Dev 57:85-94.
4. Inwald D, Brown K, Gensini F, Malone M, Goldman A 2004 Open lung biopsy in neonatal and paediatric patients referred for extracorporeal membrane oxygenation (ECMO). Thorax 59:328-333.
5. Sen P, Thakur N, Stockton DW, Langston C, Bejjani BA 2004 Expanding the phenotype of alveolar capillary dysplasia (ACD). J Pediatr 145:646-651.
6. Stankiewicz P, et al. 2009 Genomic and genic deletions of the FOX gene cluster on 16q24.1 and inactivating mutations of FOXF1 cause alveolar capillary dysplasia and other malformations. Am J Hum Genet 84:780-791.
7. Dharmadhikari AV, Szafranski P, Kalinichenko VV, Stankiewicz P 2015 Genomic and Epigenetic Complexity of the FOXF1 Locus in 16q24.1: Implications for Development and Disease. Curr Genomics 16:107-116.
8. Seo H, Kim J, Park GH, Kim Y, Cho SW 2016 Long-range enhancers modulate Foxf1 transcription in blood vessels of pulmonary vascular network. Histochem Cell Biol 146:289-300.
9. Szafranski P, et al. 2016 Pathogenetics of alveolar capillary dysplasia with misalignment of pulmonary veins. Hum Genet 135:569-586.
10. Szafranski P, et al. 2016 Narrowing the FOXF1 distant enhancer region on 16q24.1 critical for ACDMPV. Clin Epigenetics 8:112.
11. National Center for Biotechnology Information USNLoM, Genetic Testing Registry. 13 February 2020 <https://www.ncbi.nlm.nih.gov/gtr/conditions/C0031190/>
12. Genomes Project C, et al. 2015 A global reference for human genetic variation. Nature 526:68-74.
13. Smit KN, et al. 2018 Combined mutation and copy-number variation detection by targeted next-generation sequencing in uveal melanoma. Mod Pathol 31:763-771.
14. Miller SA, Dykes DD, Polesky HF 1988 A simple salting out procedure for extracting DNA from human nucleated cells. Nucleic Acids Res 16:1215.
15. Thorvaldsdottir H, Robinson JT, Mesirov JP 2013 Integrative Genomics Viewer (IGV): high-performance genomics data visualization and exploration. Brief Bioinform 14:178-192.
16. Den Dunnen J.T. DR, Maglott D. R., Hart R.K., Greenblatt M. S., McGowan-Jordan J., Roux A., Smith T., Antonarakis S.E., Taschner P.E.M., on behalf of HGVS, HVP and the HUGO 2016 HGVS Recommendations for the Description of Sequence Variants: 2016 Update. Human Mutation 37:564-569.
17. Richards S, et al. 2015 Standards and guidelines for the interpretation of sequence variants: a joint consensus recommendation of the American College of Medical Genetics and Genomics and the Association for Molecular Pathology. Genet Med 17:405-424.
18. Riggs ER, et al. 2020 Technical standards for the interpretation and reporting of constitutional copy-number variants: a joint consensus recommendation of the American College of Medical Genetics and Genomics (ACMG) and the Clinical Genome Resource (ClinGen). Genet Med 22:245-257.
19. Sen P, et al. 2013 Novel FOXF1 mutations in sporadic and familial cases of alveolar capillary dysplasia with misaligned pulmonary veins imply a role for its DNA binding domain. Hum Mutat 34:801-811.
20. Szafranski P, et al. 2013 Small noncoding differentially methylated copy-number variants, including lncRNA genes, cause a lethal lung developmental disorder. Genome Res 23:23-33.
21. Szafranski P, et al. 2019 Association of rare non-coding SNVs in the lung-specific FOXF1 enhancer with a mitigation of the lethal ACDMPV phenotype. Hum Genet 138:1301-1311.

22. Swaggart KA, Swarr DT, Tolusso LK, He H, Dawson DB, Suhrie KR 2019 Making a Genetic Diagnosis in a Level IV Neonatal Intensive Care Unit Population: Who, When, How, and at What Cost? J Pediatr.
23. Houmes RJ, et al. 2017 Risk and relevance of open lung biopsy in pediatric ECMO patients: the Dutch experience. J Pediatr Surg 52:405-409.
24. Edwards JJ, et al. 2019 Histopathologic and Genetic Features of Alveolar Capillary Dysplasia with Atypical Late Presentation and Prolonged Survival. J Pediatr 210:214-219 e212.
25. Towe CT, et al. 2017 Infants with Atypical Presentations of Alveolar Capillary Dysplasia with Misalignment of the Pulmonary Veins Who Underwent Bilateral Lung Transplantation. J Pediatr.
26. Watanabe M, et al. 2017 Estimation of age-related DNA degradation from formalin-fixed and paraffin-embedded tissue according to the extraction methods. Exp Ther Med 14:2683-2688.
27. Wong SQ, et al. 2014 Sequence artefacts in a prospective series of formalin-fixed tumours tested for mutations in hotspot regions by massively parallel sequencing. BMC Med Genomics 7:23.

SUPPLEMENTARY DATA

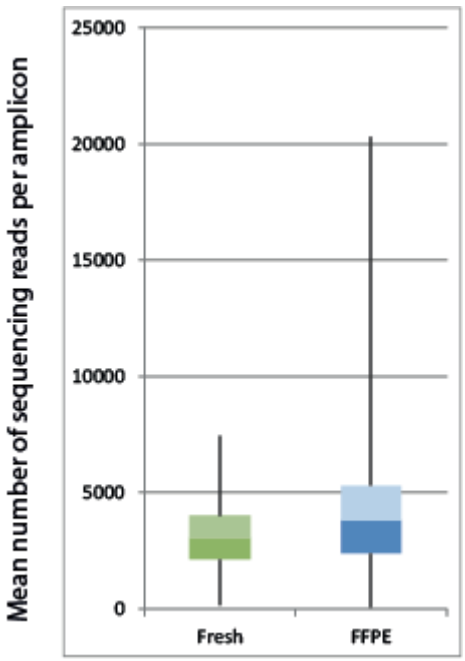

Figure S1. Illustration of the spread in sequencing depth per amplicon using DNA isolated from FFPE tissue. *The mean numbers were calculated from the read numbers per amplicon of eighteen ACD/MPV DNA samples. The use of DNA isolated from FFPE tissues resulted in too much variability in sequencing depths to detect CNVs.*

Patient no.	Year of birth	Time between birth and decompensation	Age at death	Total amount of days on ECMO	Co-malformation(s)	Mutation	Inheritance	Location	Coding effect	ACMG classification
P_003873[a]	2011	-	GA 23 4/7	-	Atrial septal defect, ventricle septal defect, gall bladder agenesis, duodenal atresia, anal atresia, intestinal malrotation	g.86544428T>A	*De novo*	Exon 1	p.(Phe85Ile)	P
P_004086	2001	< 24 hrs	12 days	8	None	g.86544336delT	Parental DNA not available	Exon 1	p.(Ile54Thrfs*16)	LP

Table S1. Clinical details and confirmed NGS results of ACD/MPV patients tested with FOXF1 targeted NGS using DNA isolated from FFPE tissue. *GA: gestational age in weeks. LP/P: likely pathogenic/pathogenic. [a]: Patient previously tested by Sen et al. (19) Genomic coordinates are based on Chr16(GRCh37); RefSeq NM_001451.2*

CHAPTER 4

GENOME WIDE DNA METHYLATION ANALYSIS OF ALVEOLAR CAPILLARY DYSPLASIA LUNG TISSUE REVEALS ABERRANT METHYLATION OF GENES INVOLVED IN DEVELOPMENT INCLUDING THE FOXF1 LOCUS

Evelien Slot[a,b], Ruben Boers[c], Joachim Boers[c], Wilfred F.J. van IJcken[d,e], Dick Tibboel[a], Joost Gribnau[c], Robbert Rottier[a,e], Annelies de Klein[b]

a. Department of Paediatric Surgery, Erasmus MC – Sophia Children's Hospital Rotterdam
b. Department of Clinical Genetics, Erasmus MC, Rotterdam
c. Department of Developmental Biology, Oncode Institute, Erasmus MC Rotterdam
d. Center for Biomics, Erasmus University Medical Center, Erasmus MC, Rotterdam
e. Department of Cell Biology, Erasmus University Medical Center, Erasmus MC, Rotterdam

Published in Clinical Epigenetics, 2021

ABSTRACT

Background

Alveolar capillary dysplasia with or without misalignment of the pulmonary veins (ACD/MPV) is a lethal congenital lung disorder associated with a variety of heterozygous genomic alterations in the FOXF1 gene or its 60 kb enhancer. Cases without a genomic alteration in the FOXF1 locus have been described as well. The mechanisms responsible for FOXF1 haploinsufficiency and the cause of ACD/MPV in patients without a genomic FOXF1 variant are poorly understood, complicating the search for potential therapeutic targets for ACD/MPV. To investigate the contribution of aberrant DNA methylation, genome wide methylation patterns of ACD/MPV lung tissues were compared with methylation patterns of control lung tissues using the recently developed technique Methylated DNA sequencing (MeD-seq).

Results

Eight ACD/MPV lung tissue samples and three control samples were sequenced and their mutual comparison resulted in identification of 319 differentially methylated regions (DMRs) genome wide, involving 115 protein coding genes. The potentially upregulated genes were significantly enriched in developmental signalling pathways, whereas potentially downregulated genes were mainly enriched in O-linked glycosylation. In patients with a large maternal deletion encompassing the 60kb FOXF1 enhancer, DNA methylation patterns in this FOXF1 enhancer were not significantly different compared to controls. However, two hypermethylated regions were detected in the 60kb FOXF1 enhancer of patients harbouring a FOXF1 point mutation. Lastly, a large hypermethylated region overlapping the first FOXF1 exon was found in one of the ACD/MPV patients without a known pathogenic FOXF1 variation.

Conclusion

This is the first study providing genome wide methylation data on lung tissue of ACD/MPV patients. DNA methylation analyses in the FOXF1 locus excludes maternal imprinting of the 60kb FOXF1 enhancer. Hypermethylation at the 60kb FOXF1 enhancer might contribute to FOXF1 haploinsufficiency caused by heterozygous mutations in the FOXF1 coding region. Interestingly, DNA methylation analyses of patients without a genomic FOXF1 variant suggest that abnormal hypermethylation of exon 1 might play a role in some ACD/MPV in patients.

BACKGROUND

Alveolar capillary dysplasia with or without misalignment of the pulmonary veins (ACD/MPV) is a lethal congenital lung disorder associated with heterozygous genomic alterations in the Forkhead Box F1 (*FOXF1)* gene locus. These genomic alterations vary from point mutations to large copy number variations (CNVs) but all seem to cause haploinsufficiency leading to ACD/MPV (1, 2). The molecular mechanism responsible for the haploinsufficiency are poorly understood which complicates the search for potential therapeutic targets for ACD/MPV. Furthermore, in approximately 30% of ACD/MPV patients no genomic variants in the *FOXF1* locus could be found, challenging the diagnostic process (3, 4).

The majority of ACD/MPV patients die within the first weeks of life due to insufficient gas exchange and therapy-resistant pulmonary hypertension. Histologically, ACD/MPV is characterized by reduced numbers of pulmonary capillaries, increased medial wall thickening in pulmonary arterioles and, in most cases, displaced pulmonary veins (reviewed in Slot et al. (2)). Genomic alterations associated with ACD/MPV are either small indel mutations in the *FOXF1* gene or large deletions that include the 60kb enhancer region (4-6). This enhancer is located 250kb upstream of the *FOXF1* transcription start site and lies within the same topologically associated domain (TAD) as *FOXF1* (4). Furthermore, this *FOXF1* enhancer region contains GLI2 binding sites that upregulate *FOXF1* expression upon Sonic hedgehog activation (4, 5, 7).

Heterozygous *FOXF1* variants seem to have a dominant negative effect that cause haploinsufficiency of FOXF1, associated with ACD/MPVPV, and it has been suggested that *FOXF1* is subjected to parental imprinting (1, 8-10). One of the well-established mechanisms of parental imprinting is allele specific DNA methylation of gene promotors (11). However, several studies have shown that the *FOXF1* promoter is not methylated in both normal and ACD/MPV lung tissue, excluding the possibility of allele specific silencing of *FOXF1* through promotor methylation (10, 12, 13). Furthermore, *FOXF1* seems to be similarly transcribed from both alleles, which opposes imprinting of the *FOXF1* transcription region itself (13, 14). However, this does not completely exclude the 60kb enhancer region to be subject to parental imprinting on the paternal allele (Suppl. figure 1), as suggested previously (4) based on the finding that all but one of the large deletions detected in ACD/MPV patients involved the 60kb enhancer on the maternal chromosome

(3, 10).Furthermore, although very unlikely, parental imprinting of the *FOXF1* enhancer on the maternal allele has never been excluded either. Up to now, studies investigating allele specific methylation in the 60kb enhancer are limited and mainly use DNA isolated from blood or skin tissue which might not be representative for methylation patterns in lung tissue (15, 16).

Although most patients have a similar clinical course, atypical cases have been described that deviate in time of disease presentation and progression or reliance on life supportive care. So far, the phenotypical differences could not be correlated with the presence, type or location of the *FOXF1* variant. Considering the complex genotype-phenotype correlation and the absence of genomic *FOXF1* alterations in some of the patients, abnormal DNA methylation might contribute to the pathogenesis of ACD/MPV.

In 2018, we developed Methylated DNA Sequencing (MeD-seq) which enables genome wide DNA-methylation profiling at single-nucleotide resolution without the need for deep sequencing (17). Using this technique, this study aimed at detection of genome wide methylation patterns in lung tissue of eight ACD/MPV patients, with specific focus on the *FOXF1* locus, to identify potential differences that might play a role in the pathogenesis of ACD/MPV.

METHODS

Sample collection

ACD/MPV and control FFPE lung tissue samples were collected from the Erasmus MC Sophia Children's Hospital in Rotterdam, the VU University Medical Centre in Amsterdam and the Hospital for Sick Children in Toronto. All specimen were obtained as part of routine autopsy following informed consent of the parents/legal representatives or as part of a diagnostic procedure to diagnose ACD/MPV based on clinical suspicion. Samples were anonymized before they were subjected to MeD-seq. The research proposal was reviewed and approved by the Daily Board of the Medical Ethics Committee (METC) Erasmus University Medical Centre Rotterdam, The Netherlands.

DNA isolation

DNA was isolated from FFPE lung tissue using the QIAamp DNA Mini Kit (Qiagen, Hilden, Germany), according to the manufacturer's instructions. Eight to ten 10µm sections were pre-treated with xylene to remove the paraffin and with sodium thiocyanate to permeabilize the tissue. Incubation with (ATL) lysis buffer and proteinase K was extended to 36 hours to allow complete lysis. DNA concentrations were measured with the Quant-iT Picogreen assay kit (ThermoFisher Scientific) according the manufacturer's instructions.

MeD-seq sample preparation

DNA samples were prepared for MeD-seq as described previously (17). In brief, DNA samples were digested with LpnPI (New England Biolabs, Ipswhich, MA, USA) and resulted in fragments of 32bp with the methylated cytosine in the centre. Fragments were either purified on 10% TBE gel before preparation or purified by Pippin system gel after preparation. The 32bp DNA fragments were prepared for sequencing using a ThruPlex DNA-seq 96D kit (Takara Bio Inc, Kusatasu, Japan) according to manufacturer's protocol. To include dual indexed barcodes, stem–loop adaptors were blunt-end ligated to repaired input DNA and amplified (4 +10 cycles) using a high-fidelity DNA polymerase. Multiplexed samples were sequenced on Illumina HiSeq2500 systems for single reads of 50bp according to the manufacturer's instructions. Dual indexed samples were demultiplexed using bcl2fastq software (Illumina).

Data processing and analysis

MeD-seq data were processed and analysed with Python 2.7.5 using specifically created scripts as described previously (17). In short, before mapping of the reads to the Hg38 genome using bowtie 2.1.0., the raw FASTQ files were subjected to Illumina adaptor trimming and filtered for the presence of LpnPI restriction sites 13-17bp from the 3' or 5' end. For visualization of the mapped reads, BAM files were generated using SAMtools. LpnPI site scores were used to produce read count scores for the transcription start sites (TSS) (1kb before and 1kb after), gene bodies (1kb after the TSS until the transcription end site) and CpG islands. Gene and CpG island annotations were downloaded from UCSC (hg38). To detect DMRs between two data sets, genome wide read counts were

compared using the Chi-Squared test. Significance was set at $p<0.05$ and was called with a Bonferroni correction or FDR using the Benjamini-Hochberg procedure. In addition, a genome-wide sliding window was used to detect sequentially differentially methylated LpnPI sites. Statistical significance was called between LpnPI sites in predetermined groups using the Chi-square test with a Bonferroni correction. Neighbouring significantly called LpnPI sites were binned and reported. Overlap of genome wide detected DMRs was reported for TSS, CpGisland or gene body regions using the annotations of UCSC (Hg38). Gene enrichment analyses were carried out using Metascape (26). Metascape identifies significant enriched terms such as Gene Ontology (GO) terms and canonical pathways, and clusters them into a tree, based on Kappa-statistical similarities among their gene memberships (26).

RESULTS

Differential methylation of developmental genes in ACD/MPV lung tissue

Formalin-fixed and paraffin-embedded (FFPE) lung tissue samples of eight ACD/MPV patients and three age-matched controls were available to study lung specific methylation (**Table 1**). All ACD/MPV patients have been previously described and tested for *FOXF1* alterations extensively (3). Three patients with a point mutation in the first *FOXF1* exon (ACD-mut), three patients with a large deletion overlapping the *FOXF1* enhancer on the maternal allele (ACD-del) and two patients without a known pathogenic variant in the *FOXF1* locus (ACD-none) (Suppl. figure 2) were selected. Control patients were age-matched individuals with a medical condition unrelated to lung development or underlying pulmonary pathology.

Table 1. Overview of included ACD/MPV patients and control samples.

Sample ID	FOXF1 alteration (Hg38)	Time of biopsy	Cause of death	Co-malformation
ACD-del1	Loss chr16: 86103904-86253076	Post mortem	ACD/MPV	None
ACD-del2	Loss chr16: 86103904-86305560	Post mortem	ACD/MPV	Omphalecele, hydronephrosis
ACD-del3	Loss chr16: 86209574-87669623	6 days of life	ACD/MPV	Chylothorax
ACD-mut1	chr16: 86510735C>G p.(L56V)	34 days of life	ACD/MPV	Hirshprung (clinical diagnosis)
ACD-mut2	chr16: 86510822T>A p.(F85I)	Post mortem	ACD/MPV	Atrial septal defect, ventricle septal defect, gall bladder agenesis, duodenal atresia, anal atresia, intestinal malrotation
ACD-mut3	chr16: 86510730delT p.(I54Tfs*16)	9 days of life	ACD/MPV	None
ACD-none1	None	Post mortem	ACD/MPV	None
ACD-none2	None*	Post mortem	ACD/MPV	None
C1	-	Post mortem	Ventriculomegaly	None
C2	-	Post mortem	Hypovolemic shock	None
C3	-	Post mortem	Asphyction	None

All ACD/MPV patients developed critical and life -threatening respiratory insufficiency within the first 24 hours after birth.
**: This patient carried a duplication in the 3'UTR of FOXF1 that was classified as likely benign according to the ACMG classification system (3).*

Genome wide DNA methylation patterns of ACD/MPV lung tissues were compared with methylation patterns of control lung tissues. Differentially methylated regions (DMRs) located on the X- and Y-chromosome were removed because samples were not gender-matched, as well as DMRs with a fold change below 2. This resulted in 319 DMRs of which 184 were hypermethylated and 135 were hypomethylated in ACD/MPV lung samples (Figure 1A). Approximately half of the DMRs (43%) were intergenic, the other 57% of DMRs fully or partly overlapped putative gene promoters (TSS) or gene bodies (Figure 1B). Depending on the location, methylation acts differently on gene regulation. In general, promotor methylation is associated with gene silencing, whereas gene body methylation is mostly associated with gene activation (18-25). Based on these assumptions, we labelled genes as potentially up- or downregulated in ACD/MPV lung tissue compared to control lung tissue. Exclusion of pseudogenes, long-non coding RNAs and duplicates resulted in 79 potentially upregulated and 36 potentially downregulated protein encoding genes (Figure 1B, supp. table 1)**.** To study if these potentially up- and downregulated genes are specifically involved in certain biological pathways, gene enrichment analyses

were performed using Metascape (26). Gene enrichment analysis of the potentially upregulated genes revealed 16 statistically significant enriched gene clusters of which the top cluster (named 'embryonic morphogenesis' (GO:0048598)) (Figure 1C) included different signalling pathways involved in developmental processes such as 'embryonic organ morphogenesis' (GO:0048562) and 'blood vessel morphogenesis' (GO: 0048514) (Supp. table 2). The genes included in this top cluster were: *COL4A2, GATA2, HOXA3, HOXB3, HOXB6, HOXD3, NOTCH1, TGFB1, SOCS3, KDM6B, TENM4, CCDC40, TIE1, NXN, DHRS3, RXRA.* Gene enrichment analysis of potentially downregulated genes revealed three significantly overrepresented gene clusters, with the most significant pathway being 'O-linked glycosylation' which included *MUC5AC, ADAMTS2* and *GALNT15.*

The FOXF1 enhancer is not maternally imprinted

Next, we focused on methylation patterns in the *FOXF1* locus (Figure 2A). Comparison of all ACD/MPV samples with controls revealed no significant DMRs in the *FOXF1* gene, the 60kb *FOXF1* enhancer nor the 250kb between these two regions (Table 2). In order to identify potential correlations between methylation patterns and patient-specific *FOXF1* variants, we separated the ACD/MPV samples with known genomic *FOXF1* variants into two groups. The first group (ACD-del) contained the three samples with a large deletion involving the *FOXF1* enhancer on the maternal chromosome (Figure 2A), the second group (ACD-mut) contained the three ACD/MPV patients with a point mutation in the first exon of *FOXF1* (ACD-mut). Both groups were compared with control samples and analysed for significant DMRs in the *FOXF1* locus. In addition, we separately compared DNA methylation patterns of the two ACD/MPV patients without a pathogenic *FOXF1* variant (ACD-none1 and ACD-none2)(3) with control samples.

We analysed DNA methylation patterns in ACD-del samples. Although methylated regions were present in both ACD-del samples and controls, no significant differences were detected between the groups (Table 2, Figure 2B). Since one of the ACD-del patients (ACD-del3) harboured a deletion starting in the middle of the 60kb enhancer, ACD-del samples ACD-del1 and ACD-del2 were also separately compared with control samples but again revealed no significant DMRs. These results indicate that the large maternal deletions in ACD-del samples have no effect on methylation patterns in the 60kb *FOXF1*

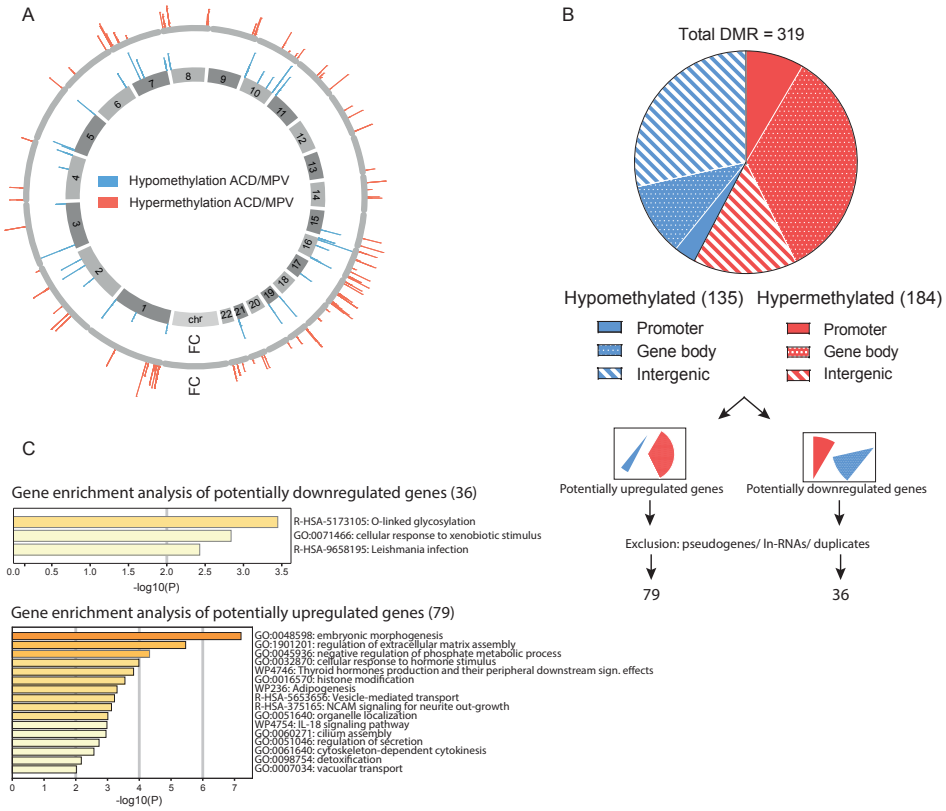

Figure 1. Genome wide methylation patterns of ACD/MPV lung tissue suggest abnormal gene regulation *A: Hypermethylated (red) and hypomethylated (blue) regions in ACD/MPV lungs that were found genome wide (X- and Y-chromosome excluded; fold change <2 excluded). The bar height indicates the relative fold change (FC) of the differentially methylated regions (DMRs). B: Pie chart of the distribution of hyper- (red) and hypomethylated (blue) DMRs. C: Results of gene ontology cluster enrichment analyses with Metascape (26) using the lists of genes that are potentially up- and downregulated based on the overlap of DMRs with promoters and gene bodies (squares with pie slices on the left indicate DMR overlap) (Suppl. table 1).*

enhancer. Szafranski and colleagues previously suggested that the 60kb *FOXF1* enhancer is subjected to allele specific imprinting through DNA methylation at the paternal allele (4). However, they did not study allele specific methylation and therefore could not exclude allele specific imprinting through DNA methylation at the maternal allele. If the 60kb *FOXF1* enhancer normally contains regions that are specifically methylated on the maternal allele, these would be lost in the ACD-del samples studied by us, resulting in significant DMRs between ACD-del and control samples (Suppl. figure 3A, left panel). Therefore, the absence of significant DMRs between ACD-del and control samples

confirms that the 60kb *FOXF1* enhancer is devoid of allele specific methylation on the maternal allele. Consequently, this means that if this *FOXF1* enhancer is subjected to allele specific imprinting through DNA methylation, this concerns the paternal allele (Suppl. figure 3A, right panel).

Table 2. DMRs in the *FOXF1* locus detected by statistical group comparisons.

Group comparison	60kb enhancer region	Between enhancer and promoter	FOXF1 promoter	FOXF1 gene body
ACD/MPV vs. Control	-	-	-	-
ACD-del vs. Control	-	-	-	-
ACD-mut vs. Control	chr16: 86210617-86211669 (FC 3.5) chr16: 86212910-86213514 (FC 2.7)	chr16: 86243281-86243394 (FC 1.1) chr16: 86345534-86345640 (FC1.4) chr16: 86504259-86504462 (FC1.1) chr16: 86504711-86505743 (FC 7.3) chr16: 86505840-86506078 (FC 1.0)*	-	-

All depicted DMRs were hypermethylated in ACD/MPV samples except for one DMR detected in the ACD-mut vs. control analysis (*), this DMR was hypomethylated in ACD-mut samples. Genomic coordinates are based on Chr16(GRCh38).

Using bisulphite sequencing, Schulze and colleagues recently identified a paternally imprinted region in the 60kb *FOXF1* enhancer 10kb upstream of LINC01082 (Hg38 chr16: 86186428-86186443) (16). Since our ACD-del and control samples carried an intact paternal allele, we investigated whether this region was methylated in our samples. We did not detect abundant CpG methylation in this region, even though MeD-seq would be able to detect methylation at half of the CpG sites in this region if methylated, questioning the validity of paternal imprinting in this region (Suppl. figure 3B).

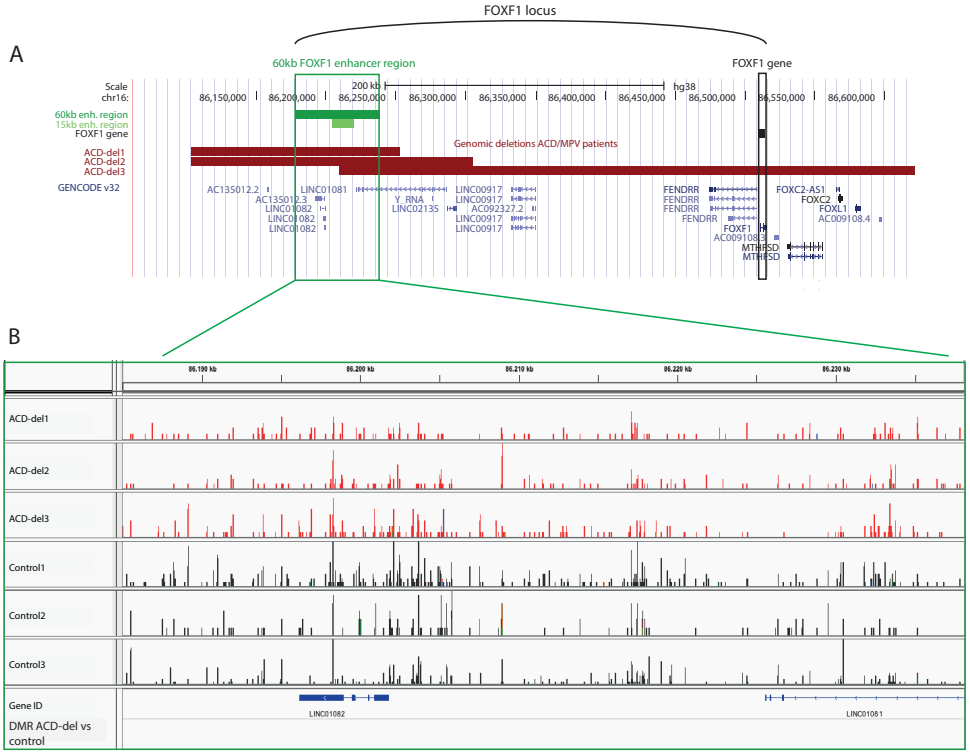

Figure 2. Absence of DMRs in ACD-del samples excludes maternal imprinting *A:* Overview of the *FOXF1* locus in the UCSC genome browser (GRCh38). The three maternal deletions of ACD-del samples involving the 60kb *FOXF1* enhancer are depicted in red. B: Methylation patterns of the three ACD-del (red) and control samples (grey) in the 60kb *FOXF1* enhancer depicted in IGV viewer. No significant DMRs were detected in the *FOXF1* enhancer as shown by the empty 'DMR ACD-del vs. control' track.

Two hypermethylated regions in the 60kb FOXF1 enhancer of ACD/MPV patients with FOXF1 point mutations

Next, we compared methylation patterns between ACD-mut and control samples and found seven DMRs distributed over the *FOXF1* enhancer and the 250kb region between the enhancer and *FOXF1* (Table 2; Figure 3A). The two DMRs located inside the 60kb *FOXF1* enhancer were both hypermethylated in ACD-mut samples compared to controls, but also compared to ACD-del and ACD-none samples (Figure 3A-B). Interestingly, both DMRs were located within the 15kb of the enhancer region which is thought to be the critical region that needs to be deleted in order to cause the typical ACD/MPV phenotype (Figure 3C)(6). Moreover, one of these DMRs (DMR2) encompasses the 250bp that have been

shown to physically interact with the *FOXF1* promoter (10). Since ACD-mut samples do not contain single nucleotide polymorphisms (SNPs) in the identified DMRs, it is unclear whether only one or both parental alleles of ACD-mut samples are hypermethylated.

Hypermethylation of the first FOXF1 exon in lung tissue of an ACD/MPV patient without a genomic FOXF1 variant

In our previous study, we described four patients with typical severe ACD/MPV phenotypes in which we could not detect genomic *FOXF1* alterations classified as pathogenic or likely pathogenic (3). To investigate whether aberrant DNA methylation could contribute to the phenotypes of these patients, we compared methylation patterns of the two patients from which we had lung tissue available (ACD-none) with methylation patterns of control lung samples (Table 2). As we only had two samples of this group, normalized read counts in the *FOXF1* locus were manually reviewed without bioinformatical analysis. In contrast to the ACD-mut samples, we did not observe DMRs located in the *FOXF1* enhancer region. However, we found a highly methylated region in sample ACD-none2 that covered exon 1 of *FOXF1* (Figure 4A). This hypermethylated region was not observed in any of the other lung samples tested in this study. Finally, since we had bowel and lymph node tissue of patient ACD-none1 available from autopsy, we compared the methylation pattern at the *FOXF1* locus in bowel, lymph node and lung tissues to explore the presence of tissue specific methylation patterns in the *FOXF1* locus. The DNA methylation patterns in bowel tissue showed no evident differences compared to the methylation pattern in lung tissue. However, lymph node tissue of ACD-none1 contained a highly methylated region covering exon 1 that was not present in lung tissue of ACD-none1 (Figure 4B). As it was remarkable that this region was similarly methylated in the lung sample of ACD-none2 and not in any of the other lung tissues tested, the origin of each tissue block was re-confirmed by the department of pathology at the Erasmus MC.

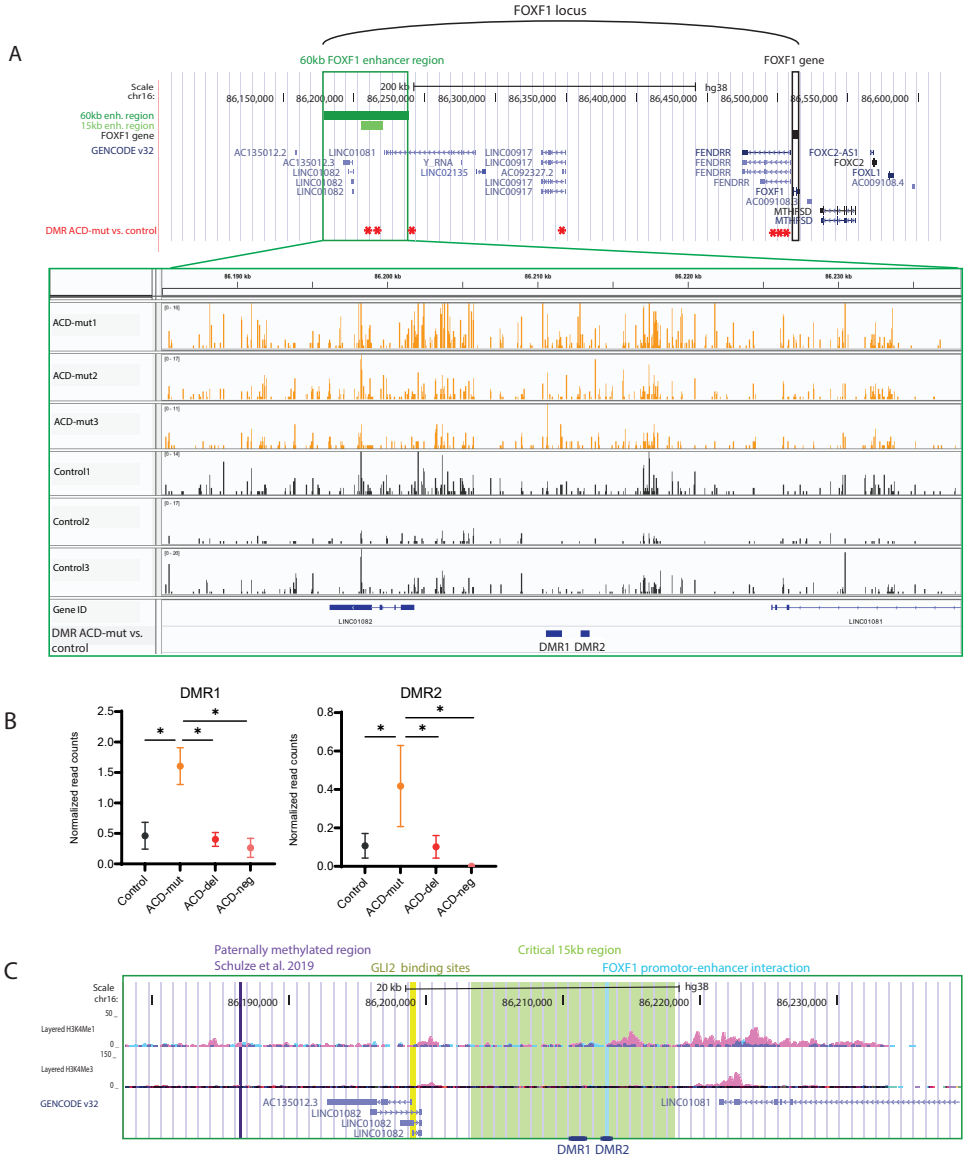

Figure 3. ACD-mut samples contain two hypermethylated regions in the 60kb FOXF1 enhancer potentially altering FOXF1 expression *A: Overview of the FOXF1 locus in UCSC genome browser (GRCh38) and methylation patterns of ACD-mut samples (orange) and control samples (grey) in the 60kb enhancer in IGV viewer. Red asterisk in upper panel: significant DMRs between ACD-mut and control samples. B: Mean and standard deviation of normalized read counts in DMR1 and DMR2 for all lung samples (*: p<0.05 in group vs. group analysis). C: Overview of the 60kb enhancer region in UCSC genome browser (GRCh38). DMR1 and DMR2 are located within the 15kb critical region (light green). DMR2 overlaps with the region that physically interacts with the FOXF1 promotor (light blue) (10) and is located close to the H3K4Me1 peak of human lung fibroblasts (pink). Both DMRs are downstream of the previous proposed paternally methylated region (purple) (15) and GLI2 binding sites (yellow) (10).*

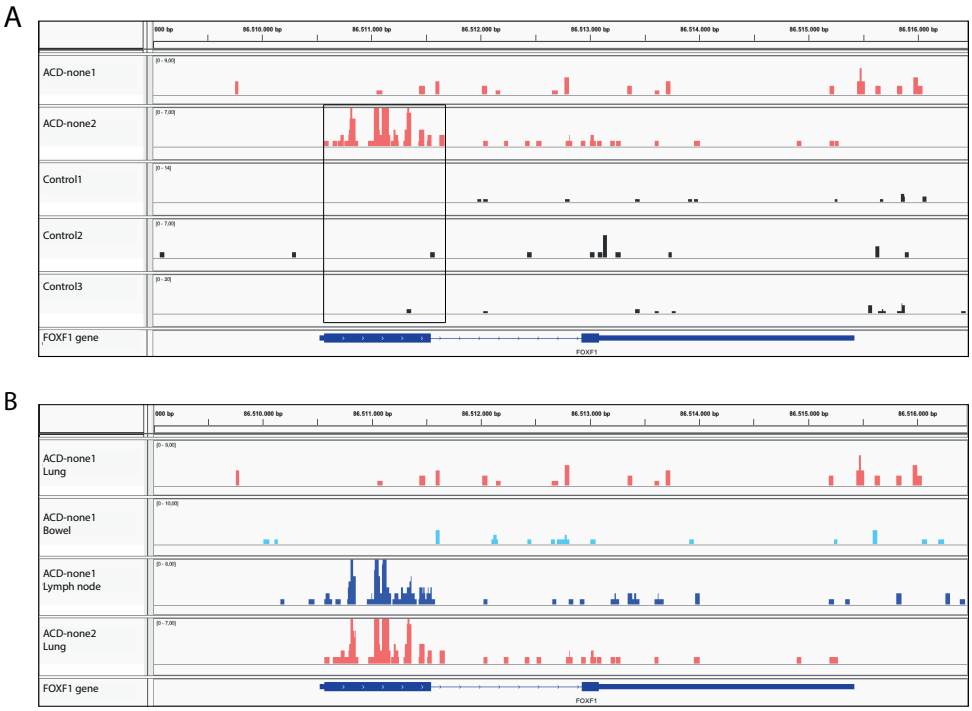

Figure 4. Hypermethylation of the first exon of FOXF1 in an ACD/MPV patient without a genomic FOXF1 variant *A: Hypermethylated region encompassing the first exon of FOXF1 in ACD-none2, demonstrated in IGV viewer. Methylation patterns of ACD-none (red) and control samples (grey) are shown. B: DNA methylation patterns of ACD-none lung tissues (light red), bowel tissue of ACD-none1 (light blue) and lymph tissue of ACD-none1 (dark blue) depicted with IGV viewer. Both lymph tissue of ACD-none1 and lung tissue of ACD-none2 demonstrate a highly methylated region covering exon 1.*

DISCUSSION

The aim of the present study was to identify genome wide methylation patterns in lung tissue of ACD/MPV patients, with specific focus on the *FOXF1* locus to identify potential differences that might play a role in the pathogenesis of ACD/MPV. Comparison of ACD/MPV lung tissue with control lung tissue resulted in 319 DMRs genome wide, possibly affecting gene regulation of 115 protein coding genes. Interestingly, pathway analysis showed that the potentially upregulated genes are mainly involved in developmental processes. This conforms the developmental delay that is indicated by histological aspects of ACD/MPV lungs, such as reduced numbers of alveolar capillaries and increased numbers of type 2 pneumocytes (2). For example, the most significantly enriched gene cluster of potentially upregulated genes included *TIE1* and *NOTCH1*, which are implicated in vascular development (27-32). Furthermore, this cluster included *COL4A2* and *TGFB1*,

which are involved in alveolar and airway branching morphogenesis respectively (33, 34). *SOCS3*, an inhibitor of the JAK/STAT signalling pathway (35, 36) was among the potentially upregulated genes as well, in line with the previously demonstrated reduction of STAT3 protein in lung tissue of ACD/MPV patients (37). The most significantly enriched gene cluster of potentially downregulated genes included *MUC5AC, ADAMTS2* and *GALNT15* which are all involved in O-linked glycosylation, a post-translational process regulating protein function. Of these, MUC5AC is secreted by goblet cells of the lower respiratory tract where it contributes to the mucocilliary clearance as part of the innate immune system (38-40). However, the relevance of downregulation of O-linked glycosylation in relation to ACD/MPV is unclear. In summary, the results of our genome-wide methylation analysis implicate up- and downregulation of a range of genes in ACD/MPV. Whether these genes are indeed dysregulated and what their specific role is in ACD/MPV, requires further investigation. Additionally, similar to the patients included in the current study, genetic testing of ACD/MPV patients has been mainly directed at the *FOXF1* locus, potentially obscuring detection of alterations in other genes. Therefore, our findings could serve as a basis to expand genetic testing in ACD/MPV patients to study whether these genes harbour genomic alterations that contribute to ACD/MPV.

Through comparison of all included ACD/MPV lung samples together with control samples we did not find significant DMRs in the *FOXF1* locus. Similarly, no significant DMRs were found in the *FOXF1* locus when we compared the group of ACD-del samples with control samples. The three ACD-del samples included in this study harbour a large deletion (partly) encompassing the *FOXF1* enhancer on the maternal allele. And thus, the absence of DMRs in comparison indicates that the methylation pattern of the unaffected paternal allele is similar to the combined methylation patterns of both alleles in control samples. In line with previous studies, these results indicate that if the *FOXF1* enhancer is imprinted through DNA methylation, this involves the paternal allele (Suppl. figure 2A, right panel) (4, 6, 9, 16). Although MeD-seq revealed multiple regions within the 60kb enhancer that are methylated on the paternal allele of ACD-del samples, additional methylation studies and analyses are needed to define if these regions are paternally imprinted. For instance, a detailed SNP analysis on methylation data from multiple control samples could indicate whether certain regions at the 60kb enhancer favour methylation at one allele. Using parental SNP data, one could identify on which parental allele the

specific methylation occurs. Furthermore, bisulphite sequencing could be applied to identify paternally methylated regions using ACD-del samples. Since this technique also sequences unmethylated regions, it is possible to perform a quantitative comparison between the methylation in ACD-del samples harbouring a maternal deletion, and control samples. If specific regions in the 60kb *FOXF1* enhancer are paternally imprinted, then 100% of the reads of the ACD-del samples would be methylated, compared to 50% of the reads in control samples. Due to DNA degradation in the FFPE tissue blocks that have been stored for many years, we were unable to perform bisulphite sequencing with the current collected samples (41).

When we compared the three ACD-mut samples with control samples, two significant hypermethylated regions were detected in the *FOXF1* enhancer, potentially interfering with normal gene regulation. Recently, it was shown that rare genomic variants in transcription factor binding sites can influence DNA methylation patterns, presumably leading to altered expression of nearby genes (42). Although the mechanisms are unclear yet, it has been proposed that mutations could cause altered transcription factor binding, leading to formation of protein complexes with the DNA methylation machinery and thereby, alter DNA methylation. To investigate whether *FOXF1* point mutations influence methylation at the *FOXF1* enhancer, it would be interesting to study the DNA methylation status in primary human lung cells before and after introduction of a site-specific mutation in the *FOXF1* gene. Endothelial colony forming cells, for instance, have a high FOXF1 expression, are easily isolated from lung tissue, and may therefore, be a suitable cell type to investigate their methylation profile in the 60kb enhancer before and after introduction of a *FOXF1* mutation(43). However, it would be ideal to study multiple cell types so that cell type specific differences in methylation patterns can be recognized. One of the mechanisms by which *FOXF1* enhancer methylation could interfere with *FOXF1* regulation is by changing the interaction between the enhancer and the *FOXF1* promoter. Therefore, it would be an interesting next step to use the ACD-mut samples to perform assay for transposase-accessible chromatin with sequencing (ATAC-Seq) (44) or universal NicE-seq (UniNicE-seq) (45). This could clarify whether enhancer methylation alters the chromatin state in the TAD harbouring the *FOXF1* enhancer and gene, leading to an altered interaction.

In one of the ACD-none samples (ACD-none2) we detected a highly methylated region completely overlapping exon 1 of *FOXF1*. According to the Eukaryotic Promoter Database (EPD), the *FOXF1* core-promoter sequence ends approximately 40bp downstream of the transcription start site (TSS) and 30bp upstream of the start of exon 1 which means that the hypermethylated region does not overlap with the *FOXF1* promoter (46). Currently, very little is known about the exact consequences of DNA methylation of exon 1 methylation on gene regulation. Therefore, it should be further investigated whether this hypermethylated region is associated with gene activation similar to other methylated regions overlapping gene bodies, or if this methylated region is close enough to the promoter to cause gene silencing, for instance by disrupting polymerase binding. Although only one lymph node sample was tested, the observation that exon 1 is hypermethylated in lymph tissue but not in the gastro-intestinal tissue or any of the lung tissues samples other than ACD-none2, could indicate that exon 1 methylation is indeed associated with reduced *FOXF1* expression since lymph node tissue is also the only tested tissue that normally does not express FOXF1 (47). However, Szafranski and colleagues also found methylation of exon 1 in a normal lung sample (10). Therefore, expression analyses in relation to exon 1 methylation are necessary before any conclusions about the relevance of the hypermethylated region in ACD-none2 can be drawn. In our previous study we showed that patient ACD-none2 carried a duplication in the 3' UTR of *FOXF1* that was also present in the healthy father of the patient (3). Although this variant has been classified as likely benign according to the ACMG classification (48), we cannot exclude that this variant contributed to the ACD/MPV phenotype, for instance through altering DNA as suggested by our findings in ACD-mut samples. As multiple ACD/MPV patients have been described without a known genomic *FOXF1* variant, it would be interesting to investigate their methylation status to get a better indication of the contribution of abnormal *FOXF1* methylation in the pathogenesis of ACD/MPV (4).

In this study we investigated methylation patterns that led to many new hypotheses about the role of DNA methylation in the pathogenesis of ACD/MPV. To fully comprehend these results, additional expression analysis would be required. However, a limitation of this study was the quality of FFPE tissue blocks which was poor and highly variable, complicating reliable expression analyses. In our experience, these type of blocks frequently have partially degraded RNA, hampering RNA in situ hybridisations or qPCR

analyses. Additional studies with FFPE blocks that have been processed similarly and stored for less than 5 years, or with fresh or frozen lung tissue, are needed to confirm our hypotheses.

Because DNA methylation is tissue specific, we used lung tissues to study methylation patterns that could contribute to the lung abnormalities observed in ACD/MPV patients (15, 21). However, lung tissue contains a heterogeneous cell population and thus, the DMRs identified are not cell type specific. In human and mice lung tissue, FOXF1 is mainly expressed in mesenchymal, smooth muscle and endothelial cells (47, 49-51). To study whether aberrant methylation of the *FOXF1* locus is specific for one of these cell types, it would be interesting to study DNA methylation patterns in sorted cells from fresh ACD/MPV lung tissues.

CONCLUSION

This study provides genome wide methylation data on lung tissue of ACD/MPV patients. A detailed investigation of the *FOXF1* locus revealed hypermethylation in the *FOXF1* enhancer in ACD/MPV patients harbouring a point mutation in the *FOXF1* gene and abnormal hypermethylation of exon 1 in a patient without a genomic *FOXF1* variant. These abnormal methylation patterns potentially change the regulation of *FOXF1* contributing to the pathogenesis of ACD/MPV. This is the first study presenting *FOXF1* specific methylation data in relation to different genomic *FOXF1* variants associated with ACD/MPV and serves as important starting point for further research.

REFERENCES

1. Stankiewicz P, Sen P, Bhatt SS, Storer M, Xia Z, Bejjani BA, et al. Genomic and genic deletions of the FOX gene cluster on 16q24.1 and inactivating mutations of FOXF1 cause alveolar capillary dysplasia and other malformations. Am J Hum Genet. 2009;84(6):780-91.
2. Slot E, Edel G, Cutz E, van Heijst A, Post M, Schnater M, et al. Alveolar capillary dysplasia with misalignment of the pulmonary veins: clinical, histological, and genetic aspects. Pulm Circ. 2018;8(3):2045894018795143.
3. Slot E, von der Thusen JH, van Heijst A, van Marion R, Magielsen F, Dubbink HJ, et al. Fast detection of FOXF1 variants in patients with alveolar capillary dysplasia with misalignment of pulmonary veins using targeted sequencing. Pediatr Res. 2020.
4. Szafranski P, Gambin T, Dharmadhikari AV, Akdemir KC, Jhangiani SN, Schuette J, et al. Pathogenetics of alveolar capillary dysplasia with misalignment of pulmonary veins. Hum Genet. 2016;135(5):569-86.
5. Szafranski P, Dharmadhikari AV, Wambach JA, Towe CT, White FV, Grady RM, et al. Two deletions overlapping a distant FOXF1 enhancer unravel the role of lncRNA LINC01081 in etiology of alveolar capillary dysplasia with misalignment of pulmonary veins. Am J Med Genet A. 2014;164A(8):2013-9.
6. Szafranski P, Herrera C, Proe LA, Coffman B, Kearney DL, Popek E, et al. Narrowing the FOXF1 distant enhancer region on 16q24.1 critical for ACDMPV. Clin Epigenetics. 2016;8:112.
7. Mahlapuu M, Enerback S, Carlsson P. Haploinsufficiency of the forkhead gene Foxf1, a target for sonic hedgehog signaling, causes lung and foregut malformations. Development. 2001;128(12):2397-406.
8. Dharmadhikari AV, Szafranski P, Kalinichenko VV, Stankiewicz P. Genomic and Epigenetic Complexity of the FOXF1 Locus in 16q24.1: Implications for Development and Disease. Curr Genomics. 2015;16(2):107-16.
9. Sen P, Gerychova R, Janku P, Jezova M, Valaskova I, Navarro C, et al. A familial case of alveolar capillary dysplasia with misalignment of pulmonary veins supports paternal imprinting of FOXF1 in human. Eur J Hum Genet. 2013;21(4):474-7.
10. Szafranski P, Dharmadhikari AV, Brosens E, Gurha P, Kolodziejska KE, Zhishuo O, et al. Small noncoding differentially methylated copy-number variants, including lncRNA genes, cause a lethal lung developmental disorder. Genome Res. 2013;23(1):23-33.
11. Deaton AM, Bird A. CpG islands and the regulation of transcription. Genes Dev. 2011;25(10):1010-22.
12. Lo PK, Lee JS, Liang X, Han L, Mori T, Fackler MJ, et al. Epigenetic inactivation of the potential tumor suppressor gene FOXF1 in breast cancer. Cancer Res. 2010;70(14):6047-58.
13. Alsina Casanova M, Monteagudo-Sanchez A, Rodiguez Guerineau L, Court F, Gazquez Serrano I, Martorell L, et al. Maternal mutations of FOXF1 cause alveolar capillary dysplasia despite not being imprinted. Hum Mutat. 2017;38(6):615-20.
14. Szafranski P, Gambin T, Karolak JA, Popek E, Stankiewicz P. Lung-specific distant enhancer cis regulates expression of FOXF1 and lncRNA FENDRR. Hum Mutat. 2021;42(6):694-8.
15. Schultz MD, He Y, Whitaker JW, Hariharan M, Mukamel EA, Leung D, et al. Human body epigenome maps reveal noncanonical DNA methylation variation. Nature. 2015;523(7559):212-6.
16. Schulze KV, Szafranski P, Lesmana H, Hopkin RJ, Hamvas A, Wambach JA, et al. Novel parent-of-origin-specific differentially methylated loci on chromosome 16. Clin Epigenetics. 2019;11(1):60.
17. Boers R, Boers J, de Hoon B, Kockx C, Ozgur Z, Molijn A, et al. Genome-wide DNA methylation profiling using the methylation-dependent restriction enzyme LpnPI. Genome Res. 2018;28(1):88-99.
18. Arechederra M, Daian F, Yim A, Bazai SK, Richelme S, Dono R, et al. Hypermethylation of gene body CpG islands predicts high dosage of functional oncogenes in liver cancer. Nat Commun. 2018;9(1):3164.

19. Bird A. DNA methylation patterns and epigenetic memory. Genes Dev. 2002;16(1):6-21.
20. Fan L, Zhang A, Deng P. LMX1B mRNA expression and its gene body CpG methylation are valuable prognostic biomarkers for laryngeal squamous cell carcinoma. Biomed Pharmacother. 2019;117:109174.
21. Greenberg MVC, Bourc'his D. The diverse roles of DNA methylation in mammalian development and disease. Nat Rev Mol Cell Biol. 2019;20(10):590-607.
22. Jones PA. Functions of DNA methylation: islands, start sites, gene bodies and beyond. Nat Rev Genet. 2012;13(7):484-92.
23. Jones PA, Baylin SB. The epigenomics of cancer. Cell. 2007;128(4):683-92.
24. Ponnaluri VK, Ehrlich KC, Zhang G, Lacey M, Johnston D, Pradhan S, et al. Association of 5-hydroxymethylation and 5-methylation of DNA cytosine with tissue-specific gene expression. Epigenetics. 2017;12(2):123-38.
25. Wang YW, Ma X, Zhang YA, Wang MJ, Yatabe Y, Lam S, et al. ITPKA Gene Body Methylation Regulates Gene Expression and Serves as an Early Diagnostic Marker in Lung and Other Cancers. J Thorac Oncol. 2016;11(9):1469-81.
26. Zhou Y, Zhou B, Pache L, Chang M, Khodabakhshi AH, Tanaseichuk O, et al. Metascape provides a biologist-oriented resource for the analysis of systems-level datasets. Nat Commun. 2019;10(1):1523.
27. Partanen J, Puri MC, Schwartz L, Fischer KD, Bernstein A, Rossant J. Cell autonomous functions of the receptor tyrosine kinase TIE in a late phase of angiogenic capillary growth and endothelial cell survival during murine development. Development. 1996;122(10):3013-21.
28. Iljin K, Petrova TV, Veikkola T, Kumar V, Poutanen M, Alitalo K. A fluorescent Tie1 reporter allows monitoring of vascular development and endothelial cell isolation from transgenic mouse embryos. FASEB J. 2002;16(13):1764-74.
29. Augustin HG, Koh GY, Thurston G, Alitalo K. Control of vascular morphogenesis and homeostasis through the angiopoietin-Tie system. Nat Rev Mol Cell Biol. 2009;10(3):165-77.
30. Benedito R, Roca C, Sorensen I, Adams S, Gossler A, Fruttiger M, et al. The notch ligands Dll4 and Jagged1 have opposing effects on angiogenesis. Cell. 2009;137(6):1124-35.
31. Hasan SS, Tsaryk R, Lange M, Wisniewski L, Moore JC, Lawson ND, et al. Endothelial Notch signalling limits angiogenesis via control of artery formation. Nat Cell Biol. 2017;19(8):928-40.
32. Benedito R, Rocha SF, Woeste M, Zamykal M, Radtke F, Casanovas O, et al. Notch-dependent VEGFR3 upregulation allows angiogenesis without VEGF-VEGFR2 signalling. Nature. 2012;484(7392):110-4.
33. Loscertales M, Nicolaou F, Jeanne M, Longoni M, Gould DB, Sun Y, et al. Type IV collagen drives alveolar epithelial-endothelial association and the morphogenetic movements of septation. BMC Biol. 2016;14:59.
34. Noe N, Shim A, Millette K, Luo Y, Azhar M, Shi W, et al. Mesenchyme-specific deletion of Tgf-beta1 in the embryonic lung disrupts branching morphogenesis and induces lung hypoplasia. Lab Invest. 2019;99(9):1363-75.
35. Babon JJ, Kershaw NJ, Murphy JM, Varghese LN, Laktyushin A, Young SN, et al. Suppression of cytokine signaling by SOCS3: characterization of the mode of inhibition and the basis of its specificity. Immunity. 2012;36(2):239-50.
36. Carow B, Rottenberg ME. SOCS3, a Major Regulator of Infection and Inflammation. Front Immunol. 2014;5:58.
37. Pradhan A, Dunn A, Ustiyan V, Bolte C, Wang G, Whitsett JA, et al. The S52F FOXF1 Mutation Inhibits STAT3 Signaling and Causes Alveolar Capillary Dysplasia. Am J Respir Crit Care Med. 2019.
38. Holmen JM, Karlsson NG, Abdullah LH, Randell SH, Sheehan JK, Hansson GC, et al. Mucins and their O-Glycans from human bronchial epithelial cell cultures. Am J Physiol Lung Cell Mol Physiol. 2004;287(4):L824-34.
39. Rose MC, Voynow JA. Respiratory tract mucin genes and mucin glycoproteins in health and disease. Physiol Rev. 2006;86(1):245-78.
40. Ridley C, Thornton DJ. Mucins: the frontline defence of the lung. Biochem Soc Trans. 2018;46(5):1099-106.

41. Ludgate JL, Wright J, Stockwell PA, Morison IM, Eccles MR, Chatterjee A. A streamlined method for analysing genome-wide DNA methylation patterns from low amounts of FFPE DNA. BMC Med Genomics. 2017;10(1):54.
42. Martin-Trujillo A, Patel N, Richter F, Jadhav B, Garg P, Morton SU, et al. Rare genetic variation at transcription factor binding sites modulates local DNA methylation profiles. PLoS Genet. 2020;16(11):e1009189.
43. Sturtzel C, Lipnik K, Hofer-Warbinek R, Testori J, Ebner B, Seigner J, et al. FOXF1 Mediates Endothelial Progenitor Functions and Regulates Vascular Sprouting. Front Bioeng Biotechnol. 2018;6:76.
44. Buenrostro JD, Giresi PG, Zaba LC, Chang HY, Greenleaf WJ. Transposition of native chromatin for fast and sensitive epigenomic profiling of open chromatin, DNA-binding proteins and nucleosome position. Nat Methods. 2013;10(12):1213-8.
45. Chin HG, Sun Z, Vishnu US, Hao P, Cejas P, Spracklin G, et al. Universal NicE-seq for high-resolution accessible chromatin profiling for formaldehyde-fixed and FFPE tissues. Clin Epigenetics. 2020;12(1):143.
46. Dreos R, Ambrosini G, Perier RC, Bucher P. The Eukaryotic Promoter Database: expansion of EPDnew and new promoter analysis tools. Nucleic Acids Res. 2015;43(Database issue):D92-6.
47. Uhlen M, Fagerberg L, Hallstrom BM, Lindskog C, Oksvold P, Mardinoglu A, et al. Proteomics. Tissue-based map of the human proteome. Science. 2015;347(6220):1260419.
48. Richards S, Aziz N, Bale S, Bick D, Das S, Gastier-Foster J, et al. Standards and guidelines for the interpretation of sequence variants: a joint consensus recommendation of the American College of Medical Genetics and Genomics and the Association for Molecular Pathology. Genet Med. 2015;17(5):405-24.
49. Kalinichenko VV, Lim L, Stolz DB, Shin B, Rausa FM, Clark J, et al. Defects in pulmonary vasculature and perinatal lung hemorrhage in mice heterozygous null for the Forkhead Box f1 transcription factor. Dev Biol. 2001;235(2):489-506.
50. Mahlapuu M, Pelto-Huikko M, Aitola M, Enerback S, Carlsson P. FREAC-1 contains a cell-type-specific transcriptional activation domain and is expressed in epithelial-mesenchymal interfaces. Dev Biol. 1998;202(2):183-95.
51. Steiner LA, Getman M, Schiralli Lester GM, Iqbal MA, Katzman P, Szafranski P, et al. Disruption of normal patterns of FOXF1 expression in a lethal disorder of lung development. J Med Genet. 2020;57(5):296-300.

SUPPLEMENTARY DATA

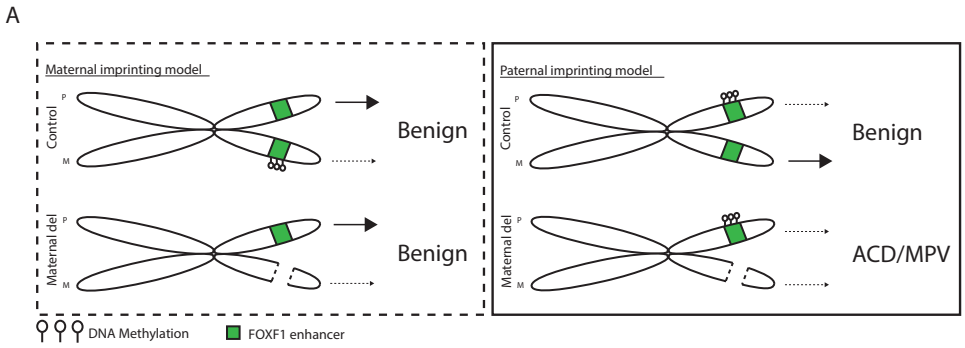

Supplementary figure 1. Simplistic illustration of the two models for parental imprinting of the 60kb FOXF1 enhancer *Based on the suggested models by Szafranski et al. (4). Continuous arrow: full function of the FOXF1 enhancer. Dotted arrow: reduced function of the FOXF1 enhancer.*

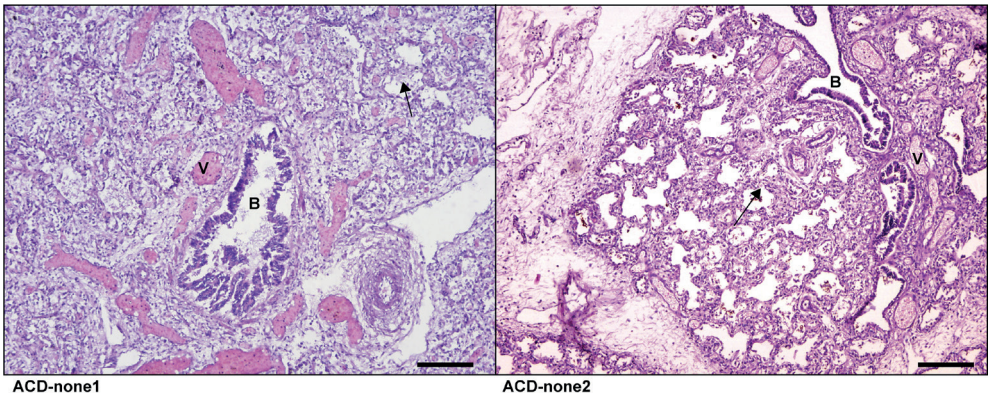

Supplementary figure 2. Haematoxylin and eosin staining of lung tissues of patients ACD-none1 and ACD-none2 demonstrating the main characteristics of ACD/MPV (2). *Arrow: thickened alveolar wall. V: misaligned pulmonary vein. B: bronchiole. Scale bar: 200µm.*

A

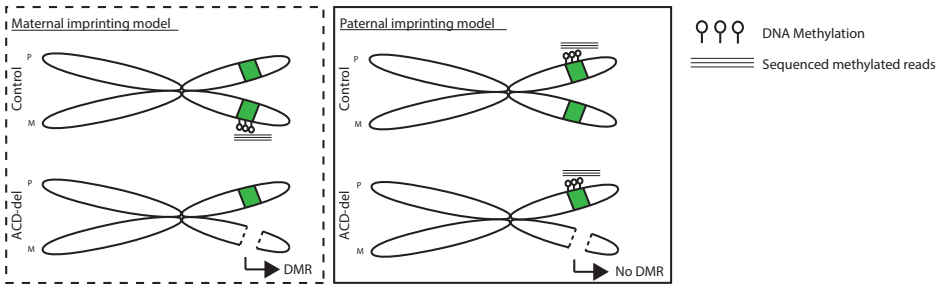

B

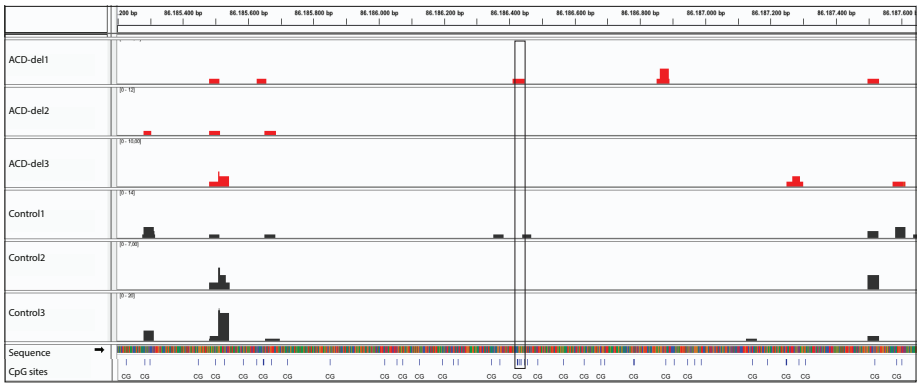

Supplementary figure 3. *A: Models of maternal and paternal imprinting of the 60kb FOXF1 enhancers through DNA methylation. The absence of DMRs in ACD-del samples makes maternal imprinting of the FOXF1 enhancer unlikely and supports a paternal imprinting model. B: Methylation status of CpG sites of previously suggested paternally methylated region (rectangular frame) (15) in ACD-del and control samples. Read counts of each individual samples is demonstrated with IGV viewer (red: ACD-del, grey: control).*

Supplementary table 1. Lists of potentially up- and downregulated genes based on methylation status and TSS/GB overlap
TSS: promotor, GB: Gene body. ↑: hypermethylated in ACD/MPV samples, ↓: hypomethylated in ACD/MPV samples.

Potentially upregulated genes

Gene ID	DMR overlap with TSS or GB	Methylation ACD/MPV	Fold Change
TIE1	GB	↑	7.91
RERE	GB	↑	5.09
SYN3	GB	↑	5.06
TIMP3	GB	↑	5.06
HOXB3	GB	↑	4.68
HOXB6	GB	↑	4.68
CIRBP	GB	↑	4.61
AMZ1	GB	↑	4.55
GEMIN4	GB	↑	4.03
HOXD3	GB	↑	4.00
BAIAP2	GB	↑	3.91
MIDN	GB	↑	3.83
VAC14	GB	↑	3.75
PEBP4	GB	↑	3.72
SOCS3	GB	↑	3.70
KDM6B	GB	↑	3.68
RIMBP2	GB	↑	3.61
ADAMTSL4	GB	↑	3.60
SH3D21	GB	↑	3.43
EVA1B	GB	↑	3.43
RAD51B	GB	↑	3.43
IRF8	GB	↑	3.38
TBC1D1	GB	↑	3.36
CCDC40	GB	↑	3.30
HOXA3	GB	↑	3.28
C6orf132	GB	↑	3.15
DHRS3	GB	↑	3.12
CHMP1A	GB	↑	3.08
CBX4	GB	↑	3.08
ARRB1	GB	↑	3.07
CYGB	GB	↑	3.02
PRCD	GB	↑	3.02
PDE11A	GB	↑	3.00
SART1	GB	↑	2.95
PKNOX2	GB	↑	2.92
PRKAR1B	GB	↑	2.91
ADAMTS17	GB	↑	2.86
TAOK2	GB	↑	2.80
CROCC	GB	↑	2.76
GATA2	GB	↑	2.75
GPR133	GB	↑	2.75
NXN	GB	↑	2.72
PTBP1	GB	↑	2.70
RXRA	GB	↑	2.69
NOTCH1	GB	↑	2.69

Gene ID	DMR overlap with TSS or GB	Methylation ACD/MPV	Fold Change
SNX33	GB	↑	2.67
CACNA1H	GB	↑	2.66
COL23A1	GB	↑	2.63
TMTC2	GB	↑	2.58
NFIC	GB	↑	2.57
ERICH1	GB	↑	2.56
SIPA1	GB	↑	2.48
PCGF3	GB	↑	2.46
PRKCZ	GB	↑	2.45
SEPT9	GB	↑	2.42
DENND3	GB	↑	2.41
SPTB	GB	↑	2.40
MRPS9	GB	↑	2.38
TGFB1	GB	↑	2.29
CCDC97	GB	↑	2.29
COL4A2	GB	↑	2.28
BAZ2A	GB	↑	2.27
RECQL5	GB	↑	2.22
FAM110A	GB	↑	2.20
SLC16A3	GB	↑	2.16
CSNK1D	GB	↑	2.16
RPTOR	GB	↑	2.15
KATNAL2	GB	↑	2.15
TCEB3CL	GB	↑	2.15
RAB12	GB	↑	2.08
CHST15	GB	↑	2.08
KIFC3	GB	↑	2.08
LRFN5	GB	↑	2.07
SEC16A	GB	↑	2.06
TENM4	GB	↑	2.04
KRTAP10-3	TSS	↓	2.04
PRDM16	GB	↑	2.02
EHMT1	GB	↑	2.01
ABCC2	GB	↑	2.01

Potentially downregulated genes

Gene ID	DMR overlap with TSS or GB	Methylation ACD/MPV	Fold change
PLEC	TSS	↑	7.11
GALNT15	GB	↓	5.65
CYP2E1	GB	↓	5.46
DPEP1	GB	↓	4.28
LBX2	TSS	↑	3.82
ADARB2	GB	↓	3.55
ZNF835	GB	↓	3.44
AK1	TSS	↑	3.29
CCDC6	GB	↓	3.08
LSG1	GB	↓	3.01
RBFOX1	GB	↓	2.88

Gene ID	DMR overlap with TSS or GB	Methylation ACD/MPV	Fold change
SUGCT	GB	↓	2.65
PDE11A	GB	↓	2.60
POLRMT	GB	↓	2.60
TOLLIP	GB	↓	2.52
SMYD3	GB	↓	2.47
ADAMTS2	GB	↓	2.46
PTH2R	GB	↓	2.46
EFTUD1	GB	↓	2.42
PCBP3	GB	↓	2.42
DLGAP2	GB	↓	2.33
TULP4	GB	↓	2.33
PIGQ	GB	↓	2.27
ERICH1	GB	↓	2.25
IL1A	GB	↓	2.24
C10orf76	GB	↓	2.21
PTPRN2	GB	↓	2.21
CCDC47	GB	↓	2.18
DIP2C	GB	↓	2.18
MUC5AC	GB	↓	2.16
PRR21	TSS	↑	2.12
KLHDC4	GB	↓	2.12
TTC34	GB	↓	2.11
MFSD8	GB	↓	2.07
INPP5E	TSS	↑	2.06
TSPEAR	GB	↓	2.04

Supplementary table 2. Results of gene ontology enrichment analysis using Metascape (36) (ONLINE ONLY)

CHAPTER 5

GENERATION OF THREE IPSC LINES FROM TWO PATIENTS WITH HETEROZYGOUS *FOXF1* MUTATIONS ASSOCIATED TO ALVEOLAR CAPILLARY DYSPLASIA WITH MISALIGNMENT OF THE PULMONARY VEINS

Evelien Slot[a,b], Annelies de Klein[b], Robbert Rottier[a,c]

a. Department of Pediatric Surgery, Sophia Children's Hospital, Rotterdam
b. Department of Clinical Genetics, Erasmus University Medical Center, Rotterdam
c. Department of Cell Biology, Erasmus MC, Rotterdam

Published in Stem Cell Research, 2020

ABSTRACT

Diagnosing Alveolar Capillary Dysplasia with Misalignment of the Pulmonary Veins (ACD/MPV) based on a genetic alteration in the *FOXF1* gene, is complicated by the poor understanding of the causal relation between *FOXF1* variants and the ACD/MPV phenotype. Here, we report the generation of human iPSC lines from two ACD/MPV patients, each carrying a different heterozygous *FOXF1* mutation, which enables disease modelling for further research on the effect of *FOXF1* variants *in vitro.* The iPSC lines were generated from skin fibroblasts using the non-integrating Sendai virus. The lines expressed pluripotency genes, retained the heterozygous mutation and were capable of trilineage differentiation.

Resource Table

Unique stem cell lines identifier	EMC127i-A EMC127i-B EMC128i-A
Alternative names of stem cell lines	EMC127i-A: ACD871C4 EMC127i-B: ACD871C8 EMC128i-A: ACD874C9
Institution	Erasmus University Medical Center Rotterdam, The Netherlands
Contact information of distributor	Robbert Rottier; r.rottier@erasmusmc.nl
Type of cell lines	iPSC
Origin	Human
Cell Source	Skin fibroblasts
Clonality	Clonal
Method of reprogramming	CytoTune-iPS 2.0 Sendai reprogramming
Multiline rationale	Two isogenic iPSC clones from ACD/MPV patient 1 and one iPSC clone from ACD/MPV patient 2.
Gene modification	Yes
Type of modification	Congenital, *de novo*
Associated disease	Alveolar Capillary Dysplasia with Misalignment of the Pulmonary Veins (ACD/MPV)
Gene/locus	Patient 1: FOXF1; 16q24.1; Chr16(GRCh37): g.86544341C>G (c.166C>G) Patient 2: FOXF1; 16q24.1; Chr16(GRCh37): g.86544428T>A (c.253T>A)
Method of modification	N/A
Name of transgene or resistance	N/A
Inducible/constitutive system	N/A
Date archived/stock date	EMC127i-A: 2019-5-1 EMC127i-B: 2019-4-25 EMC128i-A: 2019-5-28
Cell line repository/bank	https://hpscreg.eu/cell-line/EMCi127-A https://hpscreg.eu/cell-line/EMCi127-B https://hpscreg.eu/cell-line/EMCi128-A
Ethical approval	Medical Ethics Committee Erasmus MC Rotterdam, The Netherlands. Approval number: MEC-2017-302

RESOURCE UTILITY

The ACD/MPV patient specific iPSC lines are useful for disease modeling to investigate the pathogenesis of ACD/MPV. The iPSC lines will help to elucidate the effect of specific *FOXF1* mutations on the function of different cell types that are important during lung development.

RESOURCE DETAILS

Diagnosing congenital lung disorder Alveolar Capillary Dysplasia with Misalignment of the Pulmonary Veins (ACD/MPV) based on a genetic alteration in the *FOXF1* gene, is

complicated by the poor understanding of the causal relation between *FOXF1* variants and the ACD/MPV phenotype. Although several studies revealed a strong association with mutations and copy number variations in the *FOXF1* gene, an invasive lung biopsy is still necessary to confirm ACD/MPV.[1, 2] Studies in mice confirmed that FOXF1 is important in early lung development. However, rodent knock-down models do not display all ACD/MPV features that are observed in human patients.[3] Unfortunately, there is limited accessibility of patient samples, which complicates further research on ACD/MPV and FOXF1 function in human. Here, we report the generation of human iPSC lines from two ACD/MPV patients, each carrying a different heterozygous *FOXF1* mutation, which is a major contribution to the research field by enabling the investigation of FOXF1 function *in vitro.*

The iPSC lines were generated at the Erasmus MC iPS Core Facility from patient derived skin fibroblasts. From patient 1, who carried *FOXF1* mutation c.166C>G, we generated two isogenic iPSC clones. From patient 2, who carried *FOXF1* mutation c.253T>A[4], we generated one iPSC clone (Table 1). All lines showed iPSC morphology and expression of pluripotent markers NANOG, OCT4 and SSEA4 (Fig. 1A). In addition, quantitative RT-PCR revealed increased expression of NANOG and OCT3/4 compared to patients' skin fibroblasts, and similar expression compared to control line HuES9 [5] (Fig. 1B). Sanger sequencing confirmed the presence of the heterozygous mutations (Fig. 1C) and SNP arrays confirmed the absence of major copy number variations other than balanced translocations (Fig. 1D). Further, the numbers of SNP counts verified the identity of the iPSC lines (Suppl. Fig. 1B). All clones were mycoplasma free (Suppl. Fig. 1C) and able to differentiate into the three germ layers as shown by expression of trilineage markers (Fig. 1E) (Table 2).

Table 1: Summary of lines

iPSC line names	Gender	Age	Ethnicity	Genotype of locus	Disease
ACD871C4	Male	Newborn	Caucasian	c.166C>G	ACD/MPV
ACD871C8	Male	Newborn	Caucasian	c.166C>G	ACD/MPV
ACD874C9	Male	Newborn	Caucasian	c.253T>A	ACD/MPV

Fig. 1: Resource details

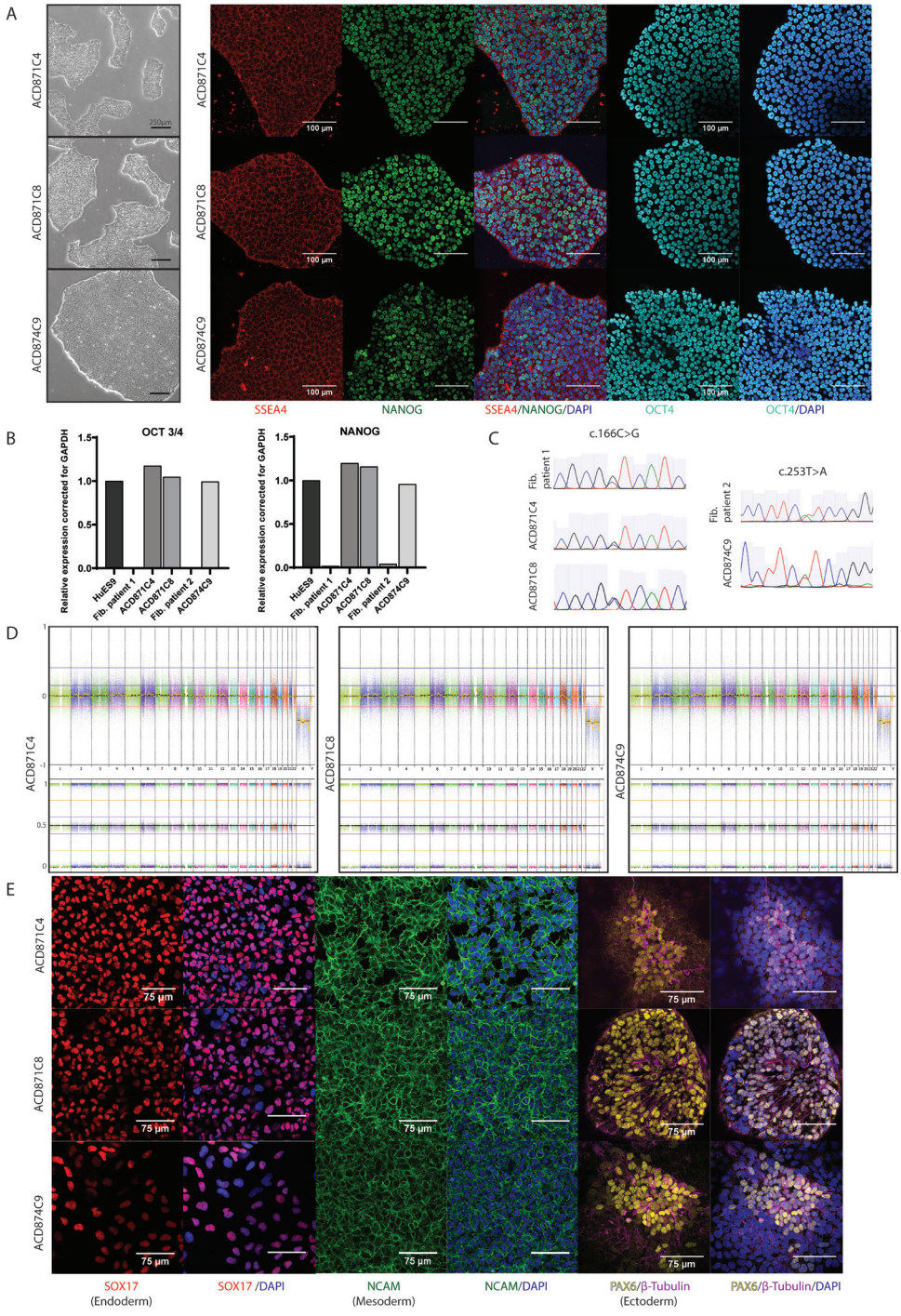

Table 2: Characterization and validation

Classification	Test	Result	Data
Morphology	Photography	Normal morphology	Fig. 1A
Phenotype	Qualitative analysis by immunohistochemistry	Expression of SSEA4, NANOG and OCT4	Fig. 1A
	Quantitative analysis by RT-qPCR	Expression of NANOG and OCT3/4	Fig. 1B
Genotype	GSAMD24 v1 Illumina Infinium SNP array 700k	Resolution 50kb: No major copy number variations or allelic changes	Fig. 1D
Identity	GSAMD24 v1 Illumina Infinium SNP array 700k	100,00% identical SNPs between fibroblasts and iPSCs	Supplementary fig. 1B
Mutation analysis	Sanger Sequencing	ACD871C4: Chr16(GRCh37): g.86544341C>G (c.166C>G) ACD871C8: Chr16(GRCh37): g.86544341C>G (c.166C>G) ACD874C9: Chr16(GRCh37): g.86544428T>A (c.253T>A)	Fig. 1C
Microbiology and virology	Mycoplasma testing by luminescence	Negative	Supplementary fig.1C
Differentiation potential	In vitro trilineage differentiation	Expression of specific germ layer markers SOX17 (endoderm), NCAM (mesoderm) and β-Tubulin (ectoderm)	Fig. 1E

MATERIALS AND METHODS

Ethical approval

iPSC lines were generated from anonymized fibroblasts that were previously isolated from skin tissues of ACD/MPV patients. The research proposal was approved by the Daily Board of the Medical Ethics Committee (METC) Erasmus University Medical Center Rotterdam, The Netherlands.

Generation and culture of human iPSC lines

Skin fibroblasts were reprogrammed using the CytoTune™-iPS 2.0 Sendai Reprogramming Kit (Invitrogen) according to the manufacturer's instructions. After reprogramming, single colonies were collected and maintained on Matrigel (Corning) plates in mTeSR™1 (STEMCELL Technologies) at 37 °C with 5% CO2. Every four days (at 80-90% confluency), the cells were passaged in an 1:6 ratio. The first five passages were done by means of mechanical passaging, all following passages were done using ReLeSR™ (Stem Cell Technologies). The absence of Sendai virus was confirmed by quantitative RT-PCR (Suppl. Fig. 1A) at passage 7 (ACD871C4-C8) and passage 9 (ACD874C9). As negative and

positive controls, RNA of non-transduced skin fibroblasts and skin fibroblasts 7 days after transduction were used.

Immunofluorescence staining

iPS cells were cultured on Geltrex (ThermoFisher Scientific) coated 4-well chamber slides (Sarstedt) and fixed for 15 min with 4% PFA at room temperature. Thereafter, cells were permeabilized with 0.1% Triton-X100 for 10 min and blocked with 1% BSA/0.05% Tween 20/PBS for 30 min at room temperature. The cells were incubated overnight at 4 °C with primary antibodies (Table 3) diluted in blocking buffer. The next day, the cells were washed and incubated with fluorophore-tagged secondary antibodies (Table 3) for 1 hour at room temperature. Finally, the cells were stained with DAPI and imaged with a Leica SP5 confocal microscope.

Quantitative gene expression analysis

RNA was isolated from iPS cells, skin fibroblasts and HuES9 cells using the ReliaPrep™ RNA Cell Miniprep System (Promega) and cDNA was prepared from mRNA using SuperScript™ II Reverse Transcriptase kit (Invitrogen). qPCR was performed with the CFX96 C1000 Thermal Cycler (Bio-rad) using SYBR Green premix (Bio-rad) and the primers listed in Table 3. mRNA expression was normalized to GAPDH.

Genotyping of the human iPSC lines

Genomic DNA was isolated from iPS cells (passage 12 for ACD871C4-C8 and passage 16 for ACD874C9) and fibroblasts (passage 7) using the QIAamp DNA Mini Kit (Qiagen) and tested for copy number variations with GSAMD24 v1 Illumina Infinium SNP array 700k (Illumina). Data was analyzed with GenomeStudio software (IIllumina) and visualized using Nexus Copy Number 9.0 (BioDiscovery). To confirm iPSC identities, we compared the number of SNPs found in iPSC lines and patient fibroblasts with R software. To assure the presence of the heterozygous *FOXF1* mutations, the regions of interest were amplified with PCR using M13 tailed primers (Table 3), followed by Sanger sequencing with the 3730xl DNA Analyzer (Applied Biosystems, ThermoFisher Scientific). The PCR was performed with the Biometra TAdvanced Thermocycler (Westburg) and consisted of 35 cycles of the following steps: 30 s at 94 °C, 30 s at 60 °C and 90 s at 72 °C.

Trilineage differentiation

In vitro trilineage differentiation was induced with the STEMdiff™ Trilineage Differentiation Kit (STEMCELL Technologies) according to manufacturer's instructions. In brief, cells were plated in a single cell suspension on Geltrex coated 4-well chamber slides (Sarstedt). The cells were daily fed with either ectoderm, mesoderm or endoderm specific medium. After five (mesoderm and endoderm) or seven (ectoderm) days, the cells were fixed with 4% PFA and used for immunofluorescence staining.

Mycoplasma detection

Cell cultures were tested for mycoplasma contamination with the MycoAlert TM Mycoplasma Detection Kit (Lonza), according to manufacturer's instructions.

Table 3: Reagents details

Antibodies used for immunocytochemistry			
	Antibody	**Dilution**	**Company Cat # and RRID**
Pluripotency markers	Mouse anti-SSEA4	1:75	Abcam, ab16287, RRID: AB_778073
	Rabbit anti- NANOG	1:75	Abcam, ab21624, RRID: AB_446437
	Rabbit anti-OCT4	1:250	Abcam, ab19857, RRID: AB_445175
Differentiation markers	Goat anti-SOX17	1:100	R&D Systems, AF1924, RRID: AB_355060
	Goat anti-NCAM	1:100	R&D Systems, AF2408, RRID: AB_442152
	Mouse anti-β-Tubulin	1:1000	Sigma-Aldrich, T8660, RRID: AB_477590
	Rabbit anti-PAX6	1:250	Biolegend, 901301, RRID: AB_2565003
Secondary antibodies	Goat anti-Mouse IgG (H+L) Alexa Fluor 546	1:500	ThermoFisher Scientific, A-11003, RRID:AB_2534071
	Goat anti-Rabbit IgG (H+L) Alexa Fluor 488	1:500	ThermoFisher Scientific, A-11008, RRID:AB_143165
	Donkey anti-Goat IgG (H+L) Alexa Fluor 488	1:500	ThermoFisher Scientific, A-11055, RRID: AB_2534102
	DyLight 594 Goat anti-Mouse IgG +IgM (H+L)	1:500	Jackson, 115-515-044, RRID: AB_2338823
	Donkey anti-Rabbit IgG (H+L) Alexa Fluor 488	1:500	Jackson, 711-545-152, RRID: AB_2313584
Primers			
	Target	**Forward/Reverse primer (5'-3')**	
Pluripotency Markers (qPCR)	NANOG	CAGCCCCGATTCTTCCACCAGTCCC/ CGGAAGATT CCCAGTCGGGTTCACC	
	OCT3/4	AGCCACATCGCTCAGACAC/ GCCCAATACGACCAAATCC	
Absence of Sendai virus	SeV	GGATCACTAGGTGATATCGAGC/ ACCAGACAAGAG TTTAAGAGATATGTATC	
House-Keeping Gene (qPCR)	GAPDH	CCTTCATTGACCTCAACTAC/ GGAAGGCCATGCCAGTGAGC	
Targeted mutation analysis (Sanger sequencing)	FOXF1 ROI (GRch37/Hg19 Chr16: 86544274-86544511; c.99-c.330; 237bp)	GGCGGCGCGGCCATGGACC/ GCCCTTGGGTAGCTTGATG	

REFERENCES

1. P. Stankiewicz, P. Sen, S.S. Bhatt, M. Storer, Z. Xia, B.A. Bejjani, Z. Ou, J. Wiszniewska, D.J. Driscoll, M.K. Maisenbacher, J. Bolivar, M. Bauer, E.H. Zackai, D. McDonald-McGinn, M.M. Nowaczyk, M. Murray, V. Hustead, K. Mascotti, R. Schultz, L. Hallam, D. McRae, A.G. Nicholson, R. Newbury, J. Durham-O'Donnell, G. Knight, U. Kini, T.H. Shaikh, V. Martin, M. Tyreman, I. Simonic, L. Willatt, J. Paterson, S. Mehta, D. Rajan, T. Fitzgerald, S. Gribble, E. Prigmore, A. Patel, L.G. Shaffer, N.P. Carter, S.W. Cheung, C. Langston, C. Shaw-Smith, Genomic and genic deletions of the FOX gene cluster on 16q24.1 and inactivating mutations of FOXF1 cause alveolar capillary dysplasia and other malformations, Am J Hum Genet, 84 (2009) 780-791 .
2. E. Slot, G. Edel, E. Cutz, A. van Heijst, M. Post, M. Schnater, R. Wijnen, D. Tibboel, R. Rottier, A. de Klein, Alveolar capillary dysplasia with misalignment of the pulmonary veins: clinical, histological, and genetic aspects, Pulm Circ, 8 (2018) 2045894018795143.
3. M. Mahlapuu, S. Enerback, P. Carlsson, Haploinsufficiency of the forkhead gene Foxf1, a target for sonic hedgehog signaling, causes lung and foregut malformations, Development, 128 (2001) 2397-2406.
4. P. Sen, Y. Yang, C. Navarro, I. Silva, P. Szafranski, K.E. Kolodziejska, A.V. Dharmadhikari, H. Mostafa, H. Kozakewich, D. Kearney, J.B. Cahill, M. Whitt, M. Bilic, L. Margraf, A. Charles, J. Goldblatt, K. Gibson, P.E. Lantz, A.J. Garvin, J. Petty, Z. Kiblawi, C. Zuppan, A. McConkie-Rosell, M.T. McDonald, S.L. Peterson-Carmichael, J.T. Gaede, B. Shivanna, D. Schady, P.S. Friedlich, S.R. Hays, I.V. Palafoll, U. Siebers-Renelt, A. Bohring, L.S. Finn, J.R. Siebert, C. Galambos, L. Nguyen, M. Riley, N. Chassaing, A. Vigouroux, G. Rocha, S. Fernandes, J. Brumbaugh, K. Roberts, L. Ho-Ming, I.F. Lo, S. Lam, R. Gerychova, M. Jezova, I. Valaskova, F. Fellmann, K. Afshar, E. Giannoni, V. Muhlethaler, J. Liang, J.S. Beckmann, J. Lioy, H. Deshmukh, L. Srinivasan, D.T. Swarr, M. Sloman, C. Shaw-Smith, R.L. van Loon, C. Hagman, Y. Sznajer, C. Barrea, C. Galant, T. Detaille, J.A. Wambach, F.S. Cole, A. Hamvas, L.S. Prince, K.E. Diderich, A.S. Brooks, R.M. Verdijk, H. Ravindranathan, E. Sugo, D. Mowat, M.L. Baker, C. Langston, S. Welty, P. Stankiewicz, Novel FOXF1 mutations in sporadic and familial cases of alveolar capillary dysplasia with misaligned pulmonary veins imply a role for its DNA binding domain, Hum Mutat, 34 (2013) 801-811.
5. C.A. Cowan, I. Klimanskaya, J. McMahon, J. Atienza, J. Witmyer, J.P. Zucker, S. Wang, C.C. Morton, A.P. McMahon, D. Powers, D.A. Melton, Derivation of embryonic stem-cell lines from human blastocysts, N Engl J Med, 350 (2004) 1353-1356.

SUPPLEMENTARY DATA

A

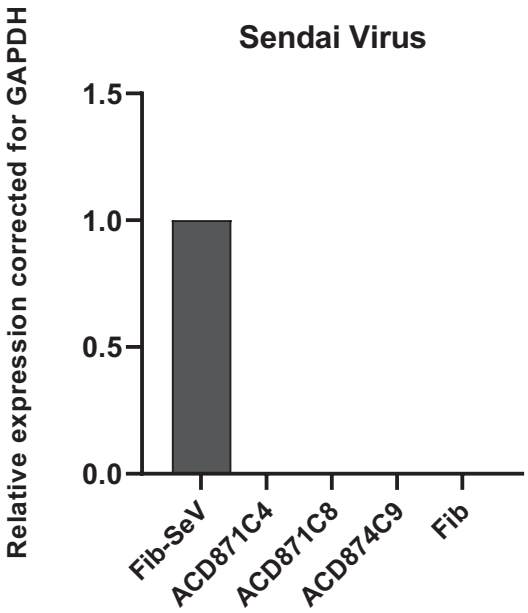

B

Fibroblast 1 (patient 1) – ACD871C4		Fibroblast 1 (patient 1) – ACD871C8	
Total passed count	708043	Total passed count	708078
Matched count	708033	Matched count	708069
Mismatch count	10	Mismatch count	9
Total Failed count	10691	Total failed count	10656
Failed count fibroblast 1	9894	Failed count fibroblast 1	9894
Failed count ACD871C4	9407	Failed count ACD871C8	9686

Fibroblast 2 (patient 2) – ACD874C9		Summary	% matched counts
Total passed count	708211	Fibroblast 1 – ACD871C4	100,00%
Matched count	708205	Fibroblast 1 – ACD871C8	100,00%
Mismatch count	6	Fibroblast 2 – ACD874C9	100,00%
Total failed count	10523		
Failed count fibroblast 2	9814		
Failed Count ACD874C9	9508		

C

Sample	A	B	B/A	Ratio	Interpretation
ACD871C4	36	18	0,5	<0,9	Negative
ACD871C8	24	8	0,33	0,9-1,2	Borderline
ACD874C9	28	18	0,69	>1,2	Positive

Supplementary figure 1. *A: Absence of Sendai virus measured by quantitative RT-PCR. B: Identification of the iPSC lines by means of SNP comparison between original human iPSC lines and the original fibroblasts used for generation of the iPSC lines. C: Mycoplasma test results.*

CHAPTER 6

ENDOTHELIAL CELL DIFFERENTIATION OF TWO PATIENT DERIVED INDUCED PLURIPOTENT STEM CELL LINES WITH *FOXF1* MUTATIONS ASSOCIATED WITH ALVEOLAR CAPILLARY DYSPLASIA

E. Slot [a, b], E. Brosens [b], G. Edel [a], A. de Klein [b], D. Tibboel [a], R. Rottier [a]

a. Department of Pediatric Surgery, Erasmus MC Sophia Children's Hospital, Rotterdam, The Netherlands
b. Department of Clinical Genetics, Erasmus MC, Rotterdam, The Netherlands

Work in progress

ABSTRACT

Alveolar capillary dysplasia with or without misalignment of the pulmonary veins (ACD/MPV) is a congenital lung disorder characterized by pulmonary vascular defects. Different types of genomic changes affecting the *FOXF1* locus have been found to result in ACD/MPV. Although it is known that FOXF1 is expressed in endothelial cells (ECs) and plays an important role during pulmonary vascular development, it is not clear how different *FOXF1* variants detected in ACD/MPV patients interfere with the function of ECs and lead to ACD/MPV. In this study, two patient derived iPSC lines are used to investigate the effects of two missense mutations (p.(L56V) and p.(F85I)) located in the DNA binding domain of FOXF1, on EC differentiation and function. So far, results show that iPSCs carrying a FOXF1 missense mutations (p.(L56V) or p.(F85I)) are able to differentiate into vascular ECs and that proliferation and tube formation capability is similar between mutated ECs and control ECs. Additional gene expression analyses and functional assays are currently ongoing to further elucidate the relation between these two *FOXF1* missense mutations and vascular defects of ACD/MPV lungs.

INTRODUCTION

Alveolar capillary dysplasia with or without misalignment of the pulmonary veins (ACD/MPV) is a congenital lung malformation associated with genomic variants in the *FOXF1* locus. ACD/MPV causes therapy resistant pulmonary hypertension and an insufficient gas exchange in new-borns, and therefore has a mortality rate of almost 100%. ACD/MPV lungs are mainly characterized by reduced numbers of alveolar capillaries, thickening of the arterial walls and, in most patients, misaligned pulmonary veins (1). These abnormalities imply a defect in the vascular patterning already at the early stages of lung development. A better understanding is needed about the mechanisms by which *FOXF1* variants cause ACD/MPV to find therapeutic targets that are able to prevent ACD/MPV or to improve the outcome..

The *FOXF1* gene encodes for transcription factor FOXF1 and has been shown to be induced by Sonic hedgehog signalling (2-4). During mouse lung development, FOXF1 is mainly expressed in the mesoderm and in mesodermal derived Pecam-1 positive alveolar endothelial cells (ECs) (5-8). Previous studies demonstrated that FOXF1 plays an important role in angiogenesis through upregulation of endothelial specific genes such as *NOTCH2, VEGFR1* and *VEGFR2* (9, 10). In line with observations in ACD/MPV lungs, heterozygous deletion of *Foxf1* in developing mice led to pulmonary vascular defects (6). Furthermore, endothelial specific knock down of *Foxf1* decreased angiogenesis in the lung, resulting in reduced vascularisation and loss of a pulmonary plexus, emphasizing the importance of FOXF1 in lung endothelial cells during pulmonary vascular development (6, 9).

In approximately 70% of ACD/MPV patients, a genomic alteration involving the *FOXF1* locus is found (11). These changes vary from *de novo* substitutions and indels located in the *FOXF1* transcription region to deletions of multiple kilo bases (kb) to mega bases (mb) in size encompassing the 60kb *FOXF1* enhancer that is located 250kb upstream of the transcription region (11-13). Studies in mice revealed that FOXF1 acts in a dosage-dependent manner and needs to be within a specific expression range to assure normal lung development (6, 14). Because the *FOXF1* enhancer is able to increase *FOXF1* transcription activity(4, 15), deletions involving the enhancer presumably reduce *FOXF1* expression as was for instance shown for the 340kb loss detected in the ACD/MPV patient described by Steiner and colleagues (16). Whether mutations located in the *FOXF1* coding

region affect *FOXF1* expression levels is not known. ACD/MPV associated mutations located in the *FOXF1* gene include missense mutations which are mainly located in the DNA binding domain (DBD), frameshift mutations which are mainly located between the cell type specific and the general activation domain, and other nonsense mutations which are found over the whole coding region (1, 11, 12, 17). As mutations in the coding region vary in type and location, it can be assumed that they alter FOXF1 expression or function through different molecular mechanisms. However, very little is currently known about these mechanisms and how they subsequently affect the development and function of ECs, and the relation towards the pulmonary vascular abnormalities that are observed in ACD/MPV.

Previously, we generated induced pluripotent stem cells (iPSCs) from two ACD/MPV patients carrying different missense mutations (p.(L56V) or p.(F85I)) located in the *FOXF1* DBD (11, 18). Through differentiation of the iPSC, we are able to study the impact of the p.(L56V) and p.(F85I) *FOXF1* mutations in different cell types. As the reduction in alveolar capillaries is one of the most prominent defects in ACD/MPV lungs, the current study investigates whether the p.(L56V) and p.(F85I) mutations affect the formation or function of vascular ECs which could contribute to abnormal vascular patterning of the lung.

MATERIAL AND METHODS

Research permission

Before the start of the study, the research proposal was reviewed and approved by the Daily Board of the Medical Ethics Committee (METC) Erasmus University Medical Center Rotterdam, The Netherlands (MEC-2017-302).

Induced pluripotent stem cells

The two ACD/MPV patient specific iPSC lines were previously generated in the Erasmus Medical Centre from skin fibroblasts using the non-integrating Sendai virus method (18). In the current study, iPSC lines ACD871C4 and ACD874C9 harbouring the pathogenic missense mutations NM_001451.3(FOXF1):c.166C>G (p.Leu56Val) and NM_001451.3(FOXF1):c.253T>C (p.Phe85Leu). these mutations are referred to as ACD-1 and ACD-2. The two control iPSC lines (control-1 and control-2) were generated in the

Leiden University Medical Centre using the same methods (hPSCreg names: LUMCi-0033C; LUMCi-003A) (19).

Cell culturing and differentiation

iPSCs were expanded on matrigel (Corning) coated plates with mTeSR™1 medium (STEMCELL technologies). Cells were passaged every 3 to 4 days in a 1:6 ratio according to the mTeSR™1 manual. iPSCs were differentiated towards vascular ECs and pericytes according to the protocol of Orlova and collaegues (20) (suppl. table 1). In brief, iPSCs were split as colonies in a 1:10 ratio once they reached 90% confluency. The following day (day 0), medium was changed to mesoderm induction medium. At day 3, the medium was changed to vascular induction medium and was refreshed on day 6 and 9. At day 10, CD31 positive ECs were isolated using magnetic CD31 recognizing Dynabeads (Thermofischer scientific) and seeded on 0.1% gelatine coated plates in EC expansion medium. ECs were passaged every 4 to 5 days in a 1:3 ratio. The CD31 negative population was collected and expanded on 0.1% gelatine coated plates in EGM-2 medium (Lonza). When cells reached 80% confluency, they were passaged in a 1:3 ratio and incubated with pericyte induction medium for three days. Thereafter, medium was changed into pericyte expansion medium. ECs were imaged with the Olympus IX70 microscope during and after differentiation.

Next generation sequencing

To exclude variants in the *FOXF1* locus in control cells, control iPSCs control-1 and control-2 were subjected to next generation sequencing with the *FOXF1* targeted panel as described previously (11). The *FOXF1* targeted library was constructed with the AmpliSeq Library Kit 2.0 (ThermoFisher Scientific). Sequences and coverages were analysed with the Ion S5 XL Sequencing System and the Torrent Suite Software v5.6 (ThermoFisher Scientific).

Flow cytometry

Cells (approximately 1 million) were collected at day 6 of differentiation and analysed with flow cytometry. Half of the cells were stained with anti-CD31 PE/Cyanine7 (Biolegend, Cat. No. 303118, dilution: 1:50) in 100µl PBS supplemented with 5% Fetal Bovine Serum (FBS) and 2mM EDTA for 30 minutes. The remaining half was used as negative control.

Thereafter, cells were washed with PBS supplemented with 5% FBS. Five minutes before flow cytometry analysis, DAPI (1:10000, BD Pharmingen) was added to distinguish dead cells form living cells. Flow cytometry was performed with the BD LSRFortessa Flow Cytometer (BD Biosciences) and analysed with BD FACSDiva 8.0.1 software (BD Biosciences).

Immunofluorescence

For immunofluorescence staining of differentiated ECs, cells were cultured on glass coverslips. Since iPSCs cannot be differentiated on glass coverslips, iPSCs were plated on Geltrex (ThermoFisher Scientific) coated 4-well chamber slides (Sarstedt) for immunofluorescence staining, and treated according to the differentiation protocol. Before staining, cells were fixed for 15 minutes with 4% PFA at room temperature. Thereafter, cells were permeabilized with 0,1% Triton-X100 for 10 minutes and blocked with 3% BSA/0,05% Tween 20/PBS for 30 minutes at room temperature. Cells were incubated overnight at 4 °C with primary antibodies (Table 1) diluted in blocking buffer. The next day, cells were washed and incubated with fluorophore-tagged secondary antibodies (Table 1) and DAPI (1:2000, BD Pharmingen) diluted in blocking buffer for 1 hour at room temperature. Cells were imaged with a Leica SP5 confocal microscope and analyzed with ImageJ software.

Table 1. List of antibodies used for immunofluorescence staining.

Primary antibody	**Host**	**Dilution**	**Company**	**Catalogue number**
CD31	Mouse	1:100	BioLegend	303101
vWF	Rabbit	1:100	Merck Millipore	Ab7356
FOXF1	Goat	1:400	R&D systems	AF4798
Brachyury	Rabbit	1:200	Sigma Aldrich	HPA003322
Secondary antibody	**Host**	**Dilution**	**Company**	**Catalogue number**
Alexa Fluor® 594 AffiniPure Anti-Mouse IgG (H+L)	Donkey	1:500	Jackson ImmunoResearch	715-585-151
Alexa Fluor® 647 AffiniPure Anti-Rabbit IgG (H+L)	Donkey	1:500	Jackson ImmunoResearch	711-605-152
Alexa Fluor® 488 AffiniPure Anti-Goat IgG (H+L)	Donkey	1:500	Jackson ImmunoResearch	705-545-147
Alexa Fluor® 594 AffiniPure Anti-Rabbit IgG (H+L)	Donkey	1:500	Jackson ImmunoResearch	711-585-152

RNA isolation

For RNA isolation, cells were dettached with TrypLE (Thermofischer scientific), quenched with 10% FCS/PBS and washed with PBS. The CD31 recognizing beads were removed from EC samples using a magnet after cell lysation. RNA was isolated with the RNeasy mini kit (Qiagen) according to manufacturer's instructions.

RNA sequencing and analysis

High quality RNA (RIN > 7.6) was used as input to create first Strand cDNA libraries using the strand-specific NEBNext Ultra II Directional RNA Library Prep Kit protocol and polyA mRNA workflow. After sequencing (40Gb, paired-end) on a Illumina NovaSeq6000 (Illumina) and quality control (see SX), reads were trimmed (Trim galore) and aligned using the CLC-Bio aligner to the hg19 reference genome. Read alignment, transcript quantification and differential expression analysis were performed using CLC Genomics Workbench version 20 (Qiagen). Alignment settings included the following: mismatch cost 2, insertion/deletion cost 3, length fraction 0.8, similarity fraction 0.8. We aligned to gene regions only counting paired reads as one. Output included total read counts, counts per million (CPM) and transcripts per million (TPM). To evaluate gene expression levels between the different time points and cell lines we used z-scores calculated from the average and standard deviations of TPM values of all cell lines at each time point.

Sanger sequencing of copy DNA

Copy DNA (cDNA) was synthesized from 2µg mRNA using M-MLV reverse transcriptase (Sigma-Aldrich) and oligo(dT) primers (self-designed: 23xT + 1A, 23xT + 1C, and 23xT + 1G). Before cDNA synthesis, mRNA was pre-treated with DNase I recombinant (Roche). 2µL of cDNA was subjected to Sanger sequencing with the 3730xl DNA Analyzer (Applied Biosystems, ThermoFisher Scientific) using custom designed primers (forward: GTCCAAGGCCAAGAAGACC; reverse: GCCCTTGGGTAGCTTGATG). Before sequencing, samples were amplified in a poly chain reaction (PCR) with the Biometra TAdvanced Thermocycler (Wetsburg), consisting of 35 cycles of the following steps: 30 seconds at 94°C, 30 seconds at 60°C and 90 seconds at 72°C. Final sequences were aligned and compared with the reference sequences GRCh37/hg19 from the Ensemble genome database (ENSG00000103241), using SeqScape Software v3.0 (Applied Biosystems, ThermoFisher Scientific).

EdU proliferation assay

An 5-ethynyl-2'-deoxyuridine (EdU) proliferation assay (21) was carried out in triplicate with ECs (passage 1 and 2) seeded on fibronectin coated glass coverslips. 24 hours after seeding, ECs were incubated with 5µM of EdU solution (CarboSynth) for 8 hours. Thereafter, cells were fixated with 4% PFA for 10 minutes at room temperature. To label the cells that incorporated EdU, cells were permeabilized with 0,1% Triton-X100 for 10 minutes followed by incubation with an EdU development cocktail (100mM Tris-buffered saline, 4nM $CuSO_4$, 2µM Sulfo-Azide-C5 (Luminoprobe), 100mM Sodium Ascorbate) for 30 minutes at room temperature. After rinsing, nuclei were labelled with DAPI (1:5000) (BD Pharmingen) for 10 minutes. Cells were imaged with the ZEISS Axiocam microscope. Percentages of EdU positive cells were counted in five random microscope fields per cell line using ImageJ software.

Tube formation assay

Tube formation assays (n=2) were carried out with the µ-Slide Angiogenesis (Ibidi). Each well of the µ-Slide Angiogenesis was coated with 10µl of growth factor reduced matrigel (Corning). After polymerization of the matrigel, 7500 ECs (passage 1) were seeded per well (three wells per cell line) in EC-SFM full medium. Cells were and imaged every two hours for the first eight hours and again 24 hours after seeding with the Olympus IX70 microscope.

RESULTS AND DISCUSSION

iPSCs with FOXF1 mutations p.(L56V) and p.(F85I) are able to differentiate into endothelial cells

To investigate whether missense *FOXF1* mutations p.(L56V) and p.(F85I) would affect the formation of mature ECs, we differentiated ACD/MPV patient specific iPSC lines (ACD-1 and ACD-2) and two control iPSC lines (control-1 and control-2) to mature ECs (22). During differentiation, cell morphologies varied slightly between cell lines and between replicates as a result of varying iPSC colony sizes at the start of the differentiation. Evident differences between patient specific iPSCs and control iPSCs were not observed (Figure 1A). Differentiated ACD-1 and ACD-2 ECs appeared morphologically identical to

differentiated control ECs, and immunofluorescence staining of EC-control-1 and EC-ACD-2 with EC markers CD31 and vWF confirmed the EC phenotype described by Orlova and colleagues who developed the differentiation protocol (Figure 1B) (22). The finding that ACD/MPV iPSC lines are able to form CD31 positive ECs *in vitro* is in line with the *in vivo* situation where vascular ECs are observed in the proximal parts of the lung and throughout the rest of the body of ACD/MPV patients, despite the presence of *FOXF1* mutations.

The exact number of iPSCs that differentiated into ECs could not be determined With the differentiation protocol that we used, since iPSCs are seeded in colonies and cannot be counted accurately. To better monitor the differentiation of each iPSC line, we analysed the percentages of living CD31 positive cells by flow cytometry at day 6 of differentiation. The mean percentages of three biological replicates (control-1: 14.9%, control-2: 6.0%, ACD-1: 5.4%, ACD-2: 26.5%), and additional experimental replicates of one control and one ACD/MPV line (control-1: 21.2%, ACD-1: 11,3%) indicated that the number of CD31 positive cells at day 6 varied per cell line and per experiment. This variation can be attributed to many factors such as the seeding size of iPSC colonies, the medium batch, or donor dependent differences in proliferation rates (23). Differentiation efficiency might also be influenced by the *FOXF1* mutations of ACD/MPV cell lines. Since FOXF1 has been shown to regulate cell proliferation (9, 24-26), *FOXF1* mutations could affect proliferation and thereby influence the subsequent differentiation efficiency. To quantify EC differentiation efficiencies and subsequently identify the impact of *FOXF1* mutations on differentiation efficiency, a large amount of flow cytometry replicates is required to rule out technical and donor dependent variance.

As *FOXF1* mutated iPSCs are able to differentiate into CD31 positive ECs, we used bulk RNA sequencing to compare the transcriptomes of mutant and control cells at different time points of differentiation (Figure 2A). Since the EC differentiation protocol allowed simultaneous differentiation of CD31 negative pericytes (22), we took pericytes along in the RNA sequencing analysis to explore whether the *FOXF1* mutations influenced pericyte formation. Preliminary analyses indicated that gene expression profiles of iPSCs (day 0), mature ECs and pericytes corresponded to published gene signatures of these cell types (Figure 2B). During differentiation, the expression trends of these signature genes were comparable between ACD/MPV and control lines, suggesting similar differentiation

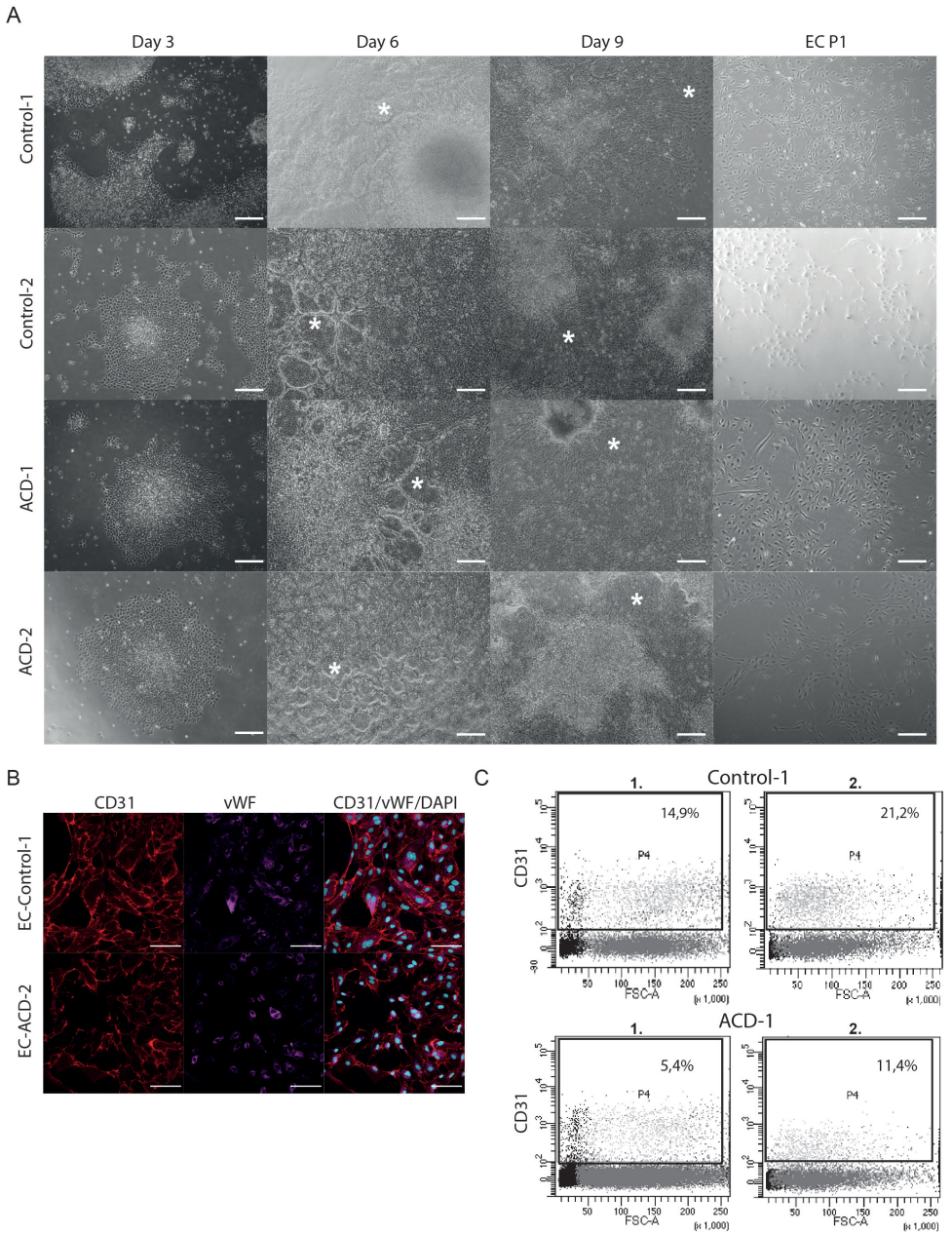

Figure 1. ACD/MPV patient specific iPSCs are capable to differentiate to CD31 positive endothelial cells *A: Cell morphologies at different time points of endothelial cell differentiation. Islands with CD31 positive cells (*) have arisen at day 3 and expanded at day 9. Scale bar: 250μM. B: Representative pictures of immunofluorescence staining on isolated control (EC-control-1) and FOXF1 mutated (EC-ACD-2) ECs. Red: CD31, purple: von Willebrand factor (vWF), cyan: DAPI. Scale bar: 100μM. C: results of the first (1.) and second (2.) flow cytometry analysis of CD31 positive cells (P4) at day 6 of differentiation of control-1 (left) and ACD-1 (right) cells.*

phases. iPSC markers decreased after day 0 in all different cell lines, whereas EC and pericyte markers gradually increased over time in all cell lines. At the final EC and pericyte stage, expression levels of EC and pericyte markers varied slightly between cell lines but were not specifically increased or decreased in ACD/MPV lines. For example, EC markers were slightly lower in EC-control-1 and EC-ACD-1 compared to EC-control-2 and EC-ACD-2 and is most likely due to interdonor variability. To summarize, morphological observations, immunofluorescence and preliminary gene expression analyses indicate that iPSCs carrying missense mutations p.(L56V) and p.(F85I) are able to form pericytes and vascular ECs *in vitro* and follow the same phases of EC differentiation as control cells.

FOXF1 expression peaks at the mesodermal stage of EC differentiation in vitro

Previous studies indicated that FOXF1 is able to homo-dimerize (14, 28). Therefore, it is possible that mutations p.(L56V) and p.(F85I), which are located in the DBD, affect FOXF1 expression. While FOXF1 expression levels have been shown to play a major role in pulmonary vascular development (6, 14), little research has been carried out investigating the effect of specific *FOXF1* mutations on FOXF1 expression levels. To study whether *FOXF1* mutations p.(L56V) and p.(F85I) affect expression of *FOXF1* or potential *FOXF1* target genes during differentiation, we analysed RNA expression levels of *FOXF1* and genes that have been identified as potential FOXF1 targets in mouse studies and *in vitro* human cell studies (3, 9, 10, 24, 27, 29-31) (Figure 3A). In all cell lines, *FOXF1* expression peaked at the mesodermal stage (day 3) of differentiation and was absent in mature ECs and pericytes. Potential FOXF1 target genes were mainly expressed after day 6 of differentiation and did not evidentially differ between ACD/MPV and control lines, similar to *FOXF1*. To confirm *FOXF1* expression patterns during differentiation on protein level, we performed immunofluorescence staining at day 3, day 6 and day 9 of differentiation. Again, all cell lines expressed FOXF1 at day 3 (Figure 3B), whereas at day 6 and 9, no FOXF1 expression was found. Mesodermal expression of FOXF1 is consistent with FOXF1 expression patterns during mouse development. During mouse development, FOXF1 is first expressed in the lateral mesoderm and continues to be expressed in the mesenchymal tissue surrounding the developing lung (2, 8). Also human *in vitro* models demonstrate FOXF1 expression in lateral mesoderm differentiated from human embryonic stem cells (32). However, the absence of FOXF1 expression in mature CD31 positive ECs differs from the observations

in mouse and human lung tissues (6, 8, 9, 16, 33). This discrepancy between *in vitro* and *in vivo* observations might be attributed to the absence of cells that surround the pulmonary ECs *in vivo.* These cells may secrete factors that activate signalling pathways leading to the induction of FOXF1 expression, such as the epithelial cells that express Sonic hedgehog. To study this in more detail, differentiated ECs could be co-cultured with other cell types that are involved in pulmonary development. Furthermore, expression of receptors in differentiated ECs could be analysed with RNA sequencing data to find the morphogens that potentially bind to ECs and influence FOXF1 expression. The absence of FOXF1 expression in mature ECs *in vitro* could also be attributed to the protocol that we used to differentiate ECs. As there is a large variety in ECs throughout the body, the type of ECs that we generated may not be representative for the ECs in human lung. Therefore, we compared the expression profiles generated with the RNA sequencing data with published single cell RNA sequencing data of human and mouse lung (34-36). First of all, pulmonary ECs lining larger blood vessels express different genes than ECs lining capillaries. Single cell RNA sequencing of human lung cells revealed a higher *FOXF1* expression in ECs lining the capillaries than ECs lining arterial or venous vessels (35). As expression of vWF in human lung ECs decreased as vessel diameter decreased, and is almost absent in alveolar capillary ECs (37-39), the observed expression of vWF suggests that our iPSC-derived ECs are not comparable with ECs lining alveolar capillaries *in vivo*. Moreover, expression of specific pulmonary EC markers identified through single cell RNA sequencing indicate that the *in vitro* differentiated cells are more related to macro-vascular ECs and the ECs located adjacent to the bronchi, than capillary ECs (Suppl. fig. 1) (34-36). Secondly, it has been shown that FOXF1 expression is higher in endothelial progenitor cells (EPCs) than mature ECs (10). Also in mice, a recent study revealed *Foxf1* expression in the alveolar capillary endothelial progenitor cells (34, 35). Since the iPSC-ECs are considered to be mature vascular ECs, their maturation state could also play a role in the absence of FOXF1 expression. Lastly, ECs form tissue specific populations throughout the body with different gene expression profiles (40-42). For FOXF1 it was demonstrated that expression is mainly restricted to tissues of the gastrointestinal-, urinary- and respiratory tract (7, 33, 40). Whether the iPSC-ECs have tissue specific characteristics, and if so, to which tissue specific population they belong, is unclear. To generate more insight in the identity of differentiated ECs, gene expression profiles will be compared with available EC expression data, which are mainly obtained from

previous studies in mice (33, 40, 43). Taken together, the absence of FOXF1 expression in differentiated ECs is likely due to the type of EC that we differentiated. As multiple EC differentiation protocols are currently available (44-48), one could choose to use another protocol for future studies into FOXF1, for instance one that specifically generates EPCs instead of mature ECs (44, 48). Since RNA sequencing data of the ECs generated by these protocols are scarce, their phenotypes are often unknown as well. Testing of different protocols will enable us to find the protocol that is best suited to study the effects of FOXF1 aberrations in pulmonary capillary ECs.

Because FOXF1 expression at day 3 was similar between *FOXF1* mutated cells and control cells, we investigated whether both the wild type (WT) and mutated alleles were expressed at RNA level. Indeed, Sanger sequencing of cDNA from *FOXF1* mutated cells at day 3 showed that both alleles were expressed (Figure 3C). This does not directly mean that the mutated and wild type alleles are similarly expressed at protein level as well. Similar to missense mutations involving succinate dehydrogenase subunit B (*SDHB*) (49), the mutated FOXF1 protein could be less stable than the wild type protein and be subjected to protein degradation. However, immunofluorescence staining of FOXF1 protein at day 3 did not show a difference between the number of cells expressing FOXF1 or the intensity of FOXF1 staining. As protein degradation presumably results in an overall reduction in FOXF1 expression, these findings insinuate that mutated FOXF1 is present at normal levels. The effect of *FOXF1* mutations p.(L56V) and p.(F85I) on the function of FOXF1 protein is unclear. Both mutations are located within the FOXF1 DBD that binds to the promoter regions of target genes to regulate their expression (50, 51). One amino acid change in the DBD might have major consequences for its bind ing capacity and therefore the regulation of target genes by FOXF1.

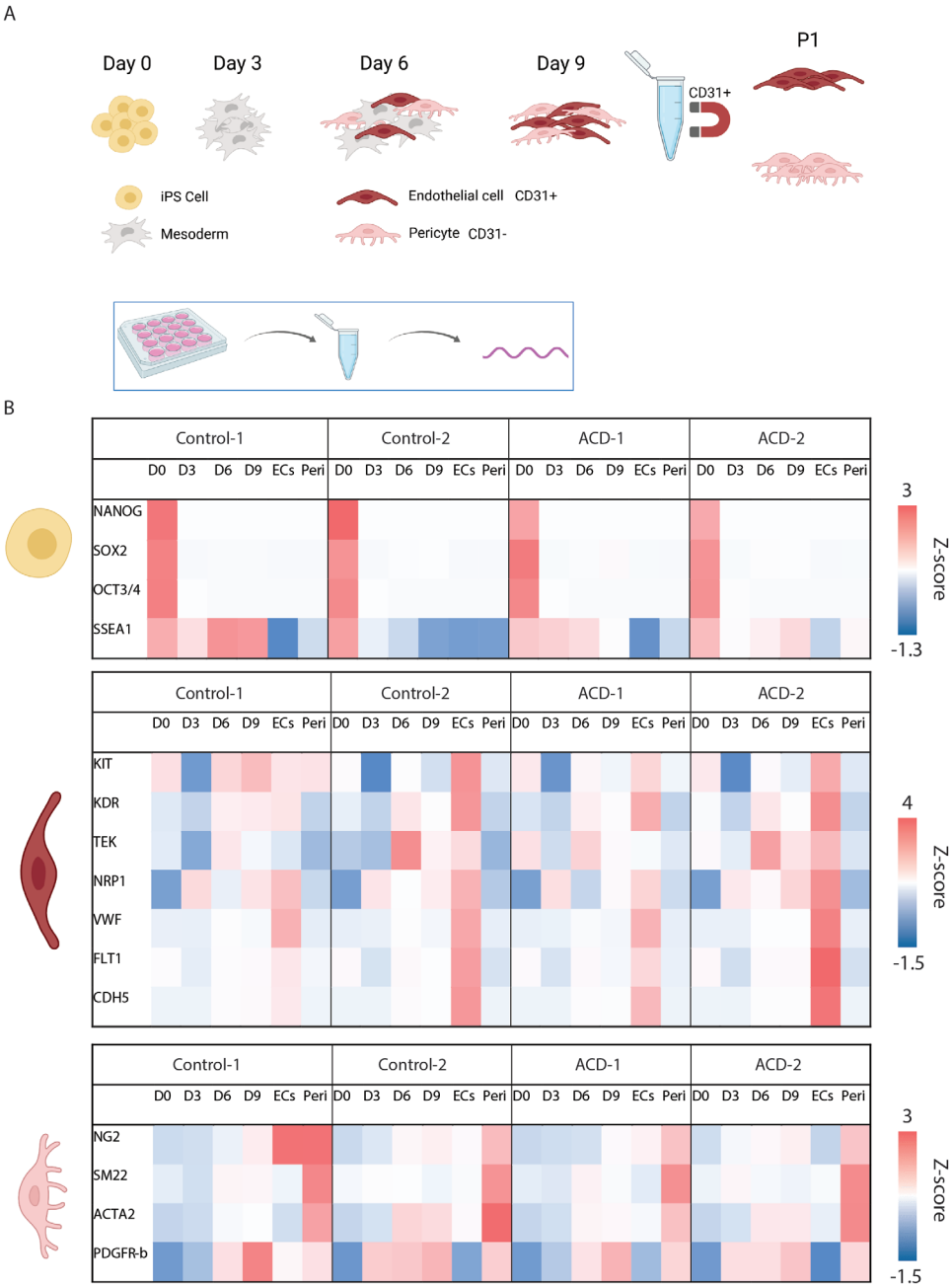

Figure 2. RNA sequencing at different time points suggests normal EC differentiation of patient derived iPSCs *A: Overview of cells harvested for RNA sequencing at different time points of EC differentiation. B: Expression levels of iPSC markers (upper panel), endothelial markers (middle panel) and pericyte markers (lower panel) at different time points of differentiation. Expression levels are depicted by colour scales that represent z-scores. Corresponding z-scores are indicated per panel.*

This was also illustrated by Pradhan and colleagues who presented the first ACD/MPV mouse model (*Foxf1*$^{WT/S52F}$) with a heterozygous missense mutation in the *FOXF1* DBD (c.155C>T, p.Ser52Phe) (29). Pradhan and colleagues showed that mutation p.S52F is located within the region of the DBD that binds *Stat3,* resulting in reduced expression of *Stat3* and *Stat3* target genes. Interestingly, we did not find any obvious effects of *FOXF1* mutations p.(L56V) and p.(F85I) on the expression of potential FOXF1 target genes in our analyses. Although it has been demonstrated that these potential FOXF1 target genes act downstream of FOXF1 (3, 9, 10, 24, 27, 29, 30), there is little to no evidence that they are direct targets of FOXF1, especially in human cells. Therefore, proteins acting between FOXF1 and downstream targets might compensate for the abnormal effects of *FOXF1* mutations during *in vitro* differentiation. For the differentiation of ECs, we supplemented the culture medium with growth factors to activate the WNT/β-catenin pathway, to inhibit the TGF-β/Activin/Nodal pathway and to induce VEGF signalling. Therefore, the modulation of these pathways may compensate for FOXF1 abnormalities. In addition, mutations p.(L56V) and p.(F85I) might affect the regulation of human lung specific genes that have not been identified as FOXF1 targets yet since studies investigating FOXF1 target genes in human cells are very scarce. Therefore, these targets are not examined in our RNA sequencing analysis. To identify (new) genes that are targeted by FOXF1 during differentiation, Cleavage Under Targets and Tagmentation (CUT&Tag) experiments combined with sequencing analysis can be performed. CUT&Tag has a low background signal and requires a minimal amount of cells, making it well suited to use during differentiation (52). To identify the genes that are significantly differentially expressed in mutated cells during differentiation, it would be interesting to repeat RNA sequencing with an increased sample size of at least three replicates per cell line, as this will allow statistical analyses on the gene expression profiles.

Since the reduced numbers of alveolar capillaries in ACD/MPV patients could be caused by defective angiogenesis, we sought to investigate whether the angiogenic potential of mutated ECs differed from control ECs. Two of the main functions required for angiogenesis are the ability to proliferate and the ability to migrate towards each other in order to form tubes. Therefore, we investigated the proliferation of the iPSC-EC by EdU incorporation. In contrast to Pradhan and colleagues who reported reduced proliferation of pulmonary ECs in *Foxf1*$^{WT/S52F}$ mice, no significant changes in proliferation between the control and ACD

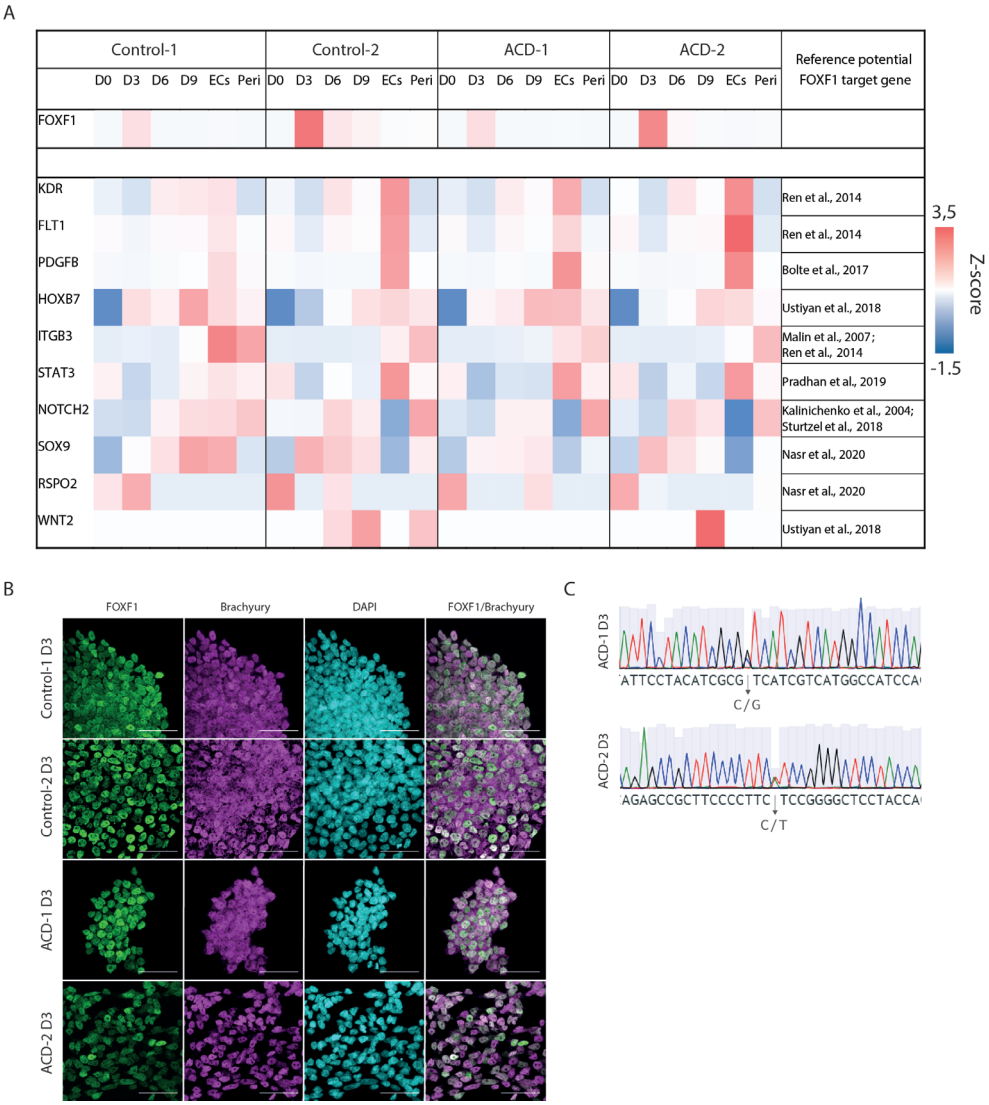

Figure 3. Mutated and control cells express FOXF1 at day 3 of differentiation *A: Indication of expression levels of FOXF1 and potential FOXF1 target genes at different time points. Expression levels are depicted by colours representing z-scores that vary between 3,5 (red) and -1,5 (blue). Studies describing presumable FOXF1 target genes are listed in the right column. B: Immunofluorescence staining with anti-FOXF1 (green), anti-brachyury (purple) and DAPI (cyan) on cells at day 3 of differentiation. D: Sanger sequencing of cDNA of ACD-1 (up) and ACD-2 (down) cells at day 3 of differentiation.*

In vitro proliferation and tube formation ability of FOXF1 mutated ECs is comparable to control ECs

iPSC-ECs was observed (10, 29) (Figure 4A). Next, we performed a tube formation assay to investigate the functionality of the iPSC-ECs. In contrast to Sturtzel and colleagues who observed reduced sprouting after knock down of *FOXF1* in EPCs, no apparent changes in network formation were detected (Figure 4B).The seemingly lack of differences between control and ACD iPSC-ECs may also be attributed to the type of ECs that are generated by the differentiation protocol. Pradhan and colleagues specifically investigated pulmonary ECs and Sturtzel and colleagues studied EPCs. In contrast to the *in vitro* differentiated ECs, these EC types have a high endogenous FOXF1 expression. In addition, the experimental set up may require optimization, for instance by performing the proliferation and tube formation assays in basal medium excluding the addition of growth factors. Furthermore, it has been shown that hypoxic conditions have a large effect on EC transcriptomes and EC behaviour which drive angiogenesis during development (55, 56). Therefore, it would be interesting to perform the functional assays under hypoxia as this might clarify whether FOXF1 plays a role in the signalling pathways that regulate hypoxia-induced angiogenesis.

So far, we have been using mono- and 2D cultures to investigate the function of ECs. *In vivo*, cells surrounding ECs influence the EC function through intercellular signalling and by creating mechanical forces. As we showed that *FOXF1* mutated cells are able to develop into vascular ECs *in vitro*, the next step could be to use these ECs for multicellular 3D cultures in order to further investigate the effects of *FOXF1* mutations on EC function in a way that is more similar to the *in vivo* situation. As we were not able to generate isogenic controls that could be used in the current study, it can still be considered to generate isogenic controls by correcting the *FOXF1* mutations using CRISPR-Cas tools for future studies (57, 58). Functional studies and gene expression comparisons between *FOXF1* mutated cells and isogenic controls, will reduce the variation between cell lines and specify the effects of *FOXF1* mutations.

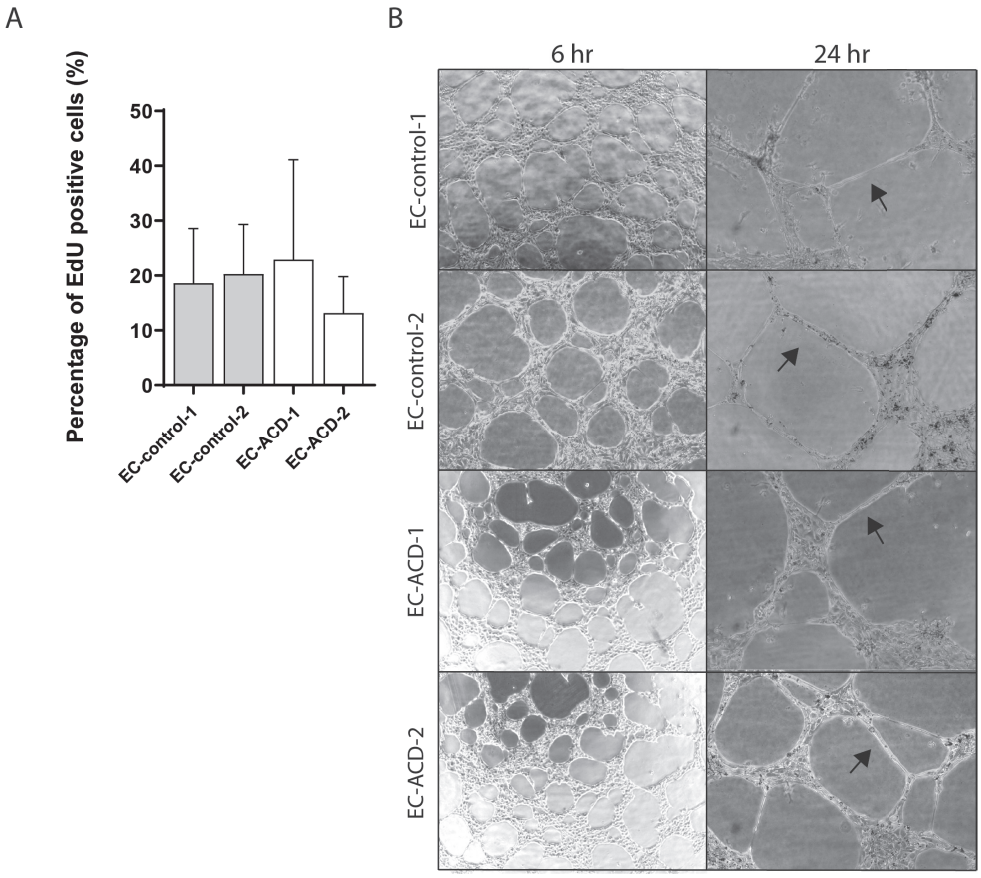

Figure 4. FOXF1 mutated ECs proliferate normally and have angiogenic potential. *A: Graphical representation of proliferation by EdU incorporation assays (n=3). Percentages of EdU positive cells were counted in five random microscope fields per EC line. Grey bars: control ECs, white bars: FOXF1 mutated ECs. B: Representative images of tube formation assays (n=2) 6 hours and 24 hours after cells were plated. Arrows indicate stable tubes after 24 hours.*

SUMMARY

To gain a better understanding of the role of *FOXF1* mutations during abnormal development of the capillary bed in ACD/MPV lungs, this study investigated the effects of *FOXF1* missense mutations p.(L56V) and p.(F85I) on EC differentiation using patient specific iPSCs. Results demonstrated that iPSCs carrying *FOXF1* mutations p.(L56V) and p.(F85I) successfully differentiated into mature vascular ECs and followed gene expression trends similar to control cells. Furthermore, *in vitro* proliferation and tube formation ability of mutated mature ECs was comparable to control ECs. To clarify whether the mature ECs differentiated *in vitro* are representative for the ECs that line the pulmonary capillaries *in*

vivo, additional gene expression analyses are currently underway. To conclude, this study provides a clear example of how ACD/MPV patient specific iPSCs can be differentiated into a cell type of interest which can be used to investigate the effects of *FOXF1* mutations on the transcriptome and function of a cell. Additional experiments and analyses are currently underway to further elucidate the relation between *FOXF1* mutations and vascular defects observed in ACD/MPV patients.

REFERENCES

1. Slot E, Edel G, Cutz E, van Heijst A, Post M, Schnater M, et al. Alveolar capillary dysplasia with misalignment of the pulmonary veins: clinical, histological, and genetic aspects. Pulm Circ. 2018;8(3):2045894018795143.
2. Mahlapuu M, Enerback S, Carlsson P. Haploinsufficiency of the forkhead gene Foxf1, a target for sonic hedgehog signaling, causes lung and foregut malformations. Development. 2001;128(12):2397-406.
3. Nasr T, Holderbaum AM, Chaturvedi P, Agarwal K, Kinney JL, Daniels K, et al. Disruption of a hedgehog-foxf1-rspo2 signaling axis leads to tracheomalacia and a loss of sox9+ tracheal chondrocytes. Dis Model Mech. 2020.
4. Szafranski P, Dharmadhikari AV, Brosens E, Gurha P, Kolodziejska KE, Zhishuo O, et al. Small noncoding differentially methylated copy-number variants, including lncRNA genes, cause a lethal lung developmental disorder. Genome Res. 2013;23(1):23-33.
5. Kalinichenko VV, Lim L, Shin B, Costa RH. Differential expression of forkhead box transcription factors following butylated hydroxytoluene lung injury. Am J Physiol Lung Cell Mol Physiol. 2001;280(4):L695-704.
6. Kalinichenko VV, Lim L, Stolz DB, Shin B, Rausa FM, Clark J, et al. Defects in pulmonary vasculature and perinatal lung hemorrhage in mice heterozygous null for the Forkhead Box f1 transcription factor. Dev Biol. 2001;235(2):489-506.
7. Mahlapuu M, Ormestad M, Enerback S, Carlsson P. The forkhead transcription factor Foxf1 is required for differentiation of extra-embryonic and lateral plate mesoderm. Development. 2001;128(2):155-66.
8. Mahlapuu M, Pelto-Huikko M, Aitola M, Enerback S, Carlsson P. FREAC-1 contains a cell-type-specific transcriptional activation domain and is expressed in epithelial-mesenchymal interfaces. Dev Biol. 1998;202(2):183-95.
9. Ren X, Ustiyan V, Pradhan A, Cai Y, Havrilak JA, Bolte CS, et al. FOXF1 transcription factor is required for formation of embryonic vasculature by regulating VEGF signaling in endothelial cells. Circ Res. 2014;115(8):709-20.
10. Sturtzel C, Lipnik K, Hofer-Warbinek R, Testori J, Ebner B, Seigner J, et al. FOXF1 Mediates Endothelial Progenitor Functions and Regulates Vascular Sprouting. Front Bioeng Biotechnol. 2018;6:76.
11. Slot E, von der Thusen JH, van Heijst A, van Marion R, Magielsen F, Dubbink HJ, et al. Fast detection of FOXF1 variants in patients with alveolar capillary dysplasia with misalignment of pulmonary veins using targeted sequencing. Pediatr Res. 2020.
12. Sen P, Yang Y, Navarro C, Silva I, Szafranski P, Kolodziejska KE, et al. Novel FOXF1 mutations in sporadic and familial cases of alveolar capillary dysplasia with misaligned pulmonary veins imply a role for its DNA binding domain. Hum Mutat. 2013;34(6):801-11.
13. Szafranski P, Gambin T, Dharmadhikari AV, Akdemir KC, Jhangiani SN, Schuette J, et al. Pathogenetics of alveolar capillary dysplasia with misalignment of pulmonary veins. Hum Genet. 2016;135(5):569-86.
14. Dharmadhikari AV, Sun JJ, Gogolewski K, Carofino BL, Ustiyan V, Hill M, et al. Lethal lung hypoplasia and vascular defects in mice with conditional Foxf1 overexpression. Biol Open. 2016;5(11):1595-606.
15. Szafranski P, Dharmadhikari AV, Wambach JA, Towe CT, White FV, Grady RM, et al. Two deletions overlapping a distant FOXF1 enhancer unravel the role of lncRNA LINC01081 in etiology of alveolar capillary dysplasia with misalignment of pulmonary veins. Am J Med Genet A. 2014;164A(8):2013-9.
16. Steiner LA, Getman M, Schiralli Lester GM, Iqbal MA, Katzman P, Szafranski P, et al. Disruption of normal patterns of FOXF1 expression in a lethal disorder of lung development. J Med Genet. 2020;57(5):296-300.
17. Sen P, Gerychova R, Janku P, Jezova M, Valaskova I, Navarro C, et al. A familial case of alveolar capillary dysplasia with misalignment of pulmonary veins supports paternal imprinting of FOXF1 in human. Eur J Hum Genet. 2013;21(4):474-7.

18. Slot E, de Klein A, Rottier RJ. Generation of three iPSC lines from two patients with heterozygous FOXF1 mutations associated to Alveolar Capillary Dysplasia with Misalignment of the Pulmonary Veins. Stem Cell Res. 2020;44:101745.
19. Buijsen RAM, Gardiner SL, Bouma MJ, van der Graaf LM, Boogaard MW, Pepers BA, et al. Generation of 3 spinocerebellar ataxia type 1 (SCA1) patient-derived induced pluripotent stem cell lines LUMCi002-A, B, and C and 2 unaffected sibling control induced pluripotent stem cell lines LUMCi003-A and B. Stem Cell Res. 2018;29:125-8.
20. Halaidych OV, Freund C, van den Hil F, Salvatori DCF, Riminucci M, Mummery CL, et al. Inflammatory Responses and Barrier Function of Endothelial Cells Derived from Human Induced Pluripotent Stem Cells. Stem Cell Reports. 2018;10(5):1642-56.
21. Salic A, Mitchison TJ. A chemical method for fast and sensitive detection of DNA synthesis in vivo. Proc Natl Acad Sci U S A. 2008;105(7):2415-20.
22. Orlova VV, van den Hil FE, Petrus-Reurer S, Drabsch Y, Ten Dijke P, Mummery CL. Generation, expansion and functional analysis of endothelial cells and pericytes derived from human pluripotent stem cells. Nat Protoc. 2014;9(6):1514-31.
23. Volpato V, Webber C. Addressing variability in iPSC-derived models of human disease: guidelines to promote reproducibility. Dis Model Mech. 2020;13(1).
24. Ustiyan V, Bolte C, Zhang Y, Han L, Xu Y, Yutzey KE, et al. FOXF1 Transcription Factor Promotes Lung Morphogenesis by Inducing Cellular Proliferation in Fetal Lung Mesenchyme. Dev Biol. 2018.
25. Wu CY, Chan CH, Dubey NK, Wei HJ, Lu JH, Chang CC, et al. Highly Expressed FOXF1 Inhibit Non-Small-Cell Lung Cancer Growth via Inducing Tumor Suppressor and G1-Phase Cell-Cycle Arrest. Int J Mol Sci. 2020;21(9).
26. Zhao J, Xue X, Fu W, Dai L, Jiang Z, Zhong S, et al. Epigenetic activation of FOXF1 confers cancer stem cell properties to cisplatinresistant nonsmall cell lung cancer. Int J Oncol. 2020;56(5):1083-92.
27. Bolte C, Flood HM, Ren X, Jagannathan S, Barski A, Kalin TV, et al. FOXF1 transcription factor promotes lung regeneration after partial pneumonectomy. Sci Rep. 2017;7 (1):10690 .
28. Ren X, Ustiyan V, Guo M, Wang G, Bolte C, Zhang Y, et al. Postnatal Alveologenesis Depends on FOXF1 Signaling in c-KIT(+) Endothelial Progenitor Cells. Am J Respir Crit Care Med. 2019.
29. Pradhan A, Dunn A, Ustiyan V, Bolte C, Wang G, Whitsett JA, et al. The S52F FOXF1 Mutation Inhibits STAT3 Signaling and Causes Alveolar Capillary Dysplasia. Am J Respir Crit Care Med. 2019.
30. Kalinichenko VV, Gusarova GA, Kim IM, Shin B, Yoder HM, Clark J, et al. Foxf1 haploinsufficiency reduces Notch-2 signaling during mouse lung development. Am J Physiol Lung Cell Mol Physiol. 2004;286(3):L521-30.
31. Malin D, Kim IM, Boetticher E, Kalin TV, Ramakrishna S, Meliton L, et al. Forkhead box F1 is essential for migration of mesenchymal cells and directly induces integrin-beta3 expression. Mol Cell Biol. 2007;27(7):2486-98.
32. Loh KM, Chen A, Koh PW, Deng TZ, Sinha R, Tsai JM, et al. Mapping the Pairwise Choices Leading from Pluripotency to Human Bone, Heart, and Other Mesoderm Cell Types. Cell. 2016;166(2):451-67.
33. Uhlen M, Fagerberg L, Hallstrom BM, Lindskog C, Oksvold P, Mardinoglu A, et al. Proteomics. Tissue-based map of the human proteome. Science. 2015;347(6220):1260419.
34. Gillich A, Zhang F, Farmer CG, Travaglini KJ, Tan SY, Gu M, et al. Capillary cell-type specialization in the alveolus. Nature. 2020;586(7831):785-9.
35. Travaglini KJ, Nabhan AN, Penland L, Sinha R, Gillich A, Sit RV, et al. A molecular cell atlas of the human lung from single-cell RNA sequencing. Nature. 2020;587(7835):619-25.
36. Zepp JA, Morley MP, Loebel C, Kremp MM, Chaudhry FN, Basil MC, et al. Genomic, epigenomic, and biophysical cues controlling the emergence of the lung alveolus. Science. 2021;371(6534).
37. Kawanami O, Jin E, Ghazizadeh M, Fujiwara M, Jiang L, Nagashima M, et al. Heterogeneous distribution of thrombomodulin and von Willebrand factor in endothelial cells in the human pulmonary microvessels. J Nippon Med Sch. 2000;67(2):118-25.
38. Muller AM, Skrzynski C, Nesslinger M, Skipka G, Muller KM. Correlation of age with in vivo expression of endothelial markers. Exp Gerontol. 2002;37(5):713-9.

39. Pusztaszeri MP, Seelentag W, Bosman FT. Immunohistochemical expression of endothelial markers CD31, CD34, von Willebrand factor, and Fli-1 in normal human tissues. J Histochem Cytochem. 2006;54(4):385-95.
40. Kalucka J, de Rooij L, Goveia J, Rohlenova K, Dumas SJ, Meta E, et al. Single-Cell Transcriptome Atlas of Murine Endothelial Cells. Cell. 2020;180(4):764-79 e20.
41. Nolan DJ, Ginsberg M, Israely E, Palikuqi B, Poulos MG, James D, et al. Molecular signatures of tissue-specific microvascular endothelial cell heterogeneity in organ maintenance and regeneration. Dev Cell. 2013;26(2):204-19.
42. Sabbagh MF, Heng JS, Luo C, Castanon RG, Nery JR, Rattner A, et al. Transcriptional and epigenomic landscapes of CNS and non-CNS vascular endothelial cells. Elife. 2018;7.
43. Tabula Muris C, Overall c, Logistical c, Organ c, processing, Library p, et al. Single-cell transcriptomics of 20 mouse organs creates a Tabula Muris. Nature. 2018;562(7727):367-72.
44. Farkas S, Simara P, Rehakova D, Veverkova L, Koutna I. Endothelial Progenitor Cells Produced From Human Pluripotent Stem Cells by a Synergistic Combination of Cytokines, Small Compounds, and Serum-Free Medium. Front Cell Dev Biol. 2020;8:309.
45. Gu M, Shao NY, Sa S, Li D, Termglinchan V, Ameen M, et al. Patient-Specific iPSC-Derived Endothelial Cells Uncover Pathways that Protect against Pulmonary Hypertension in BMPR2 Mutation Carriers. Cell Stem Cell. 2017;20(4):490-504 e5.
46. Harding A, Cortez-Toledo E, Magner NL, Beegle JR, Coleal-Bergum DP, Hao D, et al. Highly Efficient Differentiation of Endothelial Cells from Pluripotent Stem Cells Requires the MAPK and the PI3K Pathways. Stem Cells. 2017;35(4):909-19.
47. Paik DT, Tian L, Lee J, Sayed N, Chen IY, Rhee S, et al. Large-Scale Single-Cell RNA-Seq Reveals Molecular Signatures of Heterogeneous Populations of Human Induced Pluripotent Stem Cell-Derived Endothelial Cells. Circ Res. 2018;123(4):443-50.
48. Prasain N, Lee MR, Vemula S, Meador JL, Yoshimoto M, Ferkowicz MJ, et al. Differentiation of human pluripotent stem cells to cells similar to cord-blood endothelial colony-forming cells. Nat Biotechnol. 2014;32(11):1151-7.
49. Yang C, Matro JC, Huntoon KM, Ye DY, Huynh TT, Fliedner SM, et al. Missense mutations in the human SDHB gene increase protein degradation without altering intrinsic enzymatic function. FASEB J. 2012;26(11):4506-16.
50. Hellqvist M, Mahlapuu M, Samuelsson L, Enerback S, Carlsson P. Differential activation of lung-specific genes by two forkhead proteins, FREAC-1 and FREAC-2. J Biol Chem. 1996;271(8):4482-90.
51. Pierrou S, Hellqvist M, Samuelsson L, Enerback S, Carlsson P. Cloning and characterization of seven human forkhead proteins: binding site specificity and DNA bending. EMBO J. 1994;13(20):5002-12.
52. Kaya-Okur HS, Wu SJ, Codomo CA, Pledger ES, Bryson TD, Henikoff JG, et al. CUT&Tag for efficient epigenomic profiling of small samples and single cells. Nat Commun. 2019;10(1):1930.
53. Nowak-Sliwinska P, Alitalo K, Allen E, Anisimov A, Aplin AC, Auerbach R, et al. Consensus guidelines for the use and interpretation of angiogenesis assays. Angiogenesis. 2018;21(3):425-532.
54. Staton CA, Reed MW, Brown NJ. A critical analysis of current in vitro and in vivo angiogenesis assays. Int J Exp Pathol. 2009;90(3):195-221.
55. Kim YH, Choi J, Yang MJ, Hong SP, Lee CK, Kubota Y, et al. A MST1-FOXO1 cascade establishes endothelial tip cell polarity and facilitates sprouting angiogenesis. Nat Commun. 2019;10(1):838.
56. Klomp J, Hyun J, Klomp JE, Pajcini K, Rehman J, Malik AB. Comprehensive transcriptomic profiling reveals SOX7 as an early regulator of angiogenesis in hypoxic human endothelial cells. J Biol Chem. 2020;295(15):4796-808.
57. Hendriks D, Clevers H, Artegiani B. CRISPR-Cas Tools and Their Application in Genetic Engineering of Human Stem Cells and Organoids. Cell Stem Cell. 2020;27(5):705-31.
58. Maguire JA, Cardenas-Diaz FL, Gadue P, French DL. Highly Efficient CRISPR-Cas9-Mediated Genome Editing in Human Pluripotent Stem Cells. Curr Protoc Stem Cell Biol. 2019;48(1):e64.

SUPPLEMENTARY DATA

Gene	EC type	EC-control-1	EC-control-2	EC-ACD-1	EC-ACD-2	Reference
VWF	Macro EC					Zepp et al., 2021
CXCL12	Macro EC art					Zepp et al., 2021
GJA5	Art					Travaglini et al., 2020
DKK2	Art					Travaglini et al., 2020
FABP4	Macro EC ven					Zepp et al., 2021
CPE	Ven					Travaglini et al., 2020
MYC	Bron					Travaglini et al., 2020
PLVAP	Bron					Travaglini et al., 2020
HSPG2	Bron					Travaglini et al., 2020
SPRY1	Bron					Travaglini et al., 2020
GPIHBP1	Micro EC					Zepp et al., 2021
FCN3	gCap					Gillich et al., 2020
EDN1	gCap					Gillich et al., 2020
EDNRB	aCap					Gillich et al., 2020
SOSTDC1	aCap					Gillich et al., 2020
IL1RL1	aCap					Gillich et al., 2020
PROX1	Lym EC					Zepp et al., 2021
CCL21	Lym					Travaglini et al., 2020
PDPN	Lym					Travaglini et al., 2020

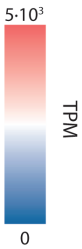

Supplementary figure 1. Expression levels of specific pulmonary EC markers in in vitro differentiated ECs *Expression levels are depicted in colour scales representing transcripts per kilobase million (TPM). EC types were specified by Zepp et al., Gillich et al. and Travaglini et al. (34-36) Macro: macro-vascular; micro: micro-vascular; art: arterial; ven: venous; bron: bronchial; gCap: general capillaries; aCap: aerocytes; lym: lymphatic.*

Mesodermal induction medium			
Reagent	**Company**	**Cat. No.**	**Final concentration**
APEL2	STEMCELL Techn.	05275	n/a
PFHM-II	Gibco	12040077	5%
CHIR 99012	STEMCELL Techn.	4423	7.5 µM
Penicillin/Streptomycin	Lonza	DE17-602e	100 U/ml; 100 µg/ml
Vascular induction medium			
Reagent	**Company**	**Cat. No.**	**Final concentration**
APEL2	STEMCELL Techn.	05275	n/a
PFHM-II	Gibco	12040077	5%
VEGF165	R&D Systems	293-VE	50 ng/ml
SB 431542	Tocris Bioscience	1614	10 µM
Penicillin/Streptomycin	Lonza	DE17-602e	100 U/ml; 100 µg/ml
EC expansion medium			
Reagent	**Company**	**Cat. No.**	**Final concentration**
EC-SFM	Gibco	11111-044	n/a
Poor-plasma-derived serum, human	Sigma-Aldrich	P2918	1%
VEGF165	R&D Systems	293-VE	30 ng/ml
bFGF	Miltenyi Biotec	130-093-842	20 ng/ml
Penicillin/Streptomycin	Lonza	DE17-602e	100 U/ml; 100 µg/ml
Pericyte induction medium			
Reagent	**Company**	**Cat. No.**	**Final concentration**
DMEM	Gibco	41966	n/a

Foetal Bovine Serum	Gibco	10270106	10%
TGF-β3	Peprotech	100-36E	2 ng/ml
PDGF-BB	Peprotech	100-14B-A	4 ng/ml
Penicillin/Streptomycin	Lonza	DE17-602e	100 U/ml; 100 µg/ml
Pericyte expansion medium			
Reagent	**Company**	**Cat. No.**	**Final concentration**
DMEM	Gibco	41966	n/a
Foetal Bovine Serum	Gibco	10270106	10%
Penicillin/Streptomycin	Lonza	DE17-602e	100 U/ml; 100 µg/ml

Supplementary table 1. *Cell culture media*

6

CHAPTER 7

GENERAL DISCUSSION

The lethal congenital lung disorder alveolar capillary dysplasia with misalignment of the pulmonary veins (ACD/MPV) is difficult to diagnose due to its low incidence and need for invasive diagnostic procedures. Therefore, patients are subjected to futile invasive therapies and prolonged hospitalization, giving false hope to the parents. Up till now, the common approach is to perform a lung biopsy in critical ill children with an inherent high risk of complications. Histologically, ACD/MPV is characterized by thickened alveolar septae, hypertrophic arterial walls and a large reduction in pulmonary capillaries. Furthermore, the majority of ACD/MPV lungs demonstrate misaligned pulmonary veins (MPV) adjacent to the arteries of bronchovascular bundles whereas in normal lungs, pulmonary veins are solely found in interlobular septae. ACD/MPV is associated with genomic variants in the *FOXF1* locus (1, 2) and genetic evaluation is increasingly used to confirm the diagnosis. Currently, there is no clear explanation for how these genomic variants cause this severe lung disorder while a better understanding could provide opportunities to define therapeutic targets. Therefore, this thesis includes the investigation of (epi)genetic *FOXF1* abnormalities contributing to the complex pathogenesis of ACD/MPV.

To improve disease management in the short run, we started our studies on ACD/MPV by developing a new, next generation sequencing (NGS) panel that enables detection of genomic *FOXF1* variants in DNA isolated from blood within 72 hours (3) (chapter 3). NGS is a relative cheap and fast method to screen for mutations in a well-defined area of the genome. In current clinical practice, four years after the start of our study, whole genome sequencing (WGS) is increasingly used as well. WGS has the advantage to cover the whole genome and therefore enables the search for genomic variants in other loci if no variants are found in the *FOXF1* locus. To test the efficacy of our *FOXF1* targeted NGS panel we collected different types of bodily material of histologically confirmed ACD/MPV patients from different clinical centres. The material enabled us to retrospectively test ACD/MPV patient DNA but also to proceed our research into the pathogenesis of ACD/MPV.

The role of FOXF1 in rodent lung development

Mouse and rat models have demonstrated the importance of FOXF1 during lung development. Already at the primitive streak stage of embryonic development, FOXF1 is expressed in the mesodermal lateral plate and continues to be expressed in the mesodermal layer of the splanchnopleure and somatopleure. As the splanchnopleure

differentiates into mesenchymal tissue, FOXF1 continues to be expressed in the mesenchyme surrounding the organs deriving from the primitive gut, from which the lungs keep the highest FOXF1 expression (4-7). From mouse embryonic day 13 onwards, FOXF1 expression within the lungs is mainly observed in the mesenchyme, endothelial cells (ECs) and airway smooth muscle cells (6, 8, 9). Homozygous deletion of *Foxf1* (*Foxf1*$^{-/-}$) is embryonically lethal due to embryonic and extra-embryonic defects such as impaired yolk sac vasculogenesis and underdevelopment of the posterior part of the embryo (10). Heterozygous deletion of *Foxf1* (*Foxf1*$^{+/-}$) results in reduced survival due to lung hypoplasia and impaired lung vasculogenesis, correlated with the level of *Foxf1* expression (5, 8, 10). The observation that *Foxf1*$^{+/-}$ mice exhibit defects in structures arising from both endodermal and mesodermal layers illustrates the importance of intercellular signalling during lung development. Moreover, *FOXF1* is a downstream target of the secreted morphogen Sonic hedgehog (SHH) which is expressed in the endodermal derived epithelium of the foregut and growing lung buds (Figure 1). SHH signals to the surrounding mesenchyme where it binds to the Patched1 (PTCH1) receptor on responsive cells and subsequently activates an intracellular signalling cascade leading to cleavage and nuclear translocation of GLI proteins (5, 11-13). Although all three GLI proteins (GLI1-3) are expressed in the lung mesenchyme during development, *Gli* knockout mice demonstrated that only GLI2 and Gli3 are essential for lung development (14, 15). Furthermore, it has been shown that GLI2 activates FOXF1 transcription, whereas GLI3 inhibits FOXF1 transcription (12, 16). Recently, a new mouse model (*Foxf1*$^{WT/S52F}$) was developed in which mice harboured a heterozygous missense mutation (c.155C>T, p.Ser52Phe) mimicking a mutation of an ACD/MPV patient (17). Besides pulmonary inflammation, hemorrhage and hypertrophy of pulmonary arteries, *Foxf1*$^{WT/S52F}$ mice also demonstrated misaligned pulmonary veins (MPVs) similar to the lungs of ACD/MPV patients. As MPVs were not observed in *Foxf1*$^{+/-}$ mice, this intriguing observation might suggest that the mutated FOXF1 protein interferes with the function of the wild-type (WT) FOXF1 protein resulting in a more severe phenotype than caused by reduced *Foxf1* expression alone. The p.S52F mutation is located in the *Foxf1* DNA binding domain and presumably leads to altered binding of target genes as was shown for *Stat3* (17). Furthermore, this mutation might lead to aberrant complex formation with protein-partners. As Pradhan and colleagues did not investigate *Foxf1* expression levels in the *Foxf1*$^{WT/S52F}$ mouse model, allele specific expression analysis needs to confirm if both mutated and WT alleles are expressed *in vivo* before further studies

are carried out to investigate if the mutated and WT proteins are indeed competing in their function. Because MPVs have also been described in patients with *FOXF1* mutations outside of the DNA binding domain, increasing our knowledge about the effects of the different genomic *FOXF1* variants on FOXF1 protein expression and function might lead to new insights that also explain the varying occurrence of MPVs in patients.

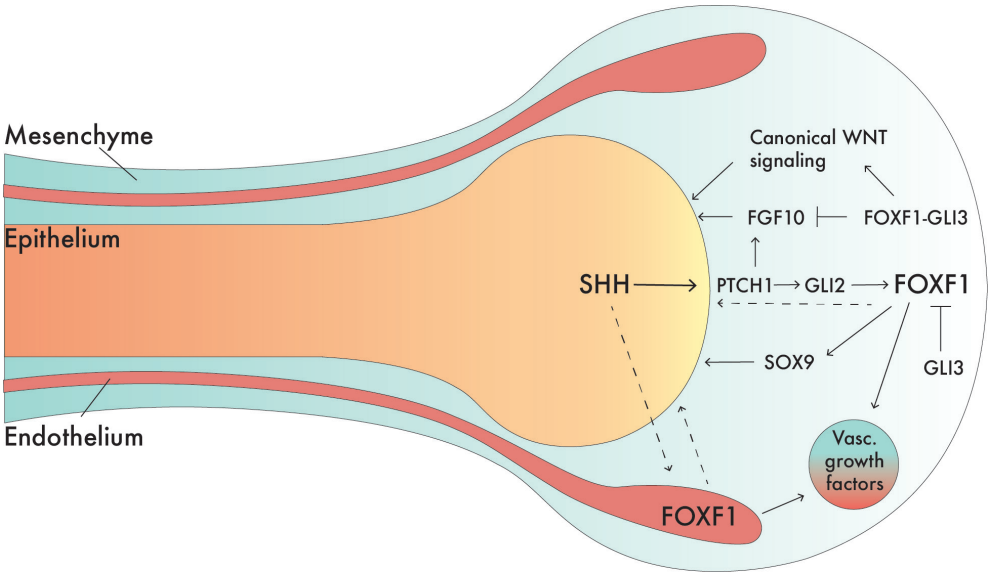

Figure 1. Intercellular signalling pathways in the developing distal lung *SHH signals to the surrounding mesenchyme and activates FOXF1 via PTCH1 and GLI2 (5, 11-13, 16). Mesenchymal and endothelial FOXF1 induces vascular development through activation of multiple vascular growth factors expressed in both the mesenchyme and endothelium. FOXF1 abnormalities presumably interfere with normal epithelial development through aberrant signalling from the mesenchyme and endothelium to the epithelium, for instance by affecting canonical WNT signalling or FGF10 signalling. Continuous arrows: known signalling; dotted arrows: hypothesized signalling.*

Patient specific iPSCs to study the effects of *FOXF1* variants in endothelial cells

Although mouse models constitute the basis for our understanding of the molecular pathways in which FOXF1 acts during lung development, humanized (lung) models are required to better study how genomic *FOXF1* variants in human lead to ACD/MPV. Therefore, we generated induced pluripotent stem cell (iPSC) lines from two patients with a *FOXF1* mutation that can be differentiated into various human cell types (18) (chapter 5). The lungs of ACD/MPV patients are mainly characterized by vascular defects of which the reduction in alveolar capillaries is most prominent. Distal vascular patterning

of the lungs is a process of angiogenesis, requiring intact and functional ECs. As this process seems affected in ACD/MPV lungs, we differentiated iPSCs into vascular ECs to investigate the effects *FOXF1* mutations on differentiation capability and EC function. In line with the presence of ECs in ACD/MPV patients *in vivo*, our results showed that cells carrying the p.L56V or p.F85I *FOXF1* mutation are able to form ECs *in vitro* (chapter 6). Furthermore, preliminary RNA expression analyses indicate that gene expression patterns during differentiation and at the EC stage, are comparable with control cells without a heterozygous *FOXF1* mutation. This implies that mutations p.L56V or p.F85I do not interfere with the expected phases of EC differentiation, and indicate that the mutations do not affect expression of *FOXF1* and *FOXF1* target genes such as *FLT1, KDR, PDGFb, and TIE2* (9, 19). Throughout the body, ECs form a heterogeneous population with tissue-specific properties (20, 21). Transcriptome analysis of organ-specific ECs from mice demonstrated expression of unique, organ-specific clusters of angiocrine factors, adhesion molecules, chemokines, transcription factors (TFs), and metabolic profiles for each EC type (20, 22). High expression levels of T*bx3, Fgf1, Cd36, Ace, Scn7a* and *Scn3a* were found to be specific for lung ECs. Since the impact of *FOXF1* mutations might be EC type specific, we are currently analysing our RNA expression data for different profiles to identify which EC type is most closely related to the mutated and control ECs generated in our study. For the most optimal representation of affected ECs in ACD/MPV lungs *in vivo*, it would be ideal to generate lung specific capillary ECs. So far, there is no available protocol to promote differentiation of lung specific capillary ECs but single cell RNA sequencing on human lung ECs will form the basis for functional *in vitro* studies investigating which (growth) factors are needed to induce lung specification. Furthermore, as epigenetic mechanisms such as DNA methylation play an important role in tissue specific gene regulation, epigenetic studies can elucidate the epigenetic marks contributing to lung specification (23, 24).

Angiogenesis is a complex process involving over fifty different proteins of which the vascular endothelial growth factor (VEGF) family and its receptors play a key role (25-27). Since VEGF receptor 1 and 2 among other endothelial growth factors are regulated by FOXF1 (9, 28), it is hypothesized that the reduction of alveolar capillaries in ACD/MPV patients can be explained by defective angiogenesis caused by FOXF1 abnormalities. Supporting this hypothesis, EC specific knockdown of *Foxf1* led to a diminished pulmonary

vasculature and impaired angiogenesis in mice (9, 29). Furthermore, it was previously shown that downregulation of *FOXF1* in human endothelial progenitor cells (EPCs) indeed reduced vascular sprouting (28). However, we did not observe a decrease in angiogenic potential in differentiated ECs carrying a *FOXF1* mutation (chapter 6). Since *FOXF1* mutations *in vivo* lead to a decrease in pulmonary capillaries, it is possible that our *in vitro* findings do not fully recapitulate the *in vivo* situation. This could be related to the type of assay that was used but also to the type of EC that was studied. Because EPCs have a higher endogenous FOXF1 expression than mature ECs, the impact of *FOXF1* abnormalities on angiogenesis could be specific for EPCs (28, 30). Whether this is the case can be studied by differentiating patient specific iPSCs to EPCs followed by different angiogenesis assays (31-33). Furthermore, by adding a *FOXF1* expression analysis in mutated EPCs, it can be defined whether angiogenic potential is related to *FOXF1* downregulation or an altered protein function.

Mimicking ACD/MPV *in vitro* using co-culture systems

The prominence of vascular defects in ACD/MPV lungs and the occurrence of pulmonary abnormalities in mice after endothelial-specific *Foxf1* deletion (29), suggest an important role for ECs in the origin of ACD/MPV. However, similar to *Foxf1*$^{+/-}$ mouse models, ACD/MPV lungs also demonstrate some epithelial defects such as increased numbers of alveolar type 2 cells, even though epithelial cells do not express FOXF1 (34, 35). As mentioned earlier, lung development is a reciprocal process of vascular morphogenesis and branching morphogenesis involving intercellular signalling between many different cell types (36-40). During lung development, mesenchymal cells are important for the mesenchymal-epithelial crosstalk which is essential for proximal-distal patterning, cellular proliferation and differentiation of various epithelial respiratory cell types (12, 41, 42). Mesenchymal-specific homozygous deletion of *Foxf1* leads to inhibited mesenchyme proliferation and delayed branching lung morphogenesis, confirming that FOXF1 plays a role in intercellular signalling (39). Furthermore, it has been shown that mesenchymal FOXF1 promotes *Sox9* transcription at the initiation of tracheal chondrogenesis and acts together with GLI3 to stimulate transcription of key WNT signalling regulators required for tracheal cartilage development (12) (Figure 1). So, aside from ECs, it would be interesting to study the impact of *FOXF1* variants on other cell types to get a more complete understanding of the pathogenesis of ACD/MPV. An interesting approach would be to

use co-cultures of endothelial, mesenchymal and epithelial cells to study the effects of *FOXF1* variants in human lung models such as Air Liquid Interface (ALI) cultures, lung-on-a-chip devices and lung organoid cultures (43-46). By differentiating patient-specific iPSCs towards endothelial-, mesenchymal- and epithelial cells, these in vitro models can be made fully or partly patient specific (47-50), depending on the research question. For instance, *FOXF1* mutated ECs can be co-cultured with normal epithelial progenitor cells to study if the presence of mutated ECs is enough to reduce the differentiation of type 1 alveolar cells. For functional studies such as rescue experiments, an *in vitro* model is preferred that represents ACD/MPV lung tissue as much as possible and thus, requires that all cell types derive from the same patient. Organoids have a self-organising 3D structure that gives a more realistic perspective of the multicellular interplay during lung development than 2D cultures. As organoids are small, they have the scalability of 2D cultures (51) and are therefore beneficial to study differences in cell differentiation and proliferation, related to multiple different *FOXF1* mutations associated with ACD/MPV. Lung-on-a-chip systems incorporating hydrodynamic forces are useful for investigating specific functions of cells that are constantly subjected to biomechanical forces *in vivo,* like ECs that are exposed to forces induced by blood pressure and blood flow (50-52). *In vitro* lung models using iPSC derived cells are preferably compared with isogenic control models. However, the generation of isogenic control models requires heterozygous editing of the *FOXF1* gene in iPSCs which can be challenging, as we have experienced. We tried to introduce heterozygous, patient-specific missense mutations in the *FOXF1* gene using separate Cas9 and gRNA expression plasmids. However, our attempts failed due to technical difficulties such as low transfection efficiency and the subsequent low iPSC survival at that time. As CRISPR-Cas gene editing methods improve constantly, I expect new effective ways for gene editing in iPSCs to be available in the near future.

The complex genetics of ACD/MPV

The ACD/MPV patient specific iPSC lines enable investigation of two *FOXF1* missense mutations. However, the genetics of ACD/MPV are far more complex. Variants detected in ACD/MPV patients vary widely from large deletions involving the 60Kb *FOXF1* enhancer to missense mutations in the *FOXF1* coding region (3, 53). Mouse studies revealed dosage-dependent effects of *Foxf1* as both downregulation and overexpression of *Foxf1* leads to lung hypoplasia and a diminished vascular network (4, 8). Whether and how the

different *FOXF1* variants detected in ACD/MPV patients affect FOXF1 expression is largely unknown as expression analyses with ACD/MPV lung tissue are scarce. In a comparative transcriptome analysis where frozen lung tissues of six ACD/MPV patients of which five carried a genomic *FOXF1* variant were pooled, *Foxf1* was not differentially expressed compared to control lung tissues (54). However, as the genomic *FOXF1* variants differed among patients, the effect of each individual variant might be diminished. In chapter 6, we found that, at the mesodermal stage, both mutated and wild type *FOXF1* alleles of ACD/MPV cell lines were equally expressed at the RNA level. However, this cannot be extrapolated to more differentiated cellular stages nor gives this an indication of the protein levels since the mutated protein might be unstable and subjected to rapid degradation through proteolytic breakdown. Extensive expression studies with ACD/MPV lung tissues are needed to define if and how each genomic *FOXF1* variant affects FOXF1 protein levels and how this could contribute to the phenotype.

Within the *FOXF1* coding region, all different types of mutations are found (Figure 2) (1, 3, 53, 55-63). Except for nonsense mutations creating a premature stop codon, each type of mutation seems to be located in a specific region of the FOXF1 protein, suggesting that ACD/MPV is related to specific changes in FOXF1 protein function. Most missense mutations are located in the DNA binding domain and presumably interfere with FOXF1 function through altering its affinity to bind target genes. Furthermore, *in silico* nuclear localisation signal (NLS) prediction models indicate that the NLS of FOXF1 is located within the DNA binding domain (64-67). Therefore, missense mutations in this region could also affect FOXF1 transport into the nucleus. Frameshift mutations are often found downstream of the cell type-specific activation domain and upstream of the general activation domain. Therefore, these mutations are likely to interfere with the function of the general activation domain. Furthermore, all these mutations might change the 3D structure of a certain protein domain which for instance, can lead to aberrant protein complex formation. To get a better understanding of the specific protein changes that might contribute to ACD/MPV, we are currently investigating whether missense mutations in the DNA binding domain indeed alter binding of FOXF1 target genes *in vitro*. Therefore, we generated constructs to express epitope tagged FOXF1 proteins with nine different patient-specific mutations located in the DNA binding domain. The results obtained with these constructs can be validated with cells differentiated from patient specific iPSCs or gene-edited primary lung cells.

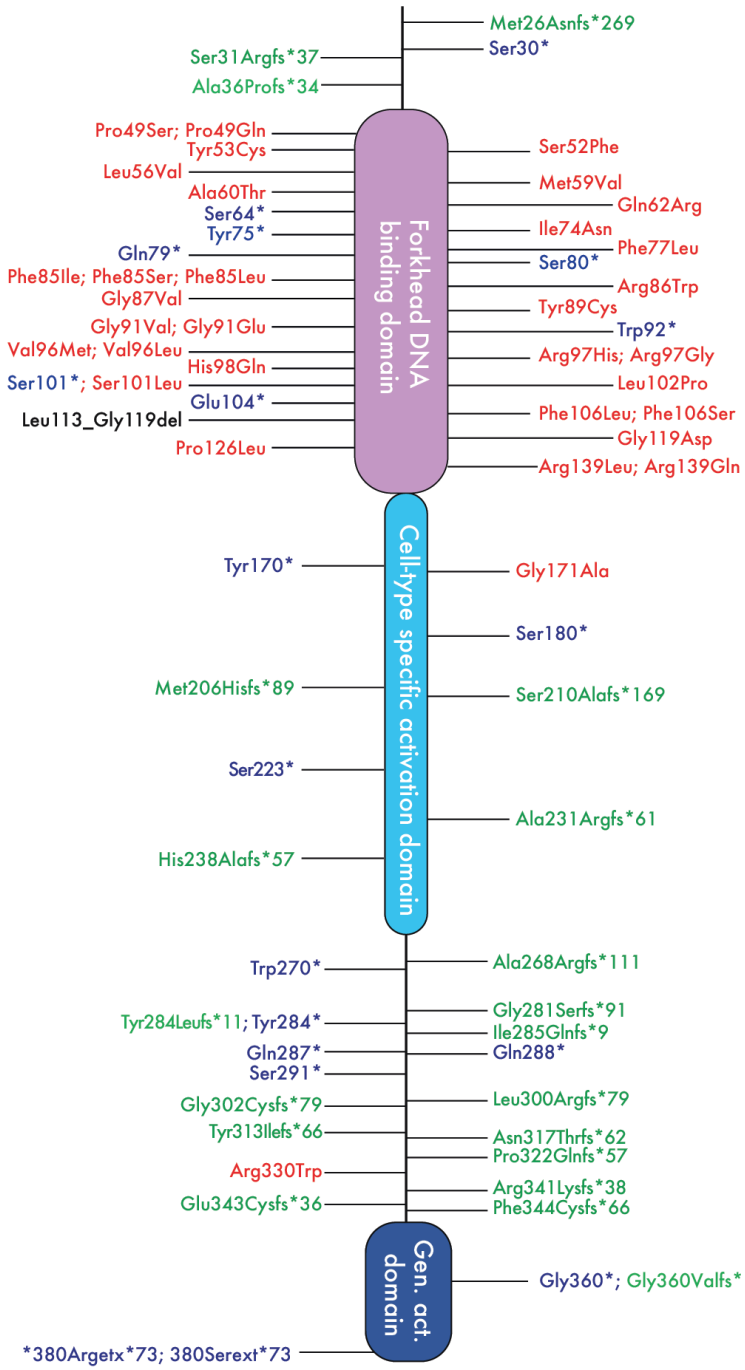

Figure 2. Overview of the different FOXF1 mutations detected in ACD/MPV patients *Blue: nonsense mutations; green: frameshift mutations; red: missense mutations; black: indel mutation without frameshift. This figure was adapted from Pradhan et al. (17), complemented with the mutations detected in chapter 3 of this thesis and case reports (1, 3, 53, 55-63).*

Phenotypical variance in ACD/MPV patients

The genotype-phenotype correlation in ACD/MPV patients is poorly understood. Phenotypic differences observed between ACD/MPV patients, for instance in severity of respiratory insufficiency, the extent of the vascular anomalies within the lung (bilateral/unilateral/one segment) and the presence of accompanying malformations, seem unrelated to the type or location of the *FOXF1* variant (3, 59, 62, 68) (chapter 3). As even patients carrying exactly the same missense mutation differ in phenotype, it could be that modifier loci are involved as well. This hypothesis is supported by the finding that the severity of lung defects in mice with heterozygous loss of *Foxf1* varied, depending on their genetic background (5). Furthermore, the severity of lung defects in mice correlated to the FOXF1 expression levels (8). Therefore, it would be interesting to investigate whether ACD/MPV patients carrying the same mutation have different FOXF1 expression levels in the lung, for instance because patient specific differences in modifier loci additionally influence *FOXF1* expression. This would also clarify if the severity of respiratory problems is correlated with FOXF1 expression levels in ACD/MPV lungs. Whether the presence of accompanying malformations can be attributed to aberrant FOXF1 expression levels in affected organs has never been studied. Steiner et al. showed in an ACD/MPV patient without co-malformations that FOXF1 levels in the lung were reduced but were normal in the intestine (69). As there are many patients with co-malformations such as intestinal malformations or heart defects, it would be interesting to study whether tissues of these affected organs have reduced FOXF1 levels, and to identify the exact role of FOXF1 in the development of these organs in a spatiotemporal manner. If the expression in affected organs is altered, this could imply that organ specific regulation of the *FOXF1* gene contributes to the variance in accompanying malformations observed in patients carrying the same mutation.

Aberrant DNA methylation of the *FOXF1* enhancer

Apart from genetic mechanisms of gene regulation, gene expression is greatly influenced by epigenetic gene regulation mechanisms such as DNA methylation. In chapter 4, we compared DNA methylation patterns in lung tissues of three ACD/MPV patients harbouring a point mutation in the *FOXF1* coding region with lung tissues of three non-ACD/MPV controls and detected two regions within the upstream 60 kb *FOXF1* enhancer region

that were significantly hypermethylated in ACD/MPV lung tissues. The *FOXF1* enhancer region is a 60 kilo base (kb) region that was identified as shortest region of overlap when comparing over 35 deletions upstream of the *FOXF1* gene detected in ACD/MPV patients (2, 16, 69, 70). The enhancer region is situated within the same topologically associated domain (TAD) as the *FOXF1* coding region and includes a long noncoding RNA *LINC01081* that upregulates FOXF1 expression in foetal lung fibroblasts (53, 70). Furthermore, this region contains GLI-binding sites that positively regulate FOXF1 expression in the presence of the SHH effector GLI2. Methylation of the CpG island overlapping these GLI-binding sites reduced *FOXF1* promoter activity *in vitro* (16). It can be hypothesized that hypermethylation of the two regions we detected in *FOXF1* mutated ACD/MPV lung tissues, of which one has been shown to physically interact with the *FOXF1* promoter (16), similarly reduces *FOXF1* promoter activity. This hypothesis should be studied in more detail by inducing specific methylation followed by expression analysis. Since we did not statistically analyse methylation patterns for the three ACD/MPV patients with a *FOXF1* point mutation separately, patient specific differentially methylated regions might be missed. In theory, patient specific differences in DNA methylation within the *FOXF1* enhancer could contribute to different *FOXF1* expression levels and therefore different clinical presentations in ACD/MPV patients carrying the same genomic mutation.

Tissue specific regulation of the *FOXF1* gene

So far, the 60kb enhancer is the only known genomic region that regulates *FOXF1* expression. Since most of the research on this 60kb enhancer has been carried out in lung derived cells (16, 53, 70), it is not certain if this region also acts as enhancer in non-lung derived tissues. High-throughput chromosome conformation capture (Hi-C) experiments demonstrated more frequent chromatin interactions between the *FOXF1* promoter and the 60kb enhancer in foetal lung fibroblasts than non-lung cell lines (53), suggesting that the 60kb enhancer is (partly) lung specific. Whether there are additional enhancers that regulate *FOXF1* expression in other organs, has not been studied yet. For our understanding of the occurrence of accompanying malformations, especially in patients carrying the same mutation, it would be helpful to identify whether these enhancers indeed exist. Genetic and epigenetic changes involving these enhancers could contribute to altered *FOXF1* regulation in specific organs leading to accompanying malformations in ACD/MPV patients. One of the approaches to identify additional enhancers would be to

perform chromosome conformation capture-on-chip (4C) experiments in different cell types, such as gastrointestinal derived ECs. It is also possible that the 60kb enhancer region is the only important *FOXF1* enhancer but acts differentially in different cell types due to the formation of cell type-specific sub-TADs which define the region of influence of an enhancer (71, 72). Genomic variance between patients could alter the organization of sub-TADs resulting in a change in *FOXF1* regulation. Using iPSCs, promoter-enhancer interactions can be investigated at different stages of cell differentiation and in different cell types. Moreover, the availability of patient specific iPSCs provides the opportunity to study abnormal interactions related to patient specific *FOXF1* variants.

Parental imprinting through DNA methylation of the *FOXF1* enhancer

To understand the regulation of *FOXF1* and to understand how heterozygote *FOXF1* variants lead to haploinsufficieny, it remains an important question whether the *FOXF1* gene locus is parentally imprinted, and if so, where and on which allele the epigenetic modification occurs. Although there is significant evidence for imprinting of the enhancer region (53), it has never been confirmed in lung tissue or lung derived cells. Our results revealed that in lung tissue, the *FOXF1* enhancer is not imprinted through DNA methylation on the maternal allele but, our methods were not sufficient to confirm imprinting of the paternal allele (chapter 4). For this we need lung tissue from uniparental disomy (UPD) 16 patients who have two paternal chromosomes 16. In comparison with lung tissue of controls who have a paternal and a maternal copy of chromosome 16, paternally imprinted regions in UPD16 lung tissue will appear as hypermethylated regions. We have to keep in mind that it is still possible that imprinting occurs on the maternal allele, but through epigenetic modifications other than DNA methylation. If the enhancer is maternally imprinted, the rarity of paternal deletions detected in ACD/MPV patients would indicate that paternal deletions are embryonically lethal, whereas in a paternal imprinting model, the rarity of paternal deletions would indicate that they are benign and therefore not found in ACD/MPV patients. If the *FOXF1* enhancer is imprinted, the bi-allelic expression of *FOXF1* during differentiation (chapter 6) indicates that the enhancer acts both in *cis* and in *trans.* These findings are in line with the *in vitro* secreted alkaline phosphatase (SEAP) reporter assays performed by Szafranski and colleagues (16). However, in this *in vitro* assay, *trans* regulation was investigated through co-transfection of two different expression constructs

in human pulmonary microvascular endothelial cells, one containing a segment of the *FOXF1* enhancer and one containing the SEAP reporter gene under the control of the *FOXF1* promoter. SEAP expression indeed increased after addition of the *FOXF1* enhancer segment illustrating that the enhancer and promoter are able to interact. *In vivo*, this interaction could for instance take place through chromatin looping. Yet, these results do not prove that *in vivo*, *FOXF1* is regulated in *trans*. To get a better understanding on *cis* and *trans* regulation of *FOXF1*, it would be interesting to create an allele specific deletion in the *FOXF1* enhancer of lung derived ECs such as endothelial colony forming cells, followed by allele specific endogenous expression analyses.

Aberrant DNA methylation of the *FOXF1* gene

Surprisingly, in 27% of the patients tested with the *FOXF1* targeted NGS panel complemented with Sanger sequencing and SNP array, there was no pathogenic *FOXF1* variant detected (3) (chapter 3). As literature mainly includes case reports of ACD/MPV patients in which a *FOXF1* variant was detected, I did not expect to find such a high percentage of patients without a *FOXF1* variant in our patient group. To investigate whether DNA methylation could contribute to ACD/MPV independent of genomic *FOXF1* variants, we studied DNA methylation patterns in lung tissues of two histologically confirmed ACD/MPV patients without known genomic *FOXF1* variants (chapter 4). Interestingly, this yielded a highly hypermethylated region overlapping exon 1 of the *FOXF1* gene in one of the two patients. Although this hypermethylated region starts approximately 30bp downstream of the *FOXF1* promoter, its proximity might still affect promoter activity, for instance trough changing binding affinity of *FOXF1* activating transcription factors. As we were the first group to test DNA methylation in patients without a genomic variant, it is important to validate if hypermethylation of exon 1 is associated with the ACD/MPV phenotype in patients without a genomic *FOXF1* variant. Whether hypermethylation of exon 1 affects *FOXF1* expression in lungs of ACD/MPV patients remains to be determined.

Reflections and future perspectives

Through development of a new NGS panel targeted at the *FOXF1* locus, we enabled a faster diagnostic process that reduces unnecessary suffering for ACD/MPV patients. Moreover, in the Erasmus MC Sophia Children's Hospital we have already been benefiting

from this test by genetically diagnosing an ACD/MPV patient during ECMO therapy in less than 72 hours. With the eventual aim to find therapeutic targets for ACD/MPV, the other studies described in this thesis are focused on understanding how (epi)genetic *FOXF1* abnormalities lead to ACD/MPV. As one of the main features of ACD/MPV is the lack of a capillary bed, we generated ACD/MPV patient specific iPSC lines and used them to investigate EC differentiation and angiogenic function. Patient specific iPSC lines with a *FOXF1* missense mutation were able to form mature vascular ECs *in vitro* and can be used for future research requiring patient specific (co-)culture systems. However, based on their gene expression, we believe that the mature ECs differentiated in our study were not representative for the type of ECs that are affected in ACD/MPV lungs and therefore did not show any effect of the *FOXF1* mutations on angiogenic function. Subsequently, this means that *in vivo,* the function of FOXF1 is restricted to a subset of ECs, presumably the ones that are particularly important for distal angiogenesis during pulmonary development. Since *in vivo* pulmonary angiogenesis always takes place in contact with the surrounding mesenchyme, the interaction between endothelial and mesenchymal cells should be further investigated to clarify whether abnormal angiogenesis in ACD/MPV lungs is attributed to mesenchymal FOXF1 abnormalities instead of EC FOXF1 abnormalities. Besides the reduction in alveolar capillaries, important characteristics of ACD/MPV include thickening of the arterial walls, reduced numbers of alveolar type 1 cells and in most patients, MPVs. These aspects were not specifically studied by us but indicate that besides distal angiogenesis, FOXF1 is involved in multiple intercellular signalling pathways required for vessel and alveolar formation. Currently, different methods are being developed and optimized to perform single cell RNA sequencing on FFPE tissue using laser capture microdissection (LCM) techniques (73, 74). This does not only enable investigation of gene expression profiles of specific cell types, but also allows for correlating gene expression to a specific location of that cell type within the lung. As the vast majority of ACD/MPV lung tissue is stored as FFPE blocks, the availability of FFPE single cell RNA sequencing techniques will open up possibilities to better define the specific cell types and signalling pathways that are affected in ACD/MPV lungs. Furthermore, single cell sequencing of ACD/MPV lung tissue might lead to identification of (modifier) genes that are responsible for the phenotypical differences between ACD/MPV patients, or the ACD/MPV phenotypes in patients without genomic *FOXF1* variants. Chromatin immunoprecipitation (ChIP) sequencing is increasingly used on FFPE tissue

as well (75, 76). Although not in use yet, combining FFPE ChIP sequencing with LCM will allow identification of direct FOXF1 target genes in specific cell types within the lung. And thus, FFPE single cell RNA sequencing and FFPE single cell ChIP sequencing will together facilitate identification of potential therapeutic targets for ACD/MPV patients with FOXF1 abnormalities using stored FFPE tissue blocks.

Besides investigating FFPE tissue, it is mandatory to increase the availability of fresh patient material. For this reason, and to reduce unnecessary suffering for patients, it is important to further shorten the time to diagnose ACD/MPV so that more patients can be diagnosed pre-mortem. Preferably, patients will be diagnosed through genetic testing instead of lung biopsy as genetic testing is less invasive and therefore increases the possibility to diagnose ACD/MPV in patients that are clinically not stable enough to undergo lung biopsy. Genetic testing techniques such as targeted NGS and WGS are still being optimized, resulting in a better coverage, higher processing rates and lower costs. Within the coming 5 years, I expect these methods to enable genetic testing within 24 hours. It would even be better to diagnose patients prenatally. However, as there are no obvious signs of ACD/MPV during pregnancy, there is often no clear indication to perform prenatal genetic testing for *FOXF1* variants, except when there is a history of ACD/MPV in the family, or if multiple co-malformations are seen during prenatal ultrasounds. Furthermore, detection of monogenetic disorders currently requires amniocentesis or chorionic villus sampling, entailing risks for the foetus. Optimization is ongoing to increase detection levels of paternally inherited or novel monogenetic disorders by non-invasive prenatal testing using cell-free foetal DNA isolated from maternal blood (77-79). Once this technique is implemented, prenatal testing for monogenetic disorders can be incorporated in standard prenatal screening procedures. Since foetal DNA can be detected in the maternal blood stream at four weeks of gestation and increases during pregnancy (80), the level of foetal DNA should be sufficient to detect *FOXF1* variants before the canalicular stage of lung development begins (16-25 weeks of gestation). Therefore, once the implications of specific *FOXF1* variants are clear and potential therapeutic targets have been defined, early prenatal detection of *FOXF1* variants will provide the opportunity to investigate antenatal administration of therapeutic compounds.

So far, studies investigating ACD/MPV mainly aimed at improving clinical outcome by increasing our understanding of the pathogenesis of ACD/MPV. Although translational

research is essential to improve disease management and eventually produce a promising treatment, clinical research is important to improve clinical outcome of ACD/MPV patients as well. Because of the rarity of ACD/MPV, diagnostic and therapeutic approaches are currently different between each hospital and are based on in-house experiences and sporadic case reports. A large clinical study comparing different approaches could result in clear guidelines for clinical management. Especially with the growing availability of genetic testing methods, a prospective clinical study is necessary to decipher which diagnostic approach is best suited for ACD/MPV patients and their parents, and which is most cost-effective. Additional to clinical research, it would also be interesting to expand the research field of ACD/MPV with transgenerational epigenetic research. As some studies indicate that certain methylation marks can be passed on to offspring (81), it might be relevant to elucidate whether environmental factors causing epigenetic changes are able to influence the occurrence and phenotype of ACD/MPV in offspring.

Altogether, this thesis includes studies investigating clinical, genetic and epigenetic aspects of ACD/MPV. Over the last four years, we have already been able to improve the diagnostics of ACD/MPV. In the next 10 years, I believe that upcoming new techniques and the continuation of ongoing functional studies using *in vitro* human lung models, will shed light on the molecular basis of ACD/MPV. This will enable identification of therapeutic targets and eventually improve the perspectives for affected ACD/MPV patients and their parents.

REFERENCES

1. Stankiewicz P, Sen P, Bhatt SS, Storer M, Xia Z, Bejjani BA, et al. Genomic and genic deletions of the FOX gene cluster on 16q24.1 and inactivating mutations of FOXF1 cause alveolar capillary dysplasia and other malformations. Am J Hum Genet. 2009;84(6):780-91.
2. Szafranski P, Yang Y, Nelson MU, Bizzarro MJ, Morotti RA, Langston C, et al. Novel FOXF1 deep intronic deletion causes lethal lung developmental disorder, alveolar capillary dysplasia with misalignment of pulmonary veins. Hum Mutat. 2013;34(11):1467-71.
3. Slot E, von der Thusen JH, van Heijst A, van Marion R, Magielsen F, Dubbink HJ, et al. Fast detection of FOXF1 variants in patients with alveolar capillary dysplasia with misalignment of pulmonary veins using targeted sequencing. Pediatr Res. 2020.
4. Dharmadhikari AV, Szafranski P, Kalinichenko VV, Stankiewicz P. Genomic and Epigenetic Complexity of the FOXF1 Locus in 16q24.1: Implications for Development and Disease. Curr Genomics. 2015;16(2):107-16.
5. Mahlapuu M, Enerback S, Carlsson P. Haploinsufficiency of the forkhead gene Foxf1, a target for sonic hedgehog signaling, causes lung and foregut malformations. Development. 2001;128(12):2397-406.
6. Mahlapuu M, Pelto-Huikko M, Aitola M, Enerback S, Carlsson P. FREAC-1 contains a cell-type-specific transcriptional activation domain and is expressed in epithelial-mesenchymal interfaces. Dev Biol. 1998;202(2):183-95.
7. Peterson RS, Lim L, Ye H, Zhou H, Overdier DG, Costa RH. The winged helix transcriptional activator HFH-8 is expressed in the mesoderm of the primitive streak stage of mouse embryos and its cellular derivatives. Mech Dev. 1997;69(1-2):53-69.
8. Kalinichenko VV, Lim L, Stolz DB, Shin B, Rausa FM, Clark J, et al. Defects in pulmonary vasculature and perinatal lung hemorrhage in mice heterozygous null for the Forkhead Box f1 transcription factor. Dev Biol. 2001;235(2):489-506.
9. Ren X, Ustiyan V, Pradhan A, Cai Y, Havrilak JA, Bolte CS, et al. FOXF1 transcription factor is required for formation of embryonic vasculature by regulating VEGF signaling in endothelial cells. Circ Res. 2014;115(8):709-20.
10. Mahlapuu M, Ormestad M, Enerback S, Carlsson P. The forkhead transcription factor Foxf1 is required for differentiation of extra-embryonic and lateral plate mesoderm. Development. 2001;128(2):155-66.
11. Madison BB, McKenna LB, Dolson D, Epstein DJ, Kaestner KH. FoxF1 and FoxL1 link hedgehog signaling and the control of epithelial proliferation in the developing stomach and intestine. J Biol Chem. 2009;284(9):5936-44.
12. Nasr T, Holderbaum AM, Chaturvedi P, Agarwal K, Kinney JL, Daniels K, et al. Disruption of a hedgehog-foxf1-rspo2 signaling axis leads to tracheomalacia and a loss of sox9+ tracheal chondrocytes. Dis Model Mech. 2020.
13. Ho UY, Wainwright BJ. Patched1 patterns Fibroblast growth factor 10 and Forkhead box F1 expression during pulmonary branch formation. Mech Dev. 2017;147:37-48.
14. Motoyama J, Liu J, Mo R, Ding Q, Post M, Hui CC. Essential function of Gli2 and Gli3 in the formation of lung, trachea and oesophagus. Nat Genet. 1998;20(1):54-7.
15. Park HL, Bai C, Platt KA, Matise MP, Beeghly A, Hui CC, et al. Mouse Gli1 mutants are viable but have defects in SHH signaling in combination with a Gli2 mutation. Development. 2000;127(8):1593-605.
16. Szafranski P, Dharmadhikari AV, Brosens E, Gurha P, Kolodziejska KE, Zhishuo O, et al. Small noncoding differentially methylated copy-number variants, including lncRNA genes, cause a lethal lung developmental disorder. Genome Res. 2013;23(1):23-33.
17. Pradhan A, Dunn A, Ustiyan V, Bolte C, Wang G, Whitsett JA, et al. The S52F FOXF1 Mutation Inhibits STAT3 Signaling and Causes Alveolar Capillary Dysplasia. Am J Respir Crit Care Med. 2019.

18. Slot E, de Klein A, Rottier RJ. Generation of three iPSC lines from two patients with heterozygous FOXF1 mutations associated to Alveolar Capillary Dysplasia with Misalignment of the Pulmonary Veins. Stem Cell Res. 2020;44:101745.
19. Bolte C, Flood HM, Ren X, Jagannathan S, Barski A, Kalin TV, et al. FOXF1 transcription factor promotes lung regeneration after partial pneumonectomy. Sci Rep. 2017;7(1):10690.
20. Nolan DJ, Ginsberg M, Israely E, Palikuqi B, Poulos MG, James D, et al. Molecular signatures of tissue-specific microvascular endothelial cell heterogeneity in organ maintenance and regeneration. Dev Cell. 2013;26(2):204-19.
21. Rafii S, Butler JM, Ding BS. Angiocrine functions of organ-specific endothelial cells. Nature. 2016;529(7586):316-25.
22. Sabbagh MF, Heng JS, Luo C, Castanon RG, Nery JR, Rattner A, et al. Transcriptional and epigenomic landscapes of CNS and non-CNS vascular endothelial cells. Elife. 2018;7.
23. Bird A. DNA methylation patterns and epigenetic memory. Genes Dev. 2002;16(1):6-21.
24. Greenberg MVC, Bourc'his D. The diverse roles of DNA methylation in mammalian development and disease. Nat Rev Mol Cell Biol. 2019;20(10):590-607.
25. Carmeliet P, Jain RK. Molecular mechanisms and clinical applications of angiogenesis. Nature. 2011;473(7347):298-307.
26. Karaman S, Leppanen VM, Alitalo K. Vascular endothelial growth factor signaling in development and disease. Development. 2018;145(14).
27. Melincovici CS, Bosca AB, Susman S, Marginean M, Mihu C, Istrate M, et al. Vascular endothelial growth factor (VEGF) - key factor in normal and pathological angiogenesis. Rom J Morphol Embryol. 2018;59(2):455-67.
28. Sturtzel C, Lipnik K, Hofer-Warbinek R, Testori J, Ebner B, Seigner J, et al. FOXF1 Mediates Endothelial Progenitor Functions and Regulates Vascular Sprouting. Front Bioeng Biotechnol. 2018;6:76.
29. Cai Y, Bolte C, Le T, Goda C, Xu Y, Kalin TV, et al. FOXF1 maintains endothelial barrier function and prevents edema after lung injury. Sci Signal. 2016;9(424):ra40.
30. Ren X, Ustiyan V, Guo M, Wang G, Bolte C, Zhang Y, et al. Postnatal Alveologenesis Depends on FOXF1 Signaling in c-KIT(+) Endothelial Progenitor Cells. Am J Respir Crit Care Med. 2019.
31. Farkas S, Simara P, Rehakova D, Veverkova L, Koutna I. Endothelial Progenitor Cells Produced From Human Pluripotent Stem Cells by a Synergistic Combination of Cytokines, Small Compounds, and Serum-Free Medium. Front Cell Dev Biol. 2020;8:309.
32. Prasain N, Lee MR, Vemula S, Meador JL, Yoshimoto M, Ferkowicz MJ, et al. Differentiation of human pluripotent stem cells to cells similar to cord-blood endothelial colony-forming cells. Nat Biotechnol. 2014;32(11):1151-7.
33. Sahara M, Hansson EM, Wernet O, Lui KO, Spater D, Chien KR. Manipulation of a VEGF-Notch signaling circuit drives formation of functional vascular endothelial progenitors from human pluripotent stem cells. Cell Res. 2014;24(7):820-41.
34. Cullinane C, Cox PN, Silver MM. Persistent pulmonary hypertension of the newborn due to alveolar capillary dysplasia. Pediatr Pathol. 1992;12(4):499-514.
35. Haraida S, Lochbuhler H, Heger A, Nerlich A, Diebold J, Wiest I, et al. Congenital alveolar capillary dysplasia: rare cause of persistent pulmonary hypertension. Pediatr Pathol Lab Med. 1997;17(6):959-75.
36. Goodwin K, Mao S, Guyomar T, Miller E, Radisky DC, Kosmrlj A, et al. Smooth muscle differentiation shapes domain branches during mouse lung development. Development. 2019;146(22).
37. Kool H, Mous D, Tibboel D, de Klein A, Rottier RJ. Pulmonary vascular development goes awry in congenital lung abnormalities. Birth Defects Res C Embryo Today. 2014;102(4):343-58.
38. Stabler CT, Morrisey EE. Developmental pathways in lung regeneration. Cell Tissue Res. 2017;367(3):677-85.
39. Ustiyan V, Bolte C, Zhang Y, Han L, Xu Y, Yutzey KE, et al. FOXF1 Transcription Factor Promotes Lung Morphogenesis by Inducing Cellular Proliferation in Fetal Lung Mesenchyme. Dev Biol. 2018.
40. Warburton D, El-Hashash A, Carraro G, Tiozzo C, Sala F, Rogers O, et al. Lung organogenesis. Curr Top Dev Biol. 2010;90:73-158.

41. Hines EA, Sun X. Tissue crosstalk in lung development. J Cell Biochem. 2014;115(9):1469-77.
42. Volckaert T, De Langhe SP. Wnt and FGF mediated epithelial-mesenchymal crosstalk during lung development. Dev Dyn. 2015;244(3):342-66.
43. Barkauskas CE, Chung MI, Fioret B, Gao X, Katsura H, Hogan BL. Lung organoids: current uses and future promise. Development. 2017;144(6):986-97.
44. Benam KH, Mazur M, Choe Y, Ferrante TC, Novak R, Ingber DE. Human Lung Small Airway-on-a-Chip Protocol. Methods Mol Biol. 2017;1612:345-65.
45. Hild M, Jaffe AB. Production of 3-D Airway Organoids From Primary Human Airway Basal Cells and Their Use in High-Throughput Screening. Curr Protoc Stem Cell Biol. 2016;37:IE 9 1-IE 9 15.
46. Wilkinson DC, Mellody M, Meneses LK, Hope AC, Dunn B, Gomperts BN. Development of a Three-Dimensional Bioengineering Technology to Generate Lung Tissue for Personalized Disease Modeling. Curr Protoc Stem Cell Biol. 2018;46(1):e56.
47. Chen YW, Huang SX, de Carvalho A, Ho SH, Islam MN, Volpi S, et al. A three-dimensional model of human lung development and disease from pluripotent stem cells. Nat Cell Biol. 2017;19(5):542-9.
48. Clevers H. Modeling Development and Disease with Organoids. Cell. 2016;165(7):1586-97.
49. Dye BR, Hill DR, Ferguson MA, Tsai YH, Nagy MS, Dyal R, et al. In vitro generation of human pluripotent stem cell derived lung organoids. Elife. 2015;4.
50. Nawroth JC, Barrile R, Conegliano D, van Riet S, Hiemstra PS, Villenave R. Stem cell-based Lung-on-Chips: The best of both worlds? Adv Drug Deliv Rev. 2019;140:12-32.
51. Sharma A, Sances S, Workman MJ, Svendsen CN. Multi-lineage Human iPSC-Derived Platforms for Disease Modeling and Drug Discovery. Cell Stem Cell. 2020;26(3):309-29.
52. Schilders KA, Eenjes E, van Riet S, Poot AA, Stamatialis D, Truckenmuller R, et al. Regeneration of the lung: Lung stem cells and the development of lung mimicking devices. Respir Res. 2016;17:44.
53. Szafranski P, Gambin T, Dharmadhikari AV, Akdemir KC, Jhangiani SN, Schuette J, et al. Pathogenetics of alveolar capillary dysplasia with misalignment of pulmonary veins. Hum Genet. 2016;135(5):569-86.
54. Sen P, Dharmadhikari AV, Majewski T, Mohammad MA, Kalin TV, Zabielska J, et al. Comparative analyses of lung transcriptomes in patients with alveolar capillary dysplasia with misalignment of pulmonary veins and in foxf1 heterozygous knockout mice. PLoS One. 2014;9(4):e94390.
55. Abu-El-Haija A, Fineman J, Connolly AJ, Murali P, Judge LM, Slavotinek AM. Two patients with FOXF1 mutations with alveolar capillary dysplasia with misalignment of pulmonary veins and other malformations: Two different presentations and outcomes. Am J Med Genet A. 2018;176(12):2877-81.
56. Goel D, Oei JL, Lui K, Ward M, Shand AW, Mowat D, et al. Antenatal gastrointestinal anomalies in neonates subsequently found to have alveolar capillary dysplasia. Clin Case Rep. 2017;5(5):559-66.
57. Hayasaka I, Cho K, Akimoto T, Ikeda M, Uzuki Y, Yamada M, et al. Genetic basis for childhood interstitial lung disease among Japanese infants and children. Pediatr Res. 2018;83(2):477-83.
58. Ito Y, Akimoto T, Cho K, Yamada M, Tanino M, Dobata T, et al. A late presenter and long-term survivor of alveolar capillary dysplasia with misalignment of the pulmonary veins. Eur J Pediatr. 2015;174(8):1123-6.
59. Jourdan-Voyen L, Touraine R, Masutti JP, Busa T, Vincent-Delorme C, Dreyfus L, et al. Phenotypic and genetic spectrum of alveolar capillary dysplasia: a retrospective cohort study. Arch Dis Child Fetal Neonatal Ed. 2019.
60. Ma Y, Jang MA, Yoo HS, Ahn SY, Sung SI, Chang YS, et al. A Novel De Novo Pathogenic Variant in FOXF1 in a Newborn with Alveolar Capillary Dysplasia with Misalignment of Pulmonary Veins. Yonsei Med J. 2017;58(3):672-5.
61. Reiter J, Szafranski P, Breuer O, Perles Z, Dagan T, Stankiewicz P, et al. Variable phenotypic presentation of a novel FOXF1 missense mutation in a single family. Pediatr Pulmonol. 2016;51(9):921-7.

62. Sen P, Gerychova R, Janku P, Jezova M, Valaskova I, Navarro C, et al. A familial case of alveolar capillary dysplasia with misalignment of pulmonary veins supports paternal imprinting of FOXF1 in human. Eur J Hum Genet. 2013;21(4):474-7.
63. Sen P, Yang Y, Navarro C, Silva I, Szafranski P, Kolodziejska KE, et al. Novel FOXF1 mutations in sporadic and familial cases of alveolar capillary dysplasia with misaligned pulmonary veins imply a role for its DNA binding domain. Hum Mutat. 2013;34(6):801-11.
64. Brameier M, Krings A, MacCallum RM. NucPred--predicting nuclear localization of proteins. Bioinformatics. 2007;23(9):1159-60.
65. Kosugi S, Hasebe M, Matsumura N, Takashima H, Miyamoto-Sato E, Tomita M, et al. Six classes of nuclear localization signals specific to different binding grooves of importin alpha. J Biol Chem. 2009;284(1):478-85.
66. Kosugi S, Hasebe M, Tomita M, Yanagawa H. Systematic identification of cell cycle-dependent yeast nucleocytoplasmic shuttling proteins by prediction of composite motifs. Proc Natl Acad Sci U S A. 2009;106(25):10171-6.
67. Nguyen Ba AN, Pogoutse A, Provart N, Moses AM. NLStradamus: a simple Hidden Markov Model for nuclear localization signal prediction. BMC Bioinformatics. 2009;10:202.
68. Slot E, Edel G, Cutz E, van Heijst A, Post M, Schnater M, et al. Alveolar capillary dysplasia with misalignment of the pulmonary veins: clinical, histological, and genetic aspects. Pulm Circ. 2018;8(3):2045894018795143.
69. Steiner LA, Getman M, Schiralli Lester GM, Iqbal MA, Katzman P, Szafranski P, et al. Disruption of normal patterns of FOXF1 expression in a lethal disorder of lung development. J Med Genet. 2020;57(5):296-300.
70. Szafranski P, Dharmadhikari AV, Wambach JA, Towe CT, White FV, Grady RM, et al. Two deletions overlapping a distant FOXF1 enhancer unravel the role of lncRNA LINC01081 in etiology of alveolar capillary dysplasia with misalignment of pulmonary veins. Am J Med Genet A. 2014;164A(8):2013-9.
71. Brown JM, Roberts NA, Graham B, Waithe D, Lagerholm C, Telenius JM, et al. A tissue-specific self-interacting chromatin domain forms independently of enhancer-promoter interactions. Nat Commun. 2018;9(1):3849.
72. Phillips-Cremins JE, Sauria ME, Sanyal A, Gerasimova TI, Lajoie BR, Bell JS, et al. Architectural protein subclasses shape 3D organization of genomes during lineage commitment. Cell. 2013;153(6):1281-95.
73. Civita P, Franceschi S, Aretini P, Ortenzi V, Menicagli M, Lessi F, et al. Laser Capture Microdissection and RNA-Seq Analysis: High Sensitivity Approaches to Explain Histopathological Heterogeneity in Human Glioblastoma FFPE Archived Tissues. Front Oncol. 2019;9:482.
74. Foley JW, Zhu C, Jolivet P, Zhu SX, Lu P, Meaney MJ, et al. Gene expression profiling of single cells from archival tissue with laser-capture microdissection and Smart-3SEQ. Genome Res. 2019;29(11):1816-25.
75. Font-Tello A, Kesten N, Xie Y, Taing L, Vareslija D, Young LS, et al. FiTAc-seq: fixed-tissue ChIP-seq for H3K27ac profiling and super-enhancer analysis of FFPE tissues. Nat Protoc. 2020;15(8):2503-18.
76. Zhong J, Ye Z, Clark CR, Lenz SW, Nguyen JH, Yan H, et al. Enhanced and controlled chromatin extraction from FFPE tissues and the application to ChIP-seq. BMC Genomics. 2019;20(1):249.
77. Breveglieri G, D'Aversa E, Finotti A, Borgatti M. Non-invasive Prenatal Testing Using Fetal DNA. Mol Diagn Ther. 2019;23(2):291-9.
78. Koumbaris G, Achilleos A, Nicolaou M, Loizides C, Tsangaras K, Kypri E, et al. Targeted capture enrichment followed by NGS: development and validation of a single comprehensive NIPT for chromosomal aneuploidies, microdeletion syndromes and monogenic diseases. Mol Cytogenet. 2019;12:48.
79. Ye X, Lin S, Song X, Tan M, Li J, Wang J, et al. Identification of copy number variants by NGS-based NIPT at low sequencing depth. Eur J Obstet Gynecol Reprod Biol. 2021;256:297-301.
80. Illanes S, Denbow M, Kailasam C, Finning K, Soothill PW. Early detection of cell-free fetal DNA in maternal plasma. Early Hum Dev. 2007;83(9):563-6.

81. Nagy C, Turecki G. Transgenerational epigenetic inheritance: an open discussion. Epigenomics. 2015;7(5):781-90.

CHAPTER 8

ENGLISH SUMMARY

NEDERLANDSE SAMENVATTING

ENGLISH SUMMARY

Alveolar capillary dysplasia with or without misalignment of the pulmonary veins (ACD/MPV) is a lethal congenital lung disorder causing therapy resistant pulmonary hypertension and an insufficient gas exchange. The majority of patients presents with respiratory distress within 24 hours after birth. Although life supportive care stabilizes the patients, withdrawal of treatment frequently follows as soon as the diagnosis is confirmed by histological examination of the lung, due to the lack of long-term treatment options apart from bilateral lung transplantation in young infants. ACD/MPV is associated with heterozygous genomic mutations and deletions in the *FOXF1* gene or the 60 kilo base pairs (kb) enhancer located 250kb upstream of the gene. However, it is not clear how these mutations and deletions affect FOXF1 and how they lead to ACD/MPV.

In this thesis, different aspects of ACD/MPV are studied with the overall aim to improve diagnosis at an early stage and, on the long run, disease management. **Chapter 1** contains the introduction into general aspects of lung development, ACD/MPV and the role of FOXF1 in lung development. In addition, this chapter gives an overview of the scope of this thesis.

The available literature about ACD/MPV, reviewed in **chapter 2**, reveals an incidence of 1/200.000 in the Netherlands (resulting in one patient per year) and learns that approximately 80% of ACD/MPV patients suffer from co-malformations that predominantly affect the gastrointestinal tract. Chapter 2 also summarizes the current diagnostic and therapeutic approaches and specifies the gaps in our understanding of the pathogenesis of ACD/MPV. For instance, case reports of rare long-term survivors and familial cases pinpoint the complex genotype-phenotype correlation.

Many ACD/MPV patients and their parents experience prolonged suffering because it often takes multiple weeks before ACD/MPV is diagnosed. Therefore, **chapter 3** presents the development and validation of a new genetic testing method. This method is based on targeted next generation sequencing (NGS) and enables fast detection of *FOXF1* variants associated with ACD/MPV. Testing of DNA in the early phase of symptom presentation could speed up the diagnostic process. The developed ACD/MPV NGS panel was validated by retrospective testing of 15 previously diagnosed ACD/MPV patients and resulted in identification of 6 novel genomic variants. In four patients, no pathogenic genomic variants in the *FOXF1* locus were found.

In **chapter 4** it is studied if, besides genomic changes, epigenetic changes contribute to the pathogenesis of ACD/MPV. Using formalin-fixed and paraffin-embedded lung tissues of eight ACD/MPV patients and three age-matched controls, DNA methylation patterns were investigated genome wide and more detailed in the *FOXF1* locus. This revealed hypermethylation of the 60kb *FOXF1* enhancer region in ACD/MPV patients harbouring a point mutation in exon 1, and hypermethylation of the first *FOXF1* exon in one of the patients without a genomic *FOXF1* variant. Based on these results, it can be hypothesized that aberrant DNA methylation contributes to the pathogenesis of ACD/MPV and possibly explains the ACD/MPV phenotype in a part of the patients without a genomic *FOXF1* variant.

Chapter 5 and **6**, focus on the investigation of two specific *FOXF1* mutations associated with ACD/MPV. On a molecular and cellular level, it is poorly understood what the effects of *FOXF1* abnormalities are on lung development and how they lead to ACD/MPV. ACD/MPV lungs are characterized by a reduction of pulmonary capillaries and the presence of misaligned pulmonary veins, indicating that vascular development is affected in particular. Correspondingly, FOXF1 is mainly expressed in vascular cells such as endothelial cells. The effect of genomic *FOXF1* abnormalities on vascular cell function is ideally studied in cells isolated from lungs of ACD/MPV patients. However, since ACD/MPV is a rare disorder and patients are often diagnosed post mortem, fresh lung tissue to isolate endothelial cells from is very scarce. To overcome this limitation, three induced pluripotent stem cell (iPSC) lines were generated from stored skin fibroblasts of two ACD/MPV patients harbouring a different *FOXF1* mutation (**chapter 5**). iPSCs have the advantage that they can be differentiated into a variety of cell types, including endothelial cells.

In **chapter 6,** it is shown that iPSCs carrying the patient specific *FOXF1* mutations are able to differentiate towards mature vascular endothelial cells and follow similar gene expression trends as control iPSCs. Furthermore, both mutated iPSCs and control iPSCs expressed FOXF1 at the mesodermal stage of differentiation. So far, functional assays indicated that mutated endothelial cells have normal angiogenic potential. However, preliminary gene expression analyses suggest that the differentiated endothelial cells might not be representative for the pulmonary capillary endothelial cells that are affected in ACD/MPV patients. Additional analyses are currently underway to further investigate the phenotype of the differentiated endothelial cells and to further investigate the impact of the two *FOXF1* mutations on the function of endothelial cells.

The general discussion (**chapter 7**) focuses on the interpretation of the most important results and their contribution to our understanding of the pathogenesis of ACD/MPV. Furthermore, this chapter elaborates on the hypotheses and perspectives for future research.

In conclusion, the studies in this thesis investigated clinical, histological and molecular aspects of ACD/MPV. This thesis provides an important basis for future research that is necessary for a better understanding of the pathogenesis of ACD/MPV and improvement of disease management.

NEDERLANDSE SAMENVATTING

Alveolaire capillaire dysplasie met of zonder verkeerd uitgelijnde pulmonaal venen (ACD/MPV) is een lethale congenitale longaandoening die leidt tot therapieresistente pulmonale hypertensie en een insufficiënte gasuitwisseling. De meerderheid van de patiënten presenteert zich binnen 24 uur met respiratoire nood waarvoor levensondersteunende behandelingen nodig zijn. Behalve een bilaterale longtransplantatie op neonatale leeftijd zijn er geen behandelopties voor de lange termijn. Daarom worden de levensondersteundende behandelingen over het algemeen gestopt zodra de diagnose ACD/MPV door middel van histologisch longonderzoek is vastgesteld, waarna de patiënt komt te overlijden. ACD/MPV is geassocieerd met heterozygote genetische mutaties en deleties in het *FOXF1* gen, en grote deleties in de *FOXF1* enhancer die 250 kilobasen (kb) voor het gen is gelegen. Hoe deze mutaties en deleties de expressie en functie van FOXF1 beïnvloeden, en hoe dit leidt tot ACD/MPV, is onduidelijk.

In dit proefschrift worden verschillende aspecten van ACD/MPV bestudeerd met het doel om de vroege diagnostiek en uiteindelijk de algehele zorg voor ACD/MPV patiënten te verbeteren. In **hoofdstuk 1** wordt een introductie gegeven in de algemene aspecten van longontwikkeling, ACD/MPV en de rol van FOXF1 tijdens de longontwikkeling. Daarnaast geeft dit hoofdstuk een overzicht van de inhoud van dit proefschrift.

De beschikbare literatuur over ACD/MPV, onderzocht in **hoofdstuk 2**, laat zien dat de incidentie van ACD/MPV in Nederland rond de 1/200.00 ligt. Dit staat gelijk aan één patiënt per jaar. Daarnaast leert de literatuur ons dat circa 80% van de ACD/MPV patiënten is aangedaan met co-malformaties, welke voornamelijk in het maagdarmstelsel voorkomen. Hoofdstuk 2 geeft ook een overzicht van de diagnostische en therapeutische procedures die momenteel worden toegepast, en specificeert de hiaten in onze kennis over de pathogenese van ACD/MPV. De case-reports van zeldzame familiaire casussen en patiënten die onverwachts lang overleven illustreren bijvoorbeeld hoe complex de genotype-fenotype relatie is.

Doordat het vaak meerdere weken duurt voordat de diagnose ACD/MPV wordt gesteld, ervaren veel ACD/MPV patiënten en hun ouders onnodig langdurig lijden. Om deze periode te verkorten presenteert **hoofdstuk 3** de ontwikkeling en validatie van een nieuwe genetische testmethode. Deze methode is gebaseerd op gerichte 'next generation sequencing' (NGS) waardoor *FOXF1* varianten snel gedetecteerd kunnen worden. Door

direct na presentatie van symptomen het DNA uit bloed te testen , kan het diagnostische proces worden bespoedigd. Het ontwikkelde ACD/MPV NGS panel is gevalideerd door DNA van 15 eerder gediagnosticeerde ACD/MPV patiënten retrospectief te testen. Hierbij werden zes genetische varianten gevonden die nog niet eerder zijn beschreven. Daarnaast viel het op dat er bij vier patiënten geen pathogene variant in de *FOXF1* locus werd gevonden.

In **hoofdstuk 4** is onderzocht of er naast genetische veranderingen ook epigenetische veranderingen aanwezig zijn in het DNA van ACD/MPV patiënten, welke zouden kunnen bijdragen aan de pathogenese. Hiervoor werden DNA-methylatiepatronen over het gehele genoom en specifiek in de *FOXF1* locus onderzocht. Het DNA werd geïsoleerd uit formaline gefixeerde en in paraffine ingebedde longweefsels van acht ACD/MPV patiënten en drie controles. Bij patiënten met een genetische puntmutatie in het *FOXF1* gen werd hypermethylatie gezien in de 60kb *FOXF1* enhancer. Bij één van de patiënten zonder genetische *FOXF1* variant werd hypermethylatie gezien in exon 1 van het *FOXF1* gen. Gebaseerd op deze resultaten kan het worden gehypothetiseerd dat afwijkende DNA-methylatiepatronen inderdaad een rol spelen bij de pathogenese van ACD/MPV.

Op cellulair en moleculair niveau is het onduidelijk wat de effecten van genetische *FOXF1* afwijkingen zijn voor de longontwikkeling en hoe deze afwijkingen resulteren in ACD/MPV. In **hoofdstuk 5** en **6** worden twee specifieke *FOXF1* mutaties die geassocieerd zijn met ACD/MPV op cellulair en moleculair niveau onderzocht. ACD/MPV longen worden gekarakteriseerd door een tekort aan alveolaire capillairen en de aanwezigheid van verkeerd uitgelijnde pulmonaal venen. Dit duidt erop dat met name de vasculaire ontwikkeling van de longen is aangedaan, wat ook overeenkomt met de bevinding dat FOXF1 met name in vasculaire cellen zoals endotheelcellen tot expressie komt. Om de effecten van genetische *FOXF1* afwijkingen te bestuderen wordt idealiter gebruik gemaakt van cellen die geïsoleerd zijn uit de longen van ACD/MPV patiënten. Echter, doordat ACD/MPV een zeldzame ziekte is, en doordat patiënten vaak pas na overlijden worden gediagnosticeerd, is vers longweefsel om cellen uit te isoleren schaars. Om dit probleem te omzeilen werden opgeslagen huidfibroblasten van twee ACD/MPV patiënten, met ieder een andere *FOXF1* mutatie, gebruikt om drie geïnduceerde pluripotente stamcel (iPSC) lijnen te genereren (**hoofdstuk 5**). Het grote voordeel van iPSCs is dat deze gedifferentieerd kunnen worden naar verschillende celtypen, waaronder endotheelcellen.

Hoofdstuk 6 laat zien dat de iPSCs met patiëntspecifieke *FOXF1* mutaties in

staat zijn om volwassen vasculaire endotheelcellen te vormen en dat ze gedurende differentiatie dezelfde trends in genexpressie volgen als controle iPSCs. Zowel de gemuteerde ACD/MPV iPSCs als de controle iPSCs brachten FOXF1 tot expressie in de mesodermale fase van differentiatie. Daarnaast lieten de functionele experimenten tot nu toe zien dat de gemuteerde gedifferentieerde endotheelcellen normale angiogenetische potentie hebben. Echter suggereren de voorlopige expressie analyses dat de *in vitro* gedifferentieerde endotheelcellen mogelijk niet volledig representatief zijn voor de specifieke endotheelcellen die zijn aangedaan in ACD/MPV patiënten. Op dit moment worden extra analyses uitgevoerd om te onderzoeken wat het fenotype van de gedifferentieerde endotheelcellen is, en om de impact van de twee *FOXF1* mutaties op de functie van de endotheelcellen verder in kaart te brengen.

De algemene discussie (**hoofdstuk 7**) bespreekt de interpretatie van de meest relevante resultaten van de studies uit dit proefschrift, en hun bijdrage aan onze kennis over de pathogenese van ACD/MPV. Daarnaast gaat de algemene discussie in op de hypothesen en perspectieven voor vervolgonderzoek.

Concluderend bevat dit proefschrift studies naar de klinische, histologische en moleculaire aspecten van ACD/MPV. Deze studies vormen een belangrijke basis voor het vervolgonderzoek dat essentieel is om meer inzicht te krijgen in de pathogenese van ACD/MPV en de zorg voor ACD/MPV patiënten te verbeteren.

APPENDIX

ABOUT THE AUTHOR

Evelien Slot was born on 15 May 1990. She graduated from secondary school at the Werkplaats Kindergemeenschap in Bilthoven in 2008. In 2009, she started her studies Bio-Pharmaceutical Sciences at the Leiden University. After completing her first year she continued her studies in Medicine at the Leiden University, from which she graduated in 2016. During this period, she developed a great interest in embryonic/fetal development and congenital malformations, which culminated in her scientific research internship at the department of Anatomy and Embryology of the Maastricht University Medical Center under supervision of Prof. Wout Lamers. For this research, she received the Student Research Award from the Leiden University Medical Center. In 2017, Evelien was able to continue her passion for research and fetal development in a PhD project at the departments of Pediatric Surgery and Clinical Genetics at the Erasmus Medical Center-Sophia Children's Hospital. The results of this research are described in this thesis. Since May 2021, Evelien works as physician at the department of Fetal Medicine at the Erasmus Medical Center. In addition to her curricular activities, Evelien always enjoyed being a member of multiple organizing committees and loves outdoor sports, yoga, singing and travelling. Evelien lives in Rotterdam, together with her husband Jules Heuberger and their daughter Isa.

LIST OF PUBLICATIONS

Slot E, Boers R, Boers J, van Ijcken WFJ, Tibboel D, Gribnau J, Rottier RJ, de Klein A. Genome wide DNA methylation analysis of alveolar capillary dysplasia lung tissue reveals aberrant methylation of genes involved in development including the FOXF1 locus. Clin. Epigenetics. 2021;13(1):148

Slot E, von der Thusen JH, van Heijst A, van Marion R, Magielsen F, Dubbink HJ, et al. Fast detection of FOXF1 variants in patients with alveolar capillary dysplasia with misalignment of pulmonary veins using targeted sequencing. Pediatr Res. 2021; 89(3):518-525.

Slot E, de Klein A, Rottier RJ. Generation of three iPSC lines from two patients with heterozygous FOXF1 mutations associated to Alveolar Capillary Dysplasia with Misalignment of the Pulmonary Veins. Stem Cell Res. 2020;44:101745.

Slot E, Edel G, Cutz E, van Heijst A, Post M, Schnater M, et al. Alveolar capillary dysplasia with misalignment of the pulmonary veins: clinical, histological, and genetic aspects. Pulm Circ. 2018;8(3):2045894018795143.

PHD PORTFOLIO

Courses		
Technology Facilities	2017	1.4
The ins and outs of CRISPR-Cas	2017	2
CPO course: Patient oriented research	2017	0.3
Genetics course	2017	3
Safely working in the Laboratory	2017	0.3
CC02A: Biostatistical Methods I: Basic Principles Part A	2018	2
Epigenetic regulation in health and disease	2018	0.8
Scientific Integrity	2019	0.3
Biomedical English Writing	2019	3
Seminars and workshops		
Weekly lab meetings	2017-2019	1
MGC PhD workshop	2017/2018	2
Weekly meeting dept. Clinical Genetics	2017-2018	1.5
Weekly meeting dept. Cell Biology	2018-2021	1.5
UCSC Gene browsing workshop	2018	0.7
Monthly ACE-PH meeting	2018	1
Bi-weekly journal club	2018-2019	1
Bi-weekly PhD meeting dept. Cell Biology	2018-2021	1
Jonge Onderzoekers Dag	2018/2019	0.5
(Inter)national conferences		
Genetics Retreat (presentation), Kerkrade	2017/2018	1.5
SMRT scientific symposium, Leiden	2017	0.5
Sophia research day (presentation), Rotterdam	2017/2018	2
CDH symposium (presentation), Liverpool	2017/2018	1
Dutch Neonatal Fellow meeting (presentation), Utrecht	2019	0.5
European Paediatric Surgeon's Association Conference (presentation), Belgrade	2019	1
Teaching		
Supervision Bachelor student Practical Laboratory School Breda	2017	1
Supervision Master student Biomolecular Sciences VU University Amsterdam	2020	2
Additional activities		
Member (president) Committee Wetenschapscafé Rotterdam	2017-2020	0.5
Member MGC PhD workshop committee	2018	0.5
Total EC		**33.8**

ACKNOWLEDGEMENTS/DANKWOORD

Beste **Dick**, ik wil u bedanken voor de kans om mijn enthousiasme voor onderzoek en fascinatie voor de ontwikkeling van de foetus te combineren in een PhD traject. Ik heb veel bewondering voor de manier waarop u ieder aspect van de patiënt belicht en verschillende disciplines weet samen te brengen om de beste zorg mogelijk te maken.

Robbert en Annelies, beiden bedankt voor de laagdrempelige begeleiding en ondersteuning tijdens mij PhD. Door jullie creativiteit en kritische vragen heb ik ontzettend veel geleerd over het doen van experimenteel onderzoek. **Annelies**, tijdens de start en afrondingsfase van mijn PhD heb ik veel gehad aan jouw besluitvaardigheid en (lange termijn) visie. Ook je persoonlijke interesse en betrokkenheid heb ik altijd erg op prijs gesteld. **Robbert**, bedankt dat je me veel ruimte gaf en vertrouwen had, hierdoor heb ik me de afgelopen jaren op verschillende vlakken enorm kunnen ontwikkelen. Ook bedankt voor al je peptalks, dat was vaak precies wat ik nodig had om op de moeilijke momenten met opgeheven hoofd weer door te zetten!

Beste **René,** ondanks dat ik technisch gezien niet onder uw supervisie viel heeft u me net als uw eigen PhD's onder uw hoede genomen en zich bekommerd om de voortgang van mijn onderzoek, mijn toekomstplannen en mijn werkplezier. Ontzettend bedankt daarvoor. Ik heb erg genoten van onze gesprekken tijdens symposia, etentjes en congressen en ik hoop deze nog lang voort te kunnen zetten!

Beste **Martin Post**, in uw lab in Toronto kreeg ik de kans om weer een andere manier van (translationeel) onderzoek mee te maken. Ik heb het ontzettend naar mijn zin gehad en ik heb grote waardering voor uw enorme kennis en manier van onderwijzen. Heel erg bedankt voor deze leuke tijd.

Erik Jan, **Jan** en **Ronald**, bedankt voor de prettige samenwerking bij het opzetten van de diagnostische test voor ACD. **Vera**, bedankt voor je hulp bij het valideren van de test! Ik ben heel trots om te zien dat je stage heeft geleid tot een baan bij de moleculaire diagnostiek en ik hoop dat je het er nog lang naar je zin zult hebben.

Iedereen van het methylatie-project, in het bijzonder **Ruben** en **Joost,** bedankt voor de fijne samenwerking. Door gebruik te maken van MeD-seq en jullie vertrouwen in ons, konden Annelies en ik onze nieuwsgierigheid naar methylatiepatronen bij ACD de vrije loop laten, wat heeft geleid tot interessante nieuwe inzichten én een publicatie.

Iedereen van de **iPS core facility,** bedankt voor jullie hulp bij het werken met de iPS cellen. De prettige werksfeer die jullie met elkaar creëren maakte alle weekenduurtjes een stuk aangenamer!!

Beste **Arno van Heijst**, bedankt voor de prettige samenwerking. Ik vond het heel leuk om via u af en toe bij de kliniek betrokken te blijven.

Iedereen van het lab van Annelies (**Frank**, **Quincy, Bert**, **Tom**, **Jolanda**, **Erwin**, **Natasha**, **Kyra**, en **Wojtek**), bedankt voor de fijne en ontzettend leerzame samenwerking! **Kyra**, bedankt voor al je hulp bij het opstarten met labwerk, zonder jou zou ik nu nog steeds niet weten hoe ik een pipet moest vasthouden ;) **Kyra**, **Natas** en **Wojtek**, onze PhD uitjes waren echt TOP! Én het is jullie gelukt om ook mij verliefd te laten worden op Rotterdam!

Everyone from lab EE1034 (**Anne**, **Marjon**, **Mieke**, **Jennifer**, **Kina**, **Evelien**, **Gabriëla**, **Isabel**, **Cinta**, **Cathy** and **Joël**), thank you all for the fun times we had in the lab. With each one of you having its own expertise and character, you form a unique group together and I'm glad that I got to be a part of that group. **Gabs**, ik ben er trots op hoe wij onze krachten hebben weten te bundelen waardoor we ons onderzoek een heel stuk leuker en beter hebben gemaakt. Je bent echt een super onderzoekster, veel succes met je laatste loodjes!

Beste **Mathijs** en **Jessica,** jullie zijn de afgelopen jaren een grote inspiratiebron voor mij geweest. Het is geweldig om te zien wat jullie tot nu toe met **Stichting ACD** hebben bereikt en ik heb grote bewondering voor jullie motivatie en doorzettingsvermogen. Jullie, **Myla** en de stichting waren voor mij dan ook een belangrijke drive om elke keer opnieuw mijn best te doen om ACD op de kaart te zetten en beter te begrijpen. Ontzettend bedankt dat ik deel mocht uitmaken van jullie grote missie en ik hoop dat we elkaar nog vaker zullen tegenkomen.

Eric, Laura, Carlijn, Willem en andere commissiegenootjes van het Wetenschapscafé, bedankt voor de fijne samenwerking en superleuke maandagavonden! Ik keek altijd uit naar onze vergaderingen die vol zaten met creativiteit en gezelligheid, en naar de cafés waar onze gemeenschappelijke interesses en nieuwgierigheid tot uiting kwamen in goede gesprekken en leuk contact met de sprekers.

Dan mijn lieve paranimfen **Isabel** en **Natas**, wat een geluk dat ik jullie beiden als goede vriendinnen aan deze PhD mag overhouden, én dat jullie naast mij staan tijdens mijn verdediging! Onze goede gesprekken en leuke momenten samen geven me altijd ontzettend veel energie. **Is**, aan het eind hebben onze koffiemomenten en hardlooprondjes me er echt doorheen gesleept; je weet me aankomend jaar te vinden ;)

Lieve **Simone, Sabine, Mady, Tirza, Jeroen, Marc (M), Marc (N), Pake, Daniel, Denise, Ilse, Marjolein, Roos, Anne, Amanda, Timothy, Stijn** en alle andere lieve vrienden, mega bedankt voor jullie eeuwig luisterend oor, altijd positieve instelling, leuke uitjes en gigantische steun over de afgelopen jaren!! Wat zou ik toch zonder jullie moeten?!

Dian, Car, Lieke en **Arne,** bedankt voor al jullie support tijdens mijn PhD! **Dian** en **Car**, al zijn we vaak duizenden kilometers van elkaar verwijderd, ik ben heel blij dat we elkaar via de telefoon altijd weten te vinden.

Leef **Heupies**, hiel erg bedaank veur al uuch steun de afgeloape joare. Geer woart altied hiel geïnteresseerd in wie t ging mit miech en mien onderzeuk en iech kos altijd beij uuch terech veur get fijne aofleiding. Geer zeet de beste sjoenfemilie dee iech miech kin winse!

Pap, mam, Jeannette en **Jan**, bedankt dat jullie me altijd hebben gestimuleerd om nieuwsgierig en kritisch te zijn, om kansen te grijpen, door te zetten en om uit het leven te halen wat er in zit. Zonder deze eigenschappen was mijn PhD nooit gelukt. Ik ben trots dat ik deze mijlpaal met jullie kan delen.

Last but not least, **Jules**. De afgelopen jaren voelde als een enorme rollercoaster. En zoals op het kaartje stond: wat ben ik blij dat jij naast me zit. Ik kan hier oneindig veel pagina's volschrijven maar het komt allemaal op hetzelfde neer: dank je, dank je en nog eens dank je, voor ALLES!!!